Impact of Clay- DNAPL Interactions on the Transport of Chlorinated Solvents in Low Permeability Subsurface Zones

by

Derya Ayral

A dissertation submitted in partial fulfillment
of the requirements for the degree of
Doctor of Philosophy
(Environmental Engineering)
in the University of Michigan
2015

Doctoral Committee:

Professor Avery H. Demond, Chair
Professor M. Clara Cruz Da Silva Castro
Assistant Professor Brian R. Ellis
Professor Mark N. Goltz, Air Force Institute of Technology
Professor Kim F. Hayes
Associate Professor Dimitrios Zekkos

Acknowledgements

I would like to thank my advisor, Prof. Avery Demond, for her guidance throughout my graduate degrees. She is one of the most influential reasons for me to continue on to the Ph.D. program after receiving my master's degree. Her support has been balanced in a great way that allowed me to progress and develop independence at the same time. I would also like to acknowledge the valuable feedback and constructive critical comments of my dissertation committee members: Drs. Clara Castro, Brian Ellis, Kim Hayes, Mark Goltz, and Dimitrios Zekkos, as well as my previous committee member Dr. Rodney Ewing. Additionally, the very beneficial discussions by Professor Peter Grathwohl from the University of Tubingen are appreciated.

There are many people within the department of Civil and Environmental Engineering that I would like to acknowledge. Andrew Henderson provided a continuous support throughout my graduate degree, and I am deeply thankful for his help and encouragements. Margarita Otero-Diaz contributed some experimental work, in particular the crack measurements and the screening experiments, and Julian Carpenter assisted me with the XRD data interpretation. Additionally, Rick Burch provided technical support in building my diffusion cells and always encouraged me with his positive attitude. Thomas Yavaraski was a valuable support for instrumental analysis and a great resource with his knowledge. Staff members Nancy Osugi and Jessica Taylor were also very helpful in addressing student service issues.

Without the funding from Turkish Educational Ministry for my master degree, I would not have been able to start my studies at the University of Michigan. The generous fellowship from Civil and Environmental Engineering Friends Association (CEEFA) and funding by the Strategic Environmental Research and Development Program (SERDP) Project ER-1737 are also appreciated. I am also grateful for the GSI appointments in the CEE department which provided funding as well as great experience to help improve my teaching.

I had the opportunity to work on the "Living Building Challenge-Mission Zero" project in BlueLab at the University of Michigan through which I learned a lot, met very inspiring people and worked with awesome teammates.

I have many friends in Ann Arbor who made it possible to survive here away from my home: (alphabetically) Ashley Burson, Devki Desai, Jenahvive Morgan, Margarita Otero-Diaz, Patrick Sheridan, Rachel Weintraub, Sarang Supekar, Sherri Cook, Tara Clancy, Yuqiang Bi, and Yvette Khachadourian. I am also blessed with having found a small, but warm Turkish community in Ann Arbor. Aysu Berk, Erkan Aktakka, Gokce Gulsoy, Sumeyra-Emrehan Turali, Tugba-Omer Aydin, Yalcin Yilmaz, Yasemin-Eren-Hakan Durmaz: thank you so much for your support and being my extended family in the U.S.

No words would be enough to express my feelings to my parents and my sister Fatma, Erdal and Elif Ayral. I would not be who I am today without you. Thank you so much for valuing my ideals and supporting me even when I was about to give up on them and no matter how hard it was for you. I am so proud of being a part of you. And Fuat,

you are a very special person, full of patience and loyalty. Thank you so much for your nonstop encouragement throughout the past six years.

Table of Contents

List of Tables

List of Figures

List of Notations

a: volumetric air content

b: Campbell soil moisture characteristic parameter

C: aqueous phase concentration of the diffusing species

C_{eq}: equilibrium concentration in the aqueous phase

C_s: initial, uniform concentration at the surface of the cylinder

C_o: constant concentration at x = 0

C_1: the concentration in the plane at t = 0 assumed to be uniform

C_2: constant concentration at x = d

d: thickness of plane sheet

D_{aq}: diffusion coefficient in bulk water

D_{app}: diffusion coefficient observed under nonsteady-state conditions in a porous medium

D_c: diffusion coefficient in the straight pores

D_e: effective diffusion coefficient

$f_{interlayer}$: fraction of porosity in the interlayers

g: gravitational acceleration constant

G: geometric factor

h: depth of the DNAPL pool

J_D: diffusional flux

K_d : Distribution coefficient

K_F: Freundlich isotherm fitting parameters

m: experimental exponent in Archie's correlation

m_{sol}: molecular weight of the solvent

M_t: total amount of diffusing substance per unit area which has entered the domain during time t

M_∞: maximum amount of diffusing substance per unit area which has entered the domain

n: Freundlich isotherm fitting parameters

P_c: capillary pressure

r: radius

R: retardation factor

t: time

T: temperature

V': molar volume of the solute at its normal boiling temperature

W: volumetric water content

x: spatial coordinate

X: empirical association factor of the solvent in Wilke-Chang correlation

α: capacity factor

γ: interfacial tension between the DNAPL and water

δ: constrictivity of the interlayer space

ε: porosity of the porous medium

η: dynamic viscosity

θ: contact angle

ρ_b: bulk density of the porous medium

ρ_s: density of the solid

$\Delta\rho$: density difference between water and the DNAPL

u, v, ζ and β: soil dependent empirical parameters

List of Acronyms

AFB: Air Force Base

AOT: Aerosol OT

ATR: Attenuated Total Reflectance

CEC: Cation Exchange Capacity

CMC: Critical Micelle Concentration

CTAB: Cetyltrimethylammonium Bromide

$C_{12}E_6$: Hexaethylene Glycol Monododecyl Ether

DNAPL: Dense Non-Aqueous Phase Liquids

ECD: Electron Capture Detector

ELSD: Evaporative Light Scattering Detector

FTIR: Fourier transform infrared

GC: Gas Chromatography

HDTMA: Hexadecyltrimethylammonium

HPLC: High-Performance Liquid Chromatography

HTO: Tritiated Water

ID: Internal Diameter

ISA: Ionic Strength Adjuster

MCL: Maximum Contaminant Level

MS: Mass Spectroscopy

MSDS: Material Safety Data Sheet

ODTMA: Octadecyltrimethylammonium

PCE: Tetrachloroethylene

RCF: Relative Centrifugal Force

RCRA: Resource Conservation and Recovery Act

TCE: Trichloroethylene

XRD: X-Ray Diffraction

Abstract

Chlorinated solvents are often disposed of in such a manner that they form pools on subsurface clay layers. There they slowly dissolve and migrate into the clay layers, accumulating therein over time. Due to the low permeability of these layers, it is assumed that the migration occurs by diffusion. However, field evidence suggests that more solvent may be stored in such layers than can be accounted for through simple diffusion.

Since there are few reported measurements of the diffusion coefficient in clayey soils for contaminants of interest, measurements were made in silt and silt-clay mixtures. The diffusion coefficient for trichloroethylene in a silt-clay mixture was at least two to four fold smaller than predictions used in field studies. Calculations based on the measurements obtained in this research suggest that there is an even greater discrepancy between the amount of mass storage in low permeability layers and that which can be attributed to diffusion.

To account for this enhanced transport, it was postulated that direct contact between the waste and these layers altered the structure of the clay, and consequently the transport properties. Measurements using X-ray diffraction showed that contact with chlorinated field wastes decreased the basal spacing of water-saturated smectites from 19 Å to 15 Å, accompanied by cracks with apertures as large as 1 mm, within weeks. Calculations showed that even minimal cracking could easily account for the enhanced mass storage observed in the field.

To investigate the mechanism of basal spacing decrease, a set of screening experiments were performed, which identified a nonionic surfactant, an anionic surfactant, and a chlorinated solvent, as the minimum waste components necessary. Sorption measurements showed enhanced synergistic sorption of the surfactants in the presence of the chlorinated solvent, while Fourier transform infrared (FTIR) spectroscopy suggested a partial displacement of water from the interlayer space. Based on all the accumulated evidence, it was hypothesized that the nonionic surfactant sorbs in the interlayer space, displacing some of the interlayer water. The anionic surfactant interacts with the nonionic surfactant through their hydrophobic moieties and enhances the dehydration of the interlayer space via its anhydrous nature.

Chapter 1
Introduction

1.1 Motivation

In the United States, the percentage of people depending on groundwater for their potable water source is greater than 50%, with groundwater withdrawals increasing almost five fold between 1950 and 2000 (Zogorski et al., 2006). Because of the importance of groundwater as a water source, its protection is vital. The contamination of groundwater can occur from leakage from hazardous waste disposal areas, landfills, septic systems or underground storage tanks. The chlorinated ethenes trichloroethylene (TCE) and tetrachloroethylene (PCE) are used extensively as cleaning solvents in processes such as degreasing and dry cleaning because they dissolve oil, dirt, and stains effectively (Williams-Johnson et al., 1997). Their improper disposal has resulted in their introduction to the subsurface environment, resulting in the fact that these compounds are two of the most common organic contaminants found at Superfund sites (SERDP, 2006) and are also frequently found in domestic wells at concentrations near or above the maximum contaminant level (MCL) (Moran et al., 2007).

TCE and PCE are often referred to as dense non-aqueous phase liquids (DNAPLs) as their density is greater than that of water and they have a low solubility in water, resulting in the fact that they can persist as a separate organic liquid phase in the subsurface. Once released to an aquifer, DNAPLs travel vertically in the groundwater column under the force of gravity because their density is greater than that of water. The vertically-downward movement is slowed significantly by low permeability layers, with the result that the

DNAPLs form pools on top of these subsurface strata (Figure 1.1). These pools then slowly dissolve into the surrounding groundwater, resulting in the transport of the contaminant, as a solute, down gradient.

Due to the long-term contact between the DNAPLs and the low permeability layers and lenses, these geologic strata can accumulate a significant mass of contamination over time, essentially becoming contaminant storage areas. Once the original source is removed or isolated, these layers or lenses then rerelease contamination into the surrounding groundwater, in a process referred to as "back diffusion" (Chapman and Parker, 2005). Studies such as that by Parker et al. (2008) show that even a clay layer thinner than 0.2 m can result in groundwater concentrations above permissible levels for decades after the original source is isolated or removed. Thus, these low permeable lenses and layers may serve as long-term secondary contamination sources (Sale et al., 2008; Stroo et al., 2012).

The most critical consequence of back diffusion from low permeable layers is its role in time to site closure. Even a thin low permeability stratum can store and then release substantial amounts of contaminants (Parker et al., 2008). Additionally, back diffusion occurs at a slower rate compared to inward diffusion because of lower concentration gradients (Chapman and Parker, 2005; Kueper et al., 2014). Simulations suggest that the contaminant concentrations in groundwater might not be reduced below MCL even after decades of aquifer remediation (Ball et al., 1997; Chapman and Parker, 2005; Parker et al., 2008). As there is no technology that can effectively and efficiently remove the contamination stored in low permeability layers, sites contaminated with DNAPLs remain some of the most difficult to remediate (Stroo et al., 2012; Kueper et al., 2014).

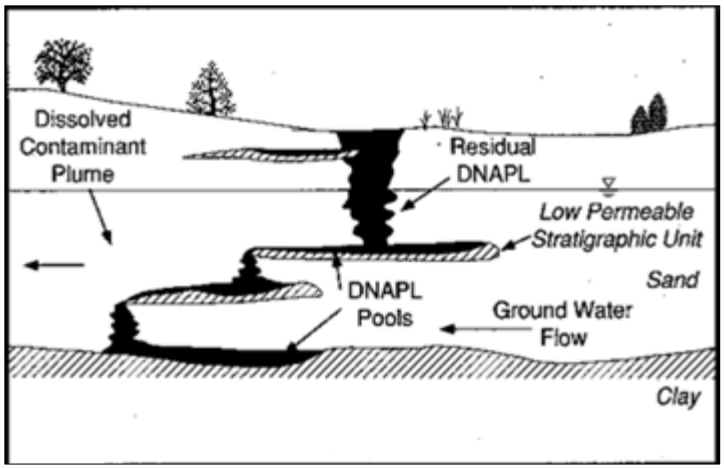

Figure 1.1 Transport of DNAPLs in the subsurface and the formation of DNAPL pools on low permeability lenses and layers (from Waterloo Centre for Groundwater Research, 1989).

The process of the accumulation of these chlorinated compounds in and their release from low permeability zones is thought to be dominated by diffusion (Mackay and Cherry, 1989; Ball et al., 1997; Wilson, 1997; Chapman and Parker, 2005; Parker et al., 2008). However, the Air Force Center for Engineering and the Environment (Sale et al., 2007) reported that the detected amounts of contaminants in some clay layers are higher than what can be attributed to diffusion only. Similarly, Ball et al. (1997) observed that the effective diffusion rates for organic compounds such as benzene, TCE, toluene, and ethylbenzene through an unweathered clay landfill liner in southwestern Ontario were 1.6 to 5 times higher than those based on estimated diffusion coefficients. An investigation of these higher than expected diffusion rates requires an understanding of the diffusive process in these geologic materials, but the literature contains surprisingly little information about the diffusion of organic compounds in saturated low permeability soils. These low permeability materials contain clay. Clay structures may undergo compression in the presence of solvents (Brown and Thomas, 1987; Li et al., 1996), which may result in the formation of macropores thus promoting greater diffusion into the clay layers. The

possibility of the modification of clay structure due to contact with organic solvents has been investigated relative to the hydraulic conductivity of landfill liners (Brown and Thomas, 1984; Anderson et al., 1985; Li et al., 1996), but its occurrence has never been addressed relative to its impact on diffusion. Given the paucity of information about the diffusion of organic compounds in clayey soils and the possibility of altered transport due to the interaction between and clay and chlorinated solvents, this dissertation seeks to examine the mechanism behind the larger than expected quantities of mass storage in low permeability lenses and layers.

1.2 Research Objectives

This dissertation aims to elucidate the mechanism behind larger than expected storage of chlorinated compounds such as TCE and PCE in low permeability geologic layers at hazardous waste sites. Specifically, the research aims to:

1.) Measure the diffusion coefficient of chlorinated organic compounds in saturated low permeable soils to ascertain the error in mass storage that may be produced by using estimates of the diffusion coefficient;

2.) Evaluate the changes that occur in clay structure in contact with chlorinated DNAPLs;

3.) Describe the mechanism by which DNAPLs may modify the structure of clay minerals; and

4.) Evaluate the impact of the structural changes on transport into low permeability soils.

Chapter 2
Background

TCE and PCE are chlorinated organic solvents that are used extensively for cleaning, especially for dry cleaning and metal surface degreasing. Their use generates waste that is comprised mainly of the chlorinated solvent, but that also contains impurities such as surfactants (ethoxylated alkylphenols, ethoxylated phosphate esters, ethoxylated alkanolamides, sodium alkylbenzene sulfonates, sulfosuccinates acid salts, amine alkylbenzene sulfonates, petroleum sulfonates, fatty acid esters of sorbitans) (Dabestani, 2001), cosolvents (hexylene glycol, 2-propanol, isopropyl alcohol, 2-butoxyethanol, diethylene glycol monobutylether, dipropylene glycol monomethylether and glycol ether) (Linn and Stupak, 2009), spot treatment chemicals, both organic (amyl acetate, acetone, ethanol, methanol, isopropyl alcohol) and inorganic (alkali lye, ammonia, potassium hydroxide or acidic acetic acid, hydrofluoric acid, oxalic acid) (Linn and Stupak, 2009), bactericides, fabric conditioners, anti-static agents (sulfonated polystyrene or sulfonated polystyrene/maleic anhydride polymers), residues removed from the fabric or surface (oil, dirt, cosmetics, etc.), and bleach (Linn and Stupak, 2009). As a result, waste DNAPLs often have very different characteristics than the pure solvent (Dwarakanath et al., 2002; Zheng et al., 2003; Hsu, 2005; Dou et al., 2008; Stroo and Ward, 2010). For example, interfacial tension is a property related to the ability of DNAPL to penetrate into water-saturated finer soil media (Zheng et al., 2003; Dou et al., 2008). The interfacial tension with water of pure TCE and PCE is reported as 34.5 dyn/cm and 47.5 dyn/cm, respectively

(Demond and Lindner, 1993). However, Parker et al. (2003) measured values of the interfacial tension of DNAPLs at sites in Connecticut and Ontario of 17.4 - 23.5 dyn/cm for TCE-based waste and 23.6 - 34.2 dyn/cm for PCE-based waste. Similarly, Dou et al. (2008) reported the interfacial tension of dry cleaning and degreasing DNAPL wastes as 10.4 dyn/cm and 8.6 - 14.6 dyn/cm, respectively. Still other studies show over an order of magnitude lower values for DNAPLs recovered from hazardous waste sites, with values of 2 - 3 dyn/cm (Hsu, 2005) and 1.2 - 2.3 dyn/cm (Dwarakanath et al., 2002) being reported.

Prior to the advent of the Resource Conservation and Recovery Act (RCRA, 1976), which mandated "cradle to grave" tracking of hazardous materials, solvents such as TCE and PCE were often disposed of directly to the land surface. Both TCE and PCE are denser than water and sparingly soluble in water so they may move as a separate organic liquid phase through the subsurface. Their vertically-downward movement is slowed by clayey lenses, or more continuous clayey layers known as aquitards, resulting in the formation of DNAPL pools. The DNAPL then slowly dissolves and moves horizontally down-gradient as a solute in the aquifer. However, the vertical advective rate of transport is minimal in the aquitards due to their low permeability. Thus, the DNAPL is thought to dissolve and penetrate into the aquitard by a diffusion-dominated process (Goodall and Quigley, 1977; Johnson et al., 1989).

As the DNAPL in the aquifer is depleted by dissolution or a remedial action, the concentration in the groundwater is expected to eventually fall below the MCL. However, field observations show that, often, the concentration does not decrease as anticipated, a phenomenon known as "plume tailing" (Chapman and Parker, 2005; Kueper et al., 2014). One explanation of these extended histories of concentrations above the MCL is that the

contamination located in the low permeable layers starts to be released back to the aquifer (Mackay and Cherry, 1989). The first field evidence of this was contributed by Ball et al. (1997) and Liu and Ball (2002) who sampled the aquitard at Dover Air Force Base and found high concentrations of PCE and TCE therein (Figure 2.1). They modeled the concentration profiles at the site and were able to match the concentrations in the aquifer by postulating the occurrence of diffusion into and out of the aquitard. Subsequently, studies at industrial sites in Connecticut (Parker et al., 2003) and Florida (Chapman and Parker, 2005) found that even though the DNAPL source was isolated, concentrations did not fall below regulatory limits. Figure 2.2 shows high concentrations of TCE in a low permeability layer at the industrial site in Florida that Chapman and Parker (2005) investigated, despite the low concentrations in the aquifer above it. Based on these studies, it is appears that the aquitards at these sites accumulated TCE and PCE over time, becoming storage units for these contaminants. After the sources were removed or isolated in the aquifer, these aquitards then served as secondary contamination sources (Sale et al., 2008; Stroo et al., 2012), releasing contamination back to the remediated aquifer.

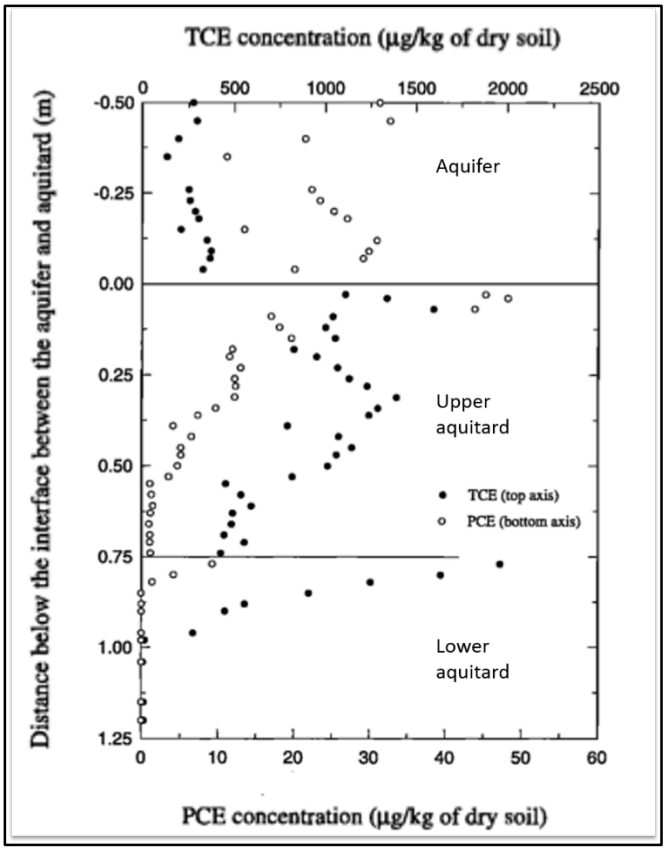

Figure 2.1 Concentration profiles showing an accumulations of TCE and PCE in the aquitards at Dover Air Force Base (Ball et al., 1997).

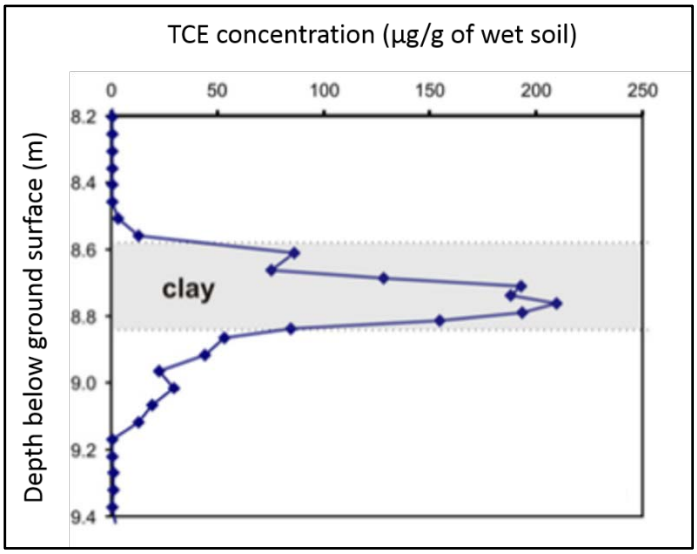

Figure 2.2 Concentration profile showing accumulation of TCE in the aquitard at an industrial site in Florida (Parker et al., 2008).

The transport mechanism of the contamination into and out of these aquitards is thought to be diffusion as the permeability, and consequently the advective rate of transport, is low. The low permeability of aquitards is attributable to the presence of fine-grained materials. Table 2.1 summarizes the grain-size distribution of several aquitards and illustrates the dominance of fine-grained materials (<50 µm). The majority of particles in the clay size fraction (< 2 µm) are made up of clay minerals. Clay minerals are layered silicates, consisting of silicon-oxygen tetrahedral sheets and aluminum-oxygen octahedral sheets stacked on top of one another. Clay minerals are divided into two groups based on the arrangement of these sheets. The first group, 1:1 minerals, has one tetrahedral silica sheet for each octahedral alumina sheet (Figure 2.3.a). This is also known as a TO structure. The second type of structural arrangement is where an octahedral alumina sheet is sandwiched between two tetrahedral silica sheets, known as a TOT structure (Figure 2.3.b).

Table 2.1 Grain size distributions of aquitards at sites contaminated with DNAPLs.

Site	Sand (>50 µm, %)	Silt (2-50 µm, %)	Clay (<2 µm, %)	Clay Mineral	Reference
Mexico City	1	25	74	-	Allen-King et al., 1995
Borden, Ontario	3	47	49	Muskovite, chlorite	Allen-King et al., 1995
Birsay, Saskatchewan	34	40	26	Muskovite, kaolinite	Allen-King et al., 1995
Dover AFB, Delaware	17-23	42-65	18-35	Kaolinite	Ball et al., 1997
Sarnia, Ontario	13	50	38	Muskovite, chlorite	Allen-King et al., 2002
Saskatoon, Saskatchewan	39	26	35		Timms and Hendry, 2007
Air Force Plant 44, Tuscan, Arizona	52.5	26.5	21	Illite, smectite	Matthieu et al. (2013)
Three Hangars Complex Tuscan, Arizona	0.1	36.5	63.5	Illite, smectite	Matthieu et al. (2013)

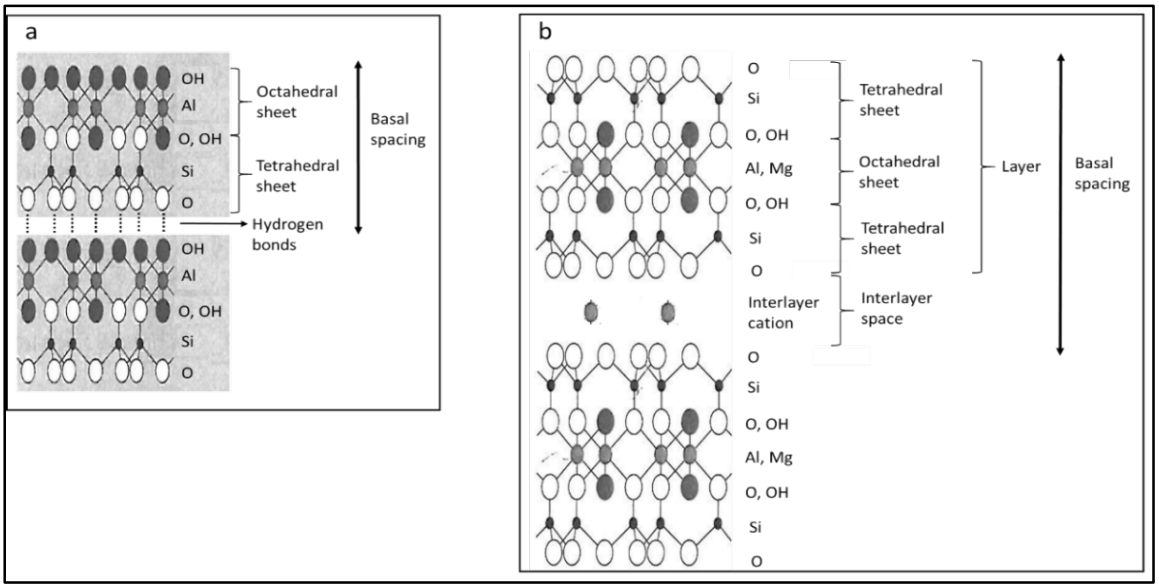

Figure 2.3 Structure of clay minerals a) 1:1 arrangement (TO structure) b) 2:1 arrangement (TOT structure). Diagrams adapted from Brady and Weil (1996).

The distance between two adjacent TO or TOT layers is known as the basal spacing or d-spacing which can expand or contract in some of the clay minerals. This ability to swell or shrink is closely related to the surface charge of clay minerals. Clay minerals can have a negative surface charge as a result of isomorphous substitution, i.e., the exchange of a higher valence silicon ion (Si^{4+}) for a lower valence alumina ion (Al^{3+}) in the octahedral sheet (Moore and Reynolds, 1997). For 1:1 clays, a neutral crystal structure is obtained at the end of the substitution (Velde, 1992). Additionally, no interlayer space exists and the layers are held together by strong hydrogen bonds, so 1:1 clays do not swell. On the other hand, a neutralization of charges is not observed in most of the 2:1 clays, so they have a net negative charge (Table 2.2). In order to balance this negative charge, cations reside in the interlayer space. Clays with a layer charge between 0.2 and 0.9 per unit formula are defined as low-layer charge clays and they retain these interlayer cations loosely. Depending on the hydration energy of the cation, water molecules are attracted and sorbed into the interlayer space, causing swelling of the structure. On the other hand,

in high-layer charge clays, potassium is held stably as the only cation due to the strong electrostatic interaction between the layers. Therefore, high-charge clays fail to swell, similar to 1:1 clays.

Table 2.2 Clay minerals classified according to layer arrangement, with the range for the layer charge. Data from Meunier and Fradin (2005).

Layer type	Group	Layer Charge (per unit layer)	Examples
1 : 1	Kaolin	0	Kaolinite, halloysite
1 : 1	Serpentine	0	Amesite, antigorite
2 : 1	Pyrophyllites	0	
2 : 1	Talc	0	
2 : 1	Smectites	-0.2 to -0.6	Montmorillonite, beidellite
2 : 1	Smectites	-0.2 to -0.6	Saponite, hectorite
2 : 1	Vermiculites	-0.6 to -0.9	
2 : 1	Vermiculites	-0.6 to -0.9	
2 : 1	Micas	1	Muskovite, paragonite
2 : 1	Micas	1	Phlogopite, biotite
2 : 1	Brittle micas	2	Margarite, clintonite
2 : 1	Illite, glauconite	2	
2 : 1	Chlorites	Variable	Donbassite
2 : 1	Chlorites	Variable	Diabantine, penninite
2 : 1	Di,trioctahedral chlorites	Variable	Cookeite, sudoite

The possibility of expansion of the lattice structure is a distinctive characteristic of 2:1 low-layer charge clay minerals, such as smectites. This expansion has been studied by measuring the basal spacing because it is the parameter that best represents the degree of separation between the layers. For smectites, the basal spacing at ambient temperature (20-25^{o}C) and air-dry conditions (at around 30% ambient relative humidity) is reported to be around 15 Å (Table 2.3) if the interlayer cation is a divalent cation such as calcium (Moore and Reynolds, 1997). On the other hand, a smaller basal spacing is observed in smectites saturated with a monovalent cation like sodium. Brindley and Brown (1980) reported that sodium montmorillonite has a basal spacing of 12.5 Å at ambient temperature and air-dry

conditions. The difference stems from the hydration energy of the cations. For monovalent cations, the hydration energy is smaller, meaning that monovalent cations attract polar water molecules weakly, resulting in only one layer of water molecules around the cations at air-dry conditions and ambient relative humidity. However, divalent cations have higher hydration energies and attract two layers of water molecules at air-dry condition, thus increasing the basal spacing. When smectite minerals are saturated with water, the basal spacing increases up to values of 19 Å. This interlayer spacing distance at saturation (100% relative humidity) agrees with the theoretical value calculated by assuming the presence of three layers of water around the interlayer cations (Brindley and Brown, 1980; Moore and Reynolds, 1997).

Table 2.3 Summary of reported basal spacings of smectite minerals, dry and wetted by water.

Basal spacing (Å) for dry smectite clays		
Sodium	**Calcium**	**Reference**
12.5	15.2 (32% humidity)	Brindley and Brown (1980)
12.8	15.2	Brindley and Brown (1980)
12.5	15.1	Brindley and Brown (1980)
-	15 (air-dry)	Moore and Reynolds (1997)
-	10 (dried at 300°C)	Moore and Reynolds (1997)
-	12.7 (20% humidity)	Chipera and Bish (2001)
10.1	-	Chipera and Bish (2001)
Basal spacing (Å) for wet smectite clays		
Sodium	**Calcium**	**Reference**
-	19.2	Barshad (1952)
-	19	Brindley et al. (1969)
indefinite[a]	19	Brindley and Brown (1980)
18.8	19	Brindley and Brown (1980)
19	18.7	Brindley and Brown (1980)
indefinite[a]	19.1	Brindley and Brown (1980)
18	-	Brown and Thomas (1987)
-	18.7	Li et al. (1996)

[a]An indefinite basal spacing was interpreted as disorder of the parallel layers or interlayer spacings (Mering, 1946), or irregular layer structure due to osmotic swelling (Brindley and Brown, 1980).

The flexibility of the clay lattice structure of smectites results in a larger basal spacing when wet and a smaller basal spacing when dry. It is well documented that hydration/dehydration cycles cause cracking in soils with clay minerals (e.g., Miller et al., 1998; Nahlawi and Kodikara, 2006; Rayhani et al., 2007). Desiccation cracks of up to 3 cm wide have been reported in natural soils (Bronswijk, 1988). Such cracking of the soil leads to large increases in hydraulic conductivity, with Omidi et al. (1996) reporting that the hydraulic conductivity of smectitic soils increased by two orders of magnitude with the first drying cycle, and another order of magnitude with the second drying cycle. Shrinkage during the first drying cycle causes irreversible changes in the clay structure (Yesiller et al., 2002), so that once the soil has undergone desiccation, the original low hydraulic conductivity is not restored by rewetting. Even in the absence of ongoing drying cycles, cracks may be present. Table 2.4 gives crack apertures and spacing for naturally-occurring cracks in clay-rich till. The data here provide evidence for cracks of up to 2 mm at depths at which aquitards occur (the depth of the aquitard at the industrial site in Florida examined by Parker et al. (2008) (Figure 2.2) is about 8.5 m). Furthermore, the contact of clayey materials with organic solvents may result in cracking. For example, Anderson and coworkers (1985) visually observed cracks and voids in their clay samples after permeation with solvents such as methanol, heptane and o-xylene. Similarly, Abdul et al. (1990) reported the formation of “distinct, large vertical cracks” following the permeation of clay with aromatic compounds. However, since the immiscible organic solvents cannot infiltrate through these low permeable water-saturated soils in a reasonable time frame, high hydraulic gradients (60-831) have been applied to the samples (Brown and Thomas, 1984; Anderson et al., 1985; Brown and Thomas, 1987; McCaulou and Huling, 1999). It

is unclear whether the cracking would have occurred under the conditions of considerably lower hydraulic gradients that are normally encountered in the field.

Table 2.4 Properties of naturally occurring cracks in subsurface clayey layers.

Depth (m)	Spacing (m)	Aperture (μm)	Soil type[1]	Clay mineral	Reference
<18	0.05-0.15	1-14	weathered/unweathered till	-	Day, 1977
<16	0.4	50	weathered till	-	Hendry et al., 1986
<12-18	<0.15	11	unweathered till	-	Keller et al., 1986
<4	0.04-1	26-32	weathered till	Muskovite, chlorite	D'Astous et al., 1989
40-50	1.2-5	140-210	unweathered till	-	Thompson, 1990
<20	1.5	30	unweathered lacustrine	-	Rudolph et al., 1991
<5	0.02-1.00	<43	weathered till	Muskovite, chlorite	McKay et al., 1993
<2.5	0.05-0.1	1-120	weathered till	-	Hinsby et al., 1996
<4-5	-	<1-5	weathered till	-	Sims et al., 1996

[1]The till soils were reported to include at least 25% clay except that in the study of Hinsby et al. (1996) where the clay content was 12%.

Cracks change the transport mechanism in porous media appreciably (Freeze and Cherry, 1979). For instance, Rayhani et al. (2007) reported that the hydraulic conductivity of soil specimens increased 12-34 times as a result of desiccation fractures in the samples. In the studies examining the impact on organic liquids on clay hydraulic conductivity, increases of two to three orders of magnitude (Anderson et al., 1985), three to four orders of magnitude (Li et al., 1996), and one to five orders of magnitude (Brown and Thomas, 1984) have been reported depending on the organic liquid, clay type and percent clay. However the vertical hydraulic gradients across many of these layers and lenses in the field are very low, significantly lower than the horizontal hydraulic gradients. Thus, even a two-order of magnitude increase in the vertical hydraulic conductivity may not increase the advective rate of transport into the clayey layers significantly.

Another possibility is that the DNAPL enters the cracks as a separate liquid. Based on the Young-Laplace equation, the height of a DNAPL pool that would be necessary to drive DNAPL into a cylindrical crack with an aperture 2r is given by:

$$P_c = \frac{2*\gamma*cos\theta}{r} = \Delta\rho * g * \mathrm{h} \qquad \text{(Equation 2.1)}$$

$$h = \frac{2*\gamma*cos\theta}{\Delta\rho*g*r} \qquad \text{(Equation 2.2)}$$

where P_c is the capillary pressure, γ is the interfacial tension between the DNAPL and water, θ is the contact angle, $\Delta\rho$ is the density difference between water and the DNAPL, g is the gravitational acceleration constant and h is the depth of the DNAPL pool.

Assuming a DNAPL density of 1.46 g/cm^3, an interfacial tension of 24 dyn/cm, and a contact angle of 0°, the DNAPL pool needs to have a height of 30 cm to enter fracture with an aperture size of 17 μm (O'Hara et al., 2000). As even lower interfacial tensions and greater contact angles are reported for field samples (Dwarakanath et al., 2002; Hsu, 2005; Dou et al., 2008), DNAPL waste can enter into such a crack even at smaller pool heights. Given that DNAPL pool heights around 1.2 -2.7 m were observed at the Hill Air Force Base Operation Unit 2 site in Utah (Oolman et al., 1995), it is possible that pure phase DNAPL might exist in the cracks of the low permeability layers and lenses, greatly increasing the mass storage in these geologic strata.

As diffusion is regarded as the dominant transport process into low permeable soils (Goodall and Quigley, 1977; Johnson et al., 1989), the mass storage of chlorinated organic solvents in aquitards at hazardous waste sites has been calculated based on rates of diffusion. However, calculated diffusion coefficients of organic compounds including TCE in a clay soil were found to be 1.6 to 5 times higher than estimated diffusion coefficients (Ball et al., 1997). Additionally, Sale et al. (2007) reported elevated mass

storage of organic contaminants in clay layers that diffusive fluxes failed to account for. Therefore, the reason for enhanced mass storage in aquitards needs to be investigated. Most of the calculations of enhanced mass storage are based on estimates of the diffusion coefficient. Since there are so few measurements of diffusion coefficients for chlorinated solvents in water-saturated clayey materials, it first needs to be determined whether the discrepancies in mass storage are attributable to errors in the diffusion coefficients used in the calculations. Furthermore, DNAPL pools resting on low permeable lenses result in direct contact between the waste and the aquitards in case of subsurface contamination with DNAPL waste. Since the previous studies citing cracking in contact with organic solvents used high head gradients, it is not known whether passive contact with chlorinated organic wastes can cause cracks to form. If cracks form, then there exists the possibility of greatly enhanced transport into these layers.

To address whether diffusion is the principal means of transport into low permeability layers, the research carried out for this dissertation is presented in the next three chapters. Chapter 3 addresses the measurement of diffusion coefficients of a chlorinated solvent, and a surfactant in low permeability materials. Chapter 4 investigates the structural changes structure of smectites as a result of contact with organic liquids and field wastes. Finally, Chapter 5 summarizes the experiments aimed at understanding the mechanism of structural changes.

Chapter 3
Diffusion of Solutes in Saturated Low Permeability Soil Materials

It has been assumed that diffusion is the mechanism governing the transport of compounds such as TCE and PCE into low permeable lenses in the subsurface (Goodall and Quigley, 1977; Johnson et al., 1989; Parker et al., 2004). These contaminants accumulate in these zones and then are released back to the aquifer, leading to concentrations above the MCL for decades. Despite of the importance of diffusion for the transport of chlorinated organic solutes in low permeable soils, few studies have actually measured the diffusion coefficient of organic solutes in saturated low permeability soils. One hypothesis for the higher than anticipated mass storage in low permeability strata is that the measured diffusion coefficients are in error. Given the criticality of this transport mechanism, this chapter reviews the fundamentals of diffusion in porous media, and literature measurements of the diffusion coefficient are summarized and discussed. Then, this chapter presents measurements of the rate of diffusion of a chlorinated organic compound and a surfactant, as both of these are important components of a DNAPL waste. Lastly, calculations are made using the measured diffusion coefficients to assess the quantity of contaminant that may accumulate in a low permeability soil due to diffusion. Parts of this chapter have been published as "Estimation of Diffusion Coefficients for Organic Solutes of Environmental Concern in Saturated Clay-Silt Mixtures" in *Clay and Clay Minerals: Geological Origin, Mechanical Properties and Industrial Application*s (L. Wesley, ed., Nova Science Publishers, Hauppauge, NY, 2014, pp. 45-66).

3.1 Background

3.1.1 Diffusion in Porous Media

Effective Diffusion Coefficient

Diffusion is defined as the transport arising from the Brownian motion of molecules due to their relative kinetic energy (Weber and Digiano, 1996). Diffusion is governed by Fick's first law, written here in one dimension for bulk water:

$$J_D = -D_{aq}\frac{dC}{dx} \qquad \text{(Equation 3.1)}$$

where J_D is the diffusional flux, D_{aq} is the diffusion coefficient in bulk water, C is the aqueous phase concentration of the diffusing species, and x is the spatial coordinate.

When considering diffusion in porous media, the cross-sectional area available for the movement of molecules is reduced due to the presence of a solid phase. If the pores can be modeled as straight capillary tubes, a continuity of flux between that measured external to the porous medium (Figure 3.1.A) and that in the porous medium (Figure 3.1.B) dictates the following relation (Weber and Digiano, 1996):

$$D_{aq}\frac{dC}{dx}\Big|_{surface} = \varepsilon D_c \frac{dC}{dx}\Big|_{within\ pore} \qquad \text{(Equation 3.2)}$$

where D_c is the diffusion coefficient in the straight pores, and ε is the porosity of the porous medium (volume of pores/total volume).

In addition to the reduced volume available for transport, the description of diffusion in a porous medium must account for the increase in the path length that the solute molecules must travel (Figure 3.1.C). Dullien (1992) compared two models of a porous medium, one with straight pores and one with tortuous pores. He defined tortuosity, τ, as the ratio of the path length travelled by the solute molecules in the tortuous pore system, L_e, to the linear path length, L, in the straight pore system:

$$\tau = \frac{L_e}{L} \qquad \text{(Equation 3.3)}$$

In order to correct for the increase in travel distance, the diffusion coefficient for the straight pore system, D_c, needs to be divided by the tortuosity, τ. Furthermore, if the number of pores is held constant in moving from the system in Figure 3.1.B to that in Figure 3.1.C, then the porosity increases by a factor of L_e/L. Thus, it is necessary to divide the porosity by this term in order to maintain the same porosity as in the straight pore system. As a result, the square of L_e/L appears in the diffusive flux equation for the tortuous pore system:

$$J_D = -D_{aq} * \frac{\varepsilon}{\frac{L_e}{L}} * \frac{dC}{dx * \frac{L_e}{L}} = -D_{aq} * \frac{\varepsilon}{\left(\frac{L_e}{L}\right)^2} * \frac{dC}{dx} \qquad \text{(Equation 3.4)}$$

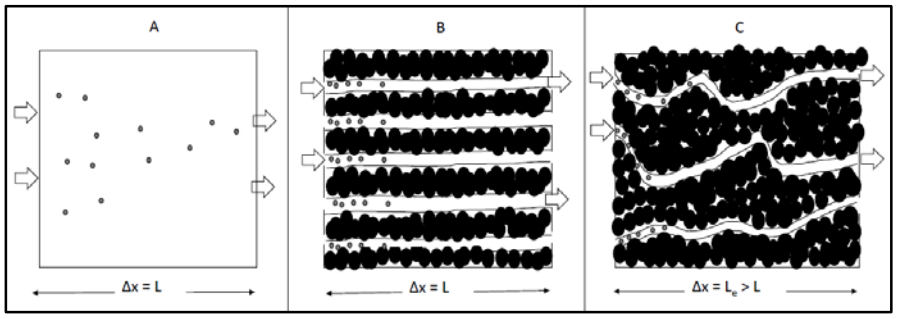

Figure 3.1 Diffusion in A) bulk aqueous phase, (B) porous medium with straight pores, (C) porous medium with tortuous pores.

The square of L_e/L is sometimes termed the tortuosity factor, denoted τ_f (Epstein, 1989):

$$\tau_f = \left(\frac{L_e}{L}\right)^2 \qquad \text{(Equation 3.5)}$$

Based on this definition, the effective diffusion coefficient, D_e, for diffusion in a porous medium is then (Grathwohl, 1998):

$$D_e = \frac{D_{aq}\,\varepsilon}{\tau_f} \qquad \text{(Equation 3.6)}$$

and the diffusive flux (per unit bulk area) in a porous medium is given by:

$$J_D = -D_e \frac{dC}{dx} \qquad \text{(Equation 3.7)}$$

The porosity in Equation 3.6 is the effective porosity, which may be less than the overall porosity of the porous medium if there are pores that do not contribute to the overall diffusive flux, such as dead-end pores (Lever et al., 1985). If the pores are sufficiently small that their diameter is on the same order as that of the diffusing solute, an additional factor, the constrictivity, δ, may be applied.

Table 3.1 provides a summary of definitions for the effective diffusion coefficient that appear in the literature. A summary was also recently included in Shackelford and Moore (2013). A number of the variations stem from the way in which tortuosity and the tortuosity factor are defined. Sometimes tortuosity is defined as the inverse of that in Equation 3.3 (Porter et al., 1960; Bear, 1972; Johnson et al., 1989; Shackelford et al., 1989; Oscarson et al., 1992), or:

$$\tau = \frac{L}{L_e} \qquad \text{(Equation 3.8)}$$

yielding a factor that is smaller than 1 rather than greater. To add to the confusion, the terms tortuosity and the tortuosity factor are sometimes used interchangeably, as Epstein (1989) pointed out. Some studies do not utilize the terminology of tortuosity or tortuosity factor, but talk instead of hindrance factors (Mott and Weber, 1991; Khandelwal et al., 1998). In addition, some studies describe effective diffusion coefficients that include porosity (Oscarson et al., 1992; Oscarson and Hume, 1994) whereas others exclude it (Johnson et al., 1989; Shackelford et al., 1989; Ball et al., 1997), as this is a parameter that can be determined independently (Shackelford, 1991).

Table 3.1 Various definitions of the effective diffusion coefficient.

D_e	Explanation	Studies
$D_{aq}\,\varepsilon\,\tau$	τ defined by Equation 3.8; ε included.	Oscarson et al. (1992); Oscarson and Hume (1994).
$\frac{D_{aq}\,\varepsilon}{\tau_f}$	τ_f defined by Equation 3.5; ε included.	Grathwohl (1998); Boving and Grathwohl (2001); García-Gutiérrez et al. (2006).
$\frac{D_{aq}}{\tau}$	τ defined by Equation 3.3; ε excluded.	Ball et al. (1997); Young and Ball (1998).
$D_{aq}\,\tau$	τ defined by Equation 3.8; ε excluded.	Johnson et al. (1989); Shackelford et al. (1989); Barone et al. (1992); Cho et al. (1993); Sawatsky et al. (1997); Roehl and Czurda (1998).

Apparent Diffusion Coefficient

Fick's first law for a porous medium given in Equation 3.7 defines the diffusive flux at steady-state. When Fick's first law is combined with a mass balance, Fick's second law is obtained (Crank, 1975), written here for diffusion in a porous medium:

$$\frac{\partial C}{\partial t} = D_{app}\frac{\partial^2 C}{\partial x^2} \qquad \text{(Equation 3.9)}$$

where D_{app} is the diffusion coefficient observed under nonsteady-state conditions in a porous medium. D_{app} is called by various names, including the apparent diffusion coefficient (Grathwohl, 1998), the reactive diffusion coefficient (Myrand et al., 1992) and the effective diffusion coefficient of a reactive solute (Shackelford et al., 1989). The primary difference between D_e and D_{app} is that D_{app} is also a function of sorption characteristics of the porous medium whereas D_e is considered to be independent of sorption, and dependent only on solute and the geometry of the porous medium.

Since sorption implies a partitioning of the solute to the solid phase, the transient diffusive flux is reduced, thus:

$$D_{app} = \frac{D_e}{R} \quad \text{(Equation 3.10)}$$

where R is the retardation factor. The form of R depends on how the sorption relationship is described. Two common forms are a linear relationship and the nonlinear Freundlich isotherm. If the sorption isotherm is linear, then:

$$R = 1 + \frac{K_d \rho_b}{\varepsilon} \quad \text{(Equation 3.11)}$$

where ρ_b is the bulk density of the porous medium and K_d is the distribution coefficient. In the case of the Freundlich isotherm, R will have the form of:

$$R = 1 + \frac{K_F C^{\frac{1}{n}-1} \rho_b}{\varepsilon} \quad \text{(Equation 3.12)}$$

where K_F and n are characteristic parameters of the isotherm, and C_{eq} is the equilibrium concentration in the aqueous phase.

Apparent diffusion coefficients have also been defined by the following relation:

$$D_{app} = \frac{D_e}{\frac{\alpha}{\varepsilon}} \quad \text{(Equation 3.13)}$$

where α is the capacity factor (Grathwohl, 1998), and $\alpha = \varepsilon R$. Since the calculation of D_e from measurements of D_{app} depends on how the isotherm relationship is described, it is critical to report the form of the sorption relationship when calculating values of D_e from measurements of D_a (Shackelford, 1991) and to recognize that the values may change depending on how the sorption relationship is modeled.

3.1.2 Measurement of the Effective Diffusion Coefficient

Measurements of diffusion coefficients of organic solutes in geologic media have been made using both steady-state and nonsteady methods. The main advantage of steady-state methods is that measured diffusion coefficients are theoretically independent of the retardation factor. But, in order to achieve a constant flux and evaluate the diffusion

coefficient from Fick's first law (Equation 3.7), the concentration gradient must be maintained constant, requiring the construction of an experimental system in which the influent and effluent concentrations can be maintained constant (Grathwohl, 1998). Furthermore, the time to establish this condition could be considerable especially for sorbing solutes or reactive soils, as García-Gutiérrez et al. (2006) determined a time to steady-state of five years for tracer diffusion through a bentonite (>90% smectites) plug with a thickness of two cm.

To avoid the long times that may be necessary to reach steady-state, transient state experiments may be preferred. Another advantage of transient methods is the concentration gradient across the domain does not need to be maintained at a constant value. However, obtaining the concentration profile along the column may require destructively slicing the column and extraction or the analysis of pore water concentrations (Mott and Weber, 1991; Parker, 1996; Donahue et al., 1999), both of which may be problematic in the case of volatile organic solutes. Furthermore, the diffusion coefficient obtained by analyzing the concentration profile is the apparent diffusion coefficient, so sorption characteristics of the soil have to be determined independently to obtain the effective diffusion coefficient (Shackelford, 1991).

Table 3.2 presents a summary of measurements of diffusion coefficients for organic solutes in saturated soils containing clay. As this table shows, the procedures vary considerably from one study to another. Nonsteady-state experiments are preferred. Most of these measurements involve the fitting of solutions to the nonsteady-state diffusion equation (Equation 3.9) to concentrations measured in the source and/or collection reservoirs (Barone et al., 1992; Myrand et al., 1992; Headley et al., 2001; Itakura et al.,

2003), or alternatively, solutions to the advection-dispersion equation (Young and Ball, 1998; Khandelwal et al., 1998).

The reported clay content ranges from 14-87 %, with the mineralogy primarily consisting of non-expansive clays. However, some studies did use appreciable percentages of expansive clays (e.g., Sawatsky et al., 1997; Donahue et al. 1999). These studies restricted the swelling by applying different pressures, but the impact of swelling on the diffusion coefficient was not discussed.

Table 3.2 Summary of literature measurements for diffusion coefficients for organic solutes in saturated clayey soils.

Solute[a]	Soil	Type of measurement	Porosity (ε)	D_e; D_{aq}; $[D_e/D_{aq}]$[b]	D_{app}[b]	R; K_d[b]	Notes	Reference
1,4-DCB 4-CP	Synthetic soil mixture containing silica sand, kaolinite, and bentonite; d = 0.3 - 0.5 cm	"Quasi steady state" (Source and collection reservoirs sampled at 10 and 20 days after an equilibration time of two weeks)	0.40 (2% bent.) 0.43 (4% bent.) 0.48 (4% bent.)	2.41; *8* [0.301] (DCB) 2.34; *8.9* [0.263] (CP) 2.65; *8* [0.331] (DCB) 2.59; *8.9* [0.291] (CP) 3.05; *8* [0.381] (DCB) 3.05; *8.9* [0.343] (CP)	-	-	Confining pressure is 4 psi. Study reported hindrance factor (H) which is defined as D_{aq}/D_e. D_e is calculated as D_{aq}/H.	Mott and Weber (1991)
Lindane	Synthetic soil mixture containing silica sand, kaolinite, and bentonite; d = 0.3 - 0.5 cm	Non-steady state (Columns sectioned at 8, 16, 32 days)	0.46 (avg. of 4% bentonite values is assumed)	2.4; 5.6 [0.429]	-	K_F = 3.84 x 10-4 ; 1/n = 1.17	Sorption of lindane is described by Freundlich isotherm, parameter values compatible with units of mg/g and mg/L; Confining pressure = 4 psi. Study reported D_e	Mott and Weber (1991)
Acetone 1,4-Dioxane Aniline Chloroform Toluene	Grey clay soil from Sarnia, Ontario, Canada (45% clay, mainly chlorite and illite); d = 1.6 cm	Non-steady state (Source and collection reservoirs sampled at two day interval over 14 days)	0.39 ρ_s = 2.73 g/cm^3 ρ_b = 1.68 g/cm^3	2.2; *12.8* [0.172] 1.6; *9.7* [0.165] 2.7; *10.5* [0.257] 4.3; *10* [0.430] 5.4; *8.5* [0.635]	1.20 0.90 0.40 0.16 0.05	1.8; [0.19] 1.7; [0.17] 6.6; [1.3] 26.8; [6.0] 113.0; [26]	Soil was placed in the cell saturated. Study reported D_e. εD_e is reported here in accordance with Eqn. 3.6. Batch tests indicated linear isotherms. R is calculated from reported values of ρ_b, K_d (fitted to data) and ε. using Eqn. 3.11 D_{app} is calculated as D_e/R.	Barone et al. (1992)

Table 3.2 Cont.

Solute[a]	Soil	Type of measurement	Porosity (ε)	D_e; D_{aq}; $[D_e/D_{aq}]^b$	$D_{app}{}^b$	R; $K_d{}^b$	Notes	Reference
Benzene TCE Toluene CB	Glaciolacustrine clay from Sarnia, Ontario, Canada (40% clay, mostly chlorite and illite); d = 10 cm	Non-steady state (Source reservoir is sampled over 23 days)	0.34 ρ_b= 1.77 g/cm^3	3.5; *10.9* [0.321] 3.5; *9.4* [0.372] 3.0; *8.5* [0.353] 2.9; *8.7* [0.333]	0.11 0.06 0.04 0.03	32.3 58.4 74 98.4	Soil used directly from soil sampler. Study reported D_{app} and R. Batch tests indicated linear isotherms. D_e is calculated from D_{app}*R (fitted to data)	Myrand et al. (1992)
DCM	Silty-clay glacial till from Sarnia, Ontario, Canada (38% clay, mainly chlorite and muscovite); d = 9 cm	Non steady state (Column sectioned at two weeks)	0.34 ρ_b= 1.71 g/cm^3	3.5; *11.5* [0.304]	2.94	1.19	Soil used directly from soil sampler. Study reported D_e and R. D_{app} was calculated from D_e /R.	Parker (1996)
1-Naphthol	Weathered shale (43 % clay, mainly montmorillo-nite) d = 0.4 cm	Steady state (Collection reservoir sampled over about 30 days; steady-state reached in 21 days)	(avg) ρ_b =1.26 g/cm^3 ρ_b =1.40 g/cm^3 ρ_b =1.57 g/cm^3	(avg) 0.17; *7.5* [0.023] 0.20; *7.5* [0.027] 0.067; *7.5* [0.009]	(avg) 0.0019 0.0017 0.00044	(avg) 94 [39] 116 [39] 151 [39]	Sample was partially saturated, compacted to a particular ρ_b, and then fully saturated. Batch tests indicated linear isotherms. Study reported D_e and R. Reported values of D_{es} were taken as D_e, based on Eqn. 3 from the paper.	Sawatsky et al. (1997)

Table 3.2 Cont.

Solute[a]	Soil	Type of measurement	Porosity (ε)	D_e; D_{aq}; [D_e/D_{aq}][b]	D_{app}[b]	R; K_d[b]	Notes	Reference
Naphthalene	Weathered shale (43 % clay, mainly montmorillonite) d = 0.4 cm		ρ_b =1.26 g/cm^3 (avg) ρ_b =1.40 g/cm^3 (avg) ρ_b =1.57 g/cm^3 (avg)	0.024; *7* [0.003]	0.00025	94 [27]	D_{app} is calculated from D_{es} and R.	Sawatsky et al. (1997)
Naphthalene	Montmorillonite (reference clay from Source Clay Repository, Columbia, MS, all cations were replaced with Ca^{2+} prior to use) d = 0.4 cm		ρ_b =1.49 g/cm^3 (avg)ρ_b =1.45 g/cm^3 (avg)	0.069; *7* [0.010]	0.069 (avg)	1 (avg)		
TCE	- Jurassic clay from Frommern, Germany (52% clay);	Steady state (Collection reservoir sampled up to 20 days)	(Avg) 0.45; ρ_s =2.67	(Avg) 0.89; *9.4* [0.095]	(Avg) 0.27	(Avg) 3.3	Material was pressed tightly into the diffusion cell ring. Study reported D_e,$D_{app.}$ and α. R is calculated from α/ε	Grathwohl (1998)
	- Jurassic clay from Lustnau, Germany (41% clay);		0.41; ρ_s =2.65	1.37; *9.4* [0.146]	0.24	5.8	$D_{app.}$ is calculated from D_e and R using Eqn. 3.11.	
	- Triassic clay from Haigerloch Germany, (55% clay);		0.46 ρ_s =2.7	0.72; *9.4* [0.077]	0.73	1.0		

Table 3.2 Cont.

Solute[a]	Soil	Type of measurement	Porosity (ε)	D_e; D_{aq}; $[D_e/D_{aq}]^b$	$D_{app}{}^b$	R; $K_d{}^b$	Notes	Reference
TCE	- Activated Na-bentonite from Friedland, Germany (87% clay);		0.55; ρ_s=2.65	0.21; *9.4* [0.022]	0.52	0.4		Grathwohl (1998)
	-Silt-clayey soil from Darmstadt, Germany (6% clay) d = 1 cm		0.34; ρ_s=2.65	1.25; *9.4* [0.133]	1.08	1.2		
TCE	Mixture of locally sourced soil (45% finer 75 micron) and 6% bentonite d = 11.8 cm (avg)	Non-steady state (Diffusion coefficient is determined by fitting the adv-dispersion equation to column exp'ts which last 25-49 days)	0.33 (avg)	1.27; *9.4* [0.135] (avg)	0.99	1.28; [0.051]	Soil was wet uniformly and placed into cell and saturated by increasing the pressure from 28 to 315 kPa. Study reported D_e/ε. D_e is calculated from D_e/ε and ε. R is calculated from K_d (fitted to data), ρ_b and ε using Eqn. 3.11.	Khandelwal et al. (1998)
Aniline				0.81; *10.5* [0.077] (avg)	0.62	1.25; [0.044]		
PCE	Silty clay loam from Dover AFB, DE (35% clay, clay minerals identified were kaolinite and chlorite) d = 25 cm Diffusion distance = 0.59 cm	Non-steady state (Diffusion coefficient determined by fitting dual domain model to breakthrough experiments lasting 11 to 112 days	0.43 ρ_b= 1.51 g/cm^3	1.8; *8.7* [0.207]	0.918	1.96	Material moistened at 20%, packed and then saturated for three weeks. Study reported D_e and R (fitted to data). D_{app} is calculated from D_e/R.	Young and Ball (1998)
1,2,4-TCB				2.0; *6.7* [0.299]	0.344	5.82		

Table 3.2 Cont.

Solute[a]	Soil	Type of measurement	Porosity (ε)	D_e; D_{aq}; $[D_e/D_{aq}]^b$	$D_{app}{}^b$	R; $K_d{}^b$	Notes	Reference
Benzene	Silty clay from Regina, Saskatchewan, Canada (70 % clay, mainly smectite) d = approx. 3 cm	Non-steady state (Source and collection reservoirs sampled over 36 days; column sectioned at end of exp'ts)	0.57 (avg) ρ_s=2.81 g/cm^3	1.8; *10.9* [0.165]	0.577	3.12 [1.0]	Soil was saturated and consolidated. Batch tests indicated linear isotherms. Study reported D_e. εD_e is reported here in accordance with Eqn. 3.6. R is calculated from K_d (fitted to data), ρ_b and ε using Eqn. 3.11. D_{app} is calculated from D_e/R.	Donahue et al. (1999)
Benzene Toluene 2-FT	Synthetic soil mixture (85% sand, 12% bentonite, 3% organophilic clay) d = approx. 3 cm	Non-steady state (The source reservoir was sampled daily for the first two weeks and then twice weekly up to 56 or 72 days)	0.34 ρ_b= 1.74 g/cm^3	1.6; *10.9* [0.144] 0.8; *8.5* [0.093] 1.1; *8.3* [0.133]	0.0076 0.0011 0.0015	206 [40] 717 [140] 717 [140]	Soil was compacted at a water content of 15% and vacuum-saturated under a pressure of 70 kPa for three days. Study reported D_e. D_e for toluene and 2-fluorotoluene are values in a three-component mixture. R is calculated from K_d (fitted to data), ρ_b and ε using Eqn. 3.11 D_{app} is calculated as εD_e /R.	Headley et al. (2001)

Table 3.2 Cont.

Solute[a]	Soil	Type of measurement	Porosity (ε)	D_e; D_{aq}; $[D_e/D_{aq}]$[b]	D_{app}[b]	R; K_d[b]	Notes	Reference
MEK TCE Toluene	Reconstituted clay (Londonderry clay from Sydney, New South Wales, Australia) (95% finer than 75 µm, mainly kaolinite and illite) d = 1.25 – 2.97 cm	Non-steady state (Source and collection reservoirs sampled over 15-27 day	Reconst. 0.41 (avg) ρ_b= 1.51 g/cm^3 (avg)	1.02; *9.4* [0.109] (MEK) 0.83; *9.4* [0.088] (TCE) 0.88; *8.5* [0.104] (Toluene)	1.02 0.53 0.57	1 [0] 1.5 [0.15] 1.5 [0.15]	Reconstituted sample mixed with distilled water at a moisture content of 40%, then placed in cell and compressed at 100 kPa to achieve field densities. Undisturbed samples used directly from corers. Study reported D_e.	Itakura et al. (2003)
	Undisturbed clay (50% finer than 75 µm, mainly kaolinite and illite) d = 1.25 cm		Undist. 0.36 (avg) ρ_b= 1.68 g/cm^3 (avg)	1.02; *9.4* [0.108] (MEK) 0.91; *9.4* [0.097] (TCE) 1.19; *8.5* [0.140] (Toluene)	0.70 0.54 0.61	1.46 [0.10] 1.69 [0.15] 1.92 [0.2]	εD_e is reported here in accordance with Eqn. 6. R is calculated from K_d (fitted to data), ρ_b and ε using Eqn. 3.11. D_{app} is calculated as εD_e /R.	

[a] CB: Chlorobenzene, CP: Chlorophenol, DCB:Dichlorobenzene, DCM: Dichloromethane, FT: Fluorotoluene, MEK: Methyl ethyl ketone, TCB:Trichlorobenzene, TCE: Trichloroethylene, PCE: Tetrachloroethylene.

[b] D_e : Effective diffusion coefficient ($cm^2/s *10^6$); D_{aq}: Aqueous diffusion coefficient ($cm^2/s *10^6$) (Montgomery, 2000); D_{app} : Apparent diffusion coefficient ($cm^2/s *10^6$); R: Retardation factor; K_d : Distribution coefficient (mL/g), K_F and n: Freundlich isotherm fitting parameters.

d: Thickness of sample; ρ_s : Soil particle density; ρ_b : Dry bulk density.

3.1.3 Estimation of Relative Diffusivity

Because of the paucity of experimental measurements, many studies examining the accumulation of organic solutes in clayey zones in the subsurface use estimated diffusion coefficients (e.g., Ball et al. 1997; Parker et al., 2004). Based on Equation 3.6, estimating the effective diffusion coefficient requires the diffusion coefficient in water, the tortuosity factor and the porosity available for diffusion. The diffusion coefficient in water of a number of organic contaminants can be obtained from the literature (Poling et al., 2001) or can be estimated using techniques such as that Wilke and Chang (1955) and Hayduk and Laudie (1974) (as in Montgomery, 2000), respectively.

$$D_{aq} = \frac{7.4*10^{-8}*T*\sqrt{Xm_{sol}}}{\eta*(V')^{0.6}} \quad \text{(Equation 3.14)}$$

$$D_{aq} = \frac{13.26*10^{-5}}{\eta^{1.14}*(V')^{0.589}} \quad \text{(Equation 3.15)}$$

where T is the temperature (K), X is an empirical association factor of the solvent (suggested as 2.6 for water, 1.9 for methanol, 1.5 for ethanol, and 1 for unassociated nonpolar solvents), m_{sol} is the molecular weight of the solvent (g/mol), η is the dynamic viscosity (cP), and V' is the molar volume of the solute at its normal boiling temperature (cm^2/mol).

The Wilke and Chang correlation was based on measurements for solutes with a molar volume less than 200 cm^3/mol and a molecular weight of 300 g/mol. On the other hand, Hayduk and Laudie (1974) extended the range of molar volumes up to 480 cm^3/mol and observed a smaller percent error (<1%) than the correlation of Wilke and Chang (around 7%) for these larger molecular-weight solutes. Another relation was developed by Hayduk and Minhas (1982) based on the same data of Hayduk and Laudie (1974) and Tyn and Calus (1975). This relation (Equation 3.16) is reported to result in a lower average

percent error (11%) than Wilke and Chang's (17% average percent error) when experimentally measured values and estimates are compared (Poling et al., 2001).

$$D_{aq} = 1.25 * 10^{-8} * [(V')^{-0.19} - 0.292] * T^{1.52} * \eta^{\varepsilon *} \qquad \text{(Equation 3.16)}$$

$$\varepsilon^* = \frac{9.5}{V'} - 1.12 \qquad \text{(Equation 3.17)}$$

Models Developed for Gas/Inorganic Species Diffusion in Unsaturated Sandy Soils

Although correlations have been developed to estimate the aqueous diffusion coefficient of solutes, independent assessments of the tortuosity factor can be challenging and, as a result, empirical methods have been developed to estimate the ratio of the effective diffusion coefficient to the aqueous diffusion coefficient, or the relative diffusivity, as a function of porosity:

$$\frac{D_e}{D_{aq}} = \frac{\varepsilon}{\tau_f} = f(\varepsilon) \qquad \text{(Equation 3.18)}$$

Since the presence of a pore structure influences more than just solute diffusion through a porous medium, the reduction in the diffusion coefficient can be estimated in analogy with other properties. The formation resistivity factor, F, is defined as the ratio of the electrical resistance of the porous medium saturated with an electrolyte (e.g., water), R_o, to the electrical resistance of the electrolyte itself, R_w. According to Archie (1942):

$$\frac{R_o}{R_w} = \varepsilon^{-m} \qquad \text{(Equation 3.19)}$$

where m is an experimental exponent whose value ranges from 1.3 to 2 for sand and sandstone (Archie, 1942). Similar to Equation 3.19, many of the models for estimating the relative diffusivity in soils give this ratio as a function of porosity only, and state that it is not affected by parameters like sorption characteristics of porous medium, type of solute (Petersen et al., 1994; Jin and Jury, 1996) or temperature (Grathwohl, 1998).

Table 3.3 summarizes methods proposed in the literature to estimate the relative diffusivity. Many of these methods are from the field of soil science where the concern is the diffusion of oxygen, for example, in the gas phase in unsaturated sandy soils. These models have been examined for their ability to predict diffusion in such systems; the Millington-Quirk (1960) and Penman (1940) models are reported to overestimate gas diffusion in unsaturated soils, whereas Millington-Quirk (1961) is said to provide underestimates (Sallam et al., 1984; Schaefer et al., 1995; Jin and Jury, 1996; Moldrup et al., 2000; Saripalli et al., 2002). On the other hand, the diffusion of inorganic solutes in unsaturated soil is overestimated by Millington-Quirk (1961). Thus, later methods added soil-dependent fitting parameters to obtain better estimates of the relative diffusivity (Troeh et al., 1982; Shimamura, 1992; Olesen et al., 1999; Moldrup et al., 2000). However, these methods have as a drawback the necessity of determining the values of empirical parameters, for which there are not adequate means to do so independently.

To adapt these models originally developed for gas or inorganics in unsaturated soils to the transport of organic solutes in saturated soils, the total pore volume can be assumed to be filled with water; thus a = θ = ε. Under these conditions, both Millington-Quirk models yield:

$$\frac{D_e}{D_{aq}} = \varepsilon^{4/3} \qquad \text{(Equation 3.20)}$$

The exponent has a value of 1.33, the same magnitude as the exponent given by Archie (1942) for sand. Thus, this method suggests an increase in effective diffusion coefficient with increasing porosity. However, it is observed that soils with a higher porosity such as clayey soils often have a lower diffusion coefficient (Grathwohl, 1998; Itakura et al., 2003). So, the possible overestimation of the effective diffusion coefficient

for clay-containing soils may be inherent to the correlation despite the report by some that this model gives the best agreement with experimental data (e.g., Mott and Weber, 1991; Jin and Jury, 1996).

Table 3.3 Methods for the determination of relative diffusivity, D_e/D_{aq}.

Method	Reference
Models developed for gas/inorganic species diffusion in unsaturated sandy soils	
0.66a	Penman (1940)
$a^{3/2}$	Marshall (1959)
$\frac{a^2}{\varepsilon^{2/3}}$	Millington and Quirk (1960)
$\frac{a^{10/3}}{\varepsilon^2}$	Millington and Quirk (1961)
$\left(\frac{a-u}{1-u}\right)^v$	Troeh et al. (1982)
$\frac{a^{3.1}}{\varepsilon^2}$	Sallam et al. (1984)
$\zeta(a-\beta)$	Shimamura (1992)
$0.45\left(\frac{W-0.022b}{\varepsilon-0.022b}\right)$	Olesen et al. (1999)
Suggested W/ε as a coefficient in Penman, Marshall and Millington-Quirk models	Moldrup et al. (2000)
Models developed for inorganic solute diffusion in clay soils	
$10^{(-0.8549\rho_b-0.0868)}$	Log-linear fit to data from Miyahara et al. (1991); Gutierrez et al. (2004); Sato et al. (1992) Equation 3.21
$\frac{\left(1-f_{interlayer}\right)+\delta_{interlayer}f_{interlayer}}{G}$	Bourg et al. (2006) Equations 3.22-3.25
Models obtained from experimental results or field studies of organic solute diffusion in clayey soils	
0.25	Johnson et al. (1989)
$-0.4619\varepsilon^2+0.926\varepsilon+0.0764$	Parker et al. (1994) Equation 3.26
0.7	Ball et al. (1997)
$10^{(2.2517\rho_b-4.3364)}$	Grathwohl (1998) Equation 3.27

ε: total porosity; a: volumetric air content; W: volumetric water content; u, v, ζ and β: soil dependent empirical parameters; b: Campbell soil moisture characteristic parameter (Campbell, 1974), ρ_b: dry bulk density, $f_{interlayer}$: fraction of porosity in the interlayer of clay minerals, δ: constrictivity of the interlayer space, G: geometric factor.

Models Developed for Inorganic Solute Diffusion in Clay Soils

The issues arising with methods that extrapolate from sandy soils for calculating relative diffusivities in clays have been recognized by, for example, Olesen et al. (1999) who pointed out that the goodness of the Millington-Quirk method appeared to depend on the clay content of the soil. As the clay content increased over 21%, the method gave increasingly large overestimates for solutes such as chloride in unsaturated soils. There may be a number of reasons for this increase. As Shackelford and Moore (2013) point out, the total porosity does not reflect the porosity available for diffusion for these soils because water in the micropores and some fraction of the macropores is not available for diffusion, so one needs to think in terms of "diffusion-accessible porosity." Clay soils that contain clay minerals such as smectites (montmorillonite and bentonite) include macropores or interparticle void volume, and micropores or interlayer void volume (Bourg et al., 2003). Additionally, diffusion-accessible porosity depends on the charge of the solute. Because of the negative charge of the clay surfaces, anions may be excluded from some pores due to the repulsive force between the negatively-charged solute and the surface. As a result, diffusion-accessible porosity for anions may be much smaller than the total porosity (García-Gutiérrez et al., 2004; Appelo and Wersin, 2007; Montavon et al., 2009; Shackelford and Moore, 2013). For example, the relative diffusivity of iodide in Opalinus clay was found to be 40% smaller than the relative diffusivity of a neutral inorganic species, tritiated water (HTO) (Appelo and Wersin, 2007). Additionally, García-Gutiérrez et al. (2004) measured the effective diffusion coefficient of HTO and chloride and determined that the diffusion coefficient of chloride was 6-100 times lower and the diffusion-accessible porosity was 3-20 times smaller for iodide, depending on the dry bulk density of the

bentonite soil. Furthermore, the diffusion of anions may be related to the ionic strength of the pore solution (Bourg et al., 2003; García-Gutiérrez et al., 2004; Van Loon et al., 2007; Shackelford and Moore, 2013).

Unlike anionic species, the accessible porosity was found to be equal to the total porosity for uncharged inorganic species such as HTO based on experiments with expanding clays with large fractions of interlayer water (García-Gutiérrez et al., 2004; Montavon et al., 2009). Although the diffusion-accessible porosity may be equal to the total porosity for uncharged species, the morphology of the pores differ. In their literature review, Yang and Aplin (2010) emphasized that the relation between porosity and permeability needs to be adjusted to include the clay content as a parameter since the pore radii are smaller at higher clay content. Thus, the relative diffusivity in clay soils may be smaller than in sandy soils due to the smaller pore size and resultant greater tortuosity, despite the larger porosities. In addition, expansive clays may have variable porosities depending on their degree of compaction. Thus, a number of studies have addressed the relationship between the bulk density of clay materials and the diffusivity of inorganic species. Figure 3.2 shows the data from three studies (Miyahara et al., 1991; Sato et al., 1992; García-Gutiérrez et al., 2004) for HTO diffusion in montmorillonite compacted to different bulk densities. These data show that relative diffusivity decreases with increasing bulk density and that the relationship between the relative diffusivity and the bulk density is log-linear. Fitting such a model to the combined data yields:

$$\log\left(\frac{D_e}{D_{aq}}\right) = -0.8549\rho_b - 0.0868 \qquad \text{(Equation 3.21)}$$

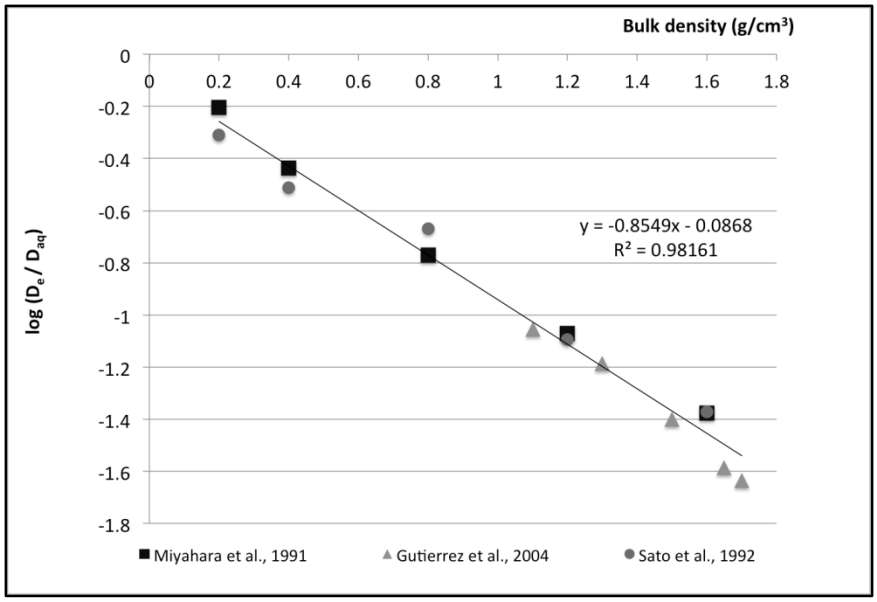

Figure 3.2 Relative diffusivities of tritiated water (HTO) in montmorillonite as a function of bulk density.

Alternatively, Bourg et al. (2006) described relative diffusivity as the weighted average of the relative diffusivities in macropores and interlayer space. Assuming that the constrictivity of macropores is equal to 1 and the geometric factor for the macropores and interlayer space is the same, they proposed that the relative diffusivity in montmorillonite can be given by:

$$\frac{D_e}{D_{aq}} = \frac{(1-f_{interlayer})+\delta_{interlayer} f_{interlayer}}{G} \qquad \text{(Equation 3.22)}$$

where G is a geometric factor that has a value of 4.0 for both macropores and interlayer space, δ, the constrictivity of the interlayer space, has a value of 0.3, and $f_{interlayer}$ is the fraction of porosity in the interlayers. The fraction of interlayer pores as a function of bulk density is given in Bourg et al. (2006) and plotted in Figure 3.3. Fitting piecewise linear models yields:

$$f_{interlayer} = 0.87\rho_b - 0.348, \text{ for } 1 < \rho_b < 1.3 \text{ g/cm}^3 \quad \text{(Equation 3.23)}$$

$$f_{interlayer} = 0.78 \text{ for } 1.3 < \rho_b < 1.5 \text{ g/cm}^3 \quad \text{(Equation 3.24)}$$

$$f_{interlayer} = 0.9\rho_b - 0.58 \text{ , for } 1.5 < \rho_b < 1.7 \text{ g/cm}^3 \quad \text{(Equation 3.25)}$$

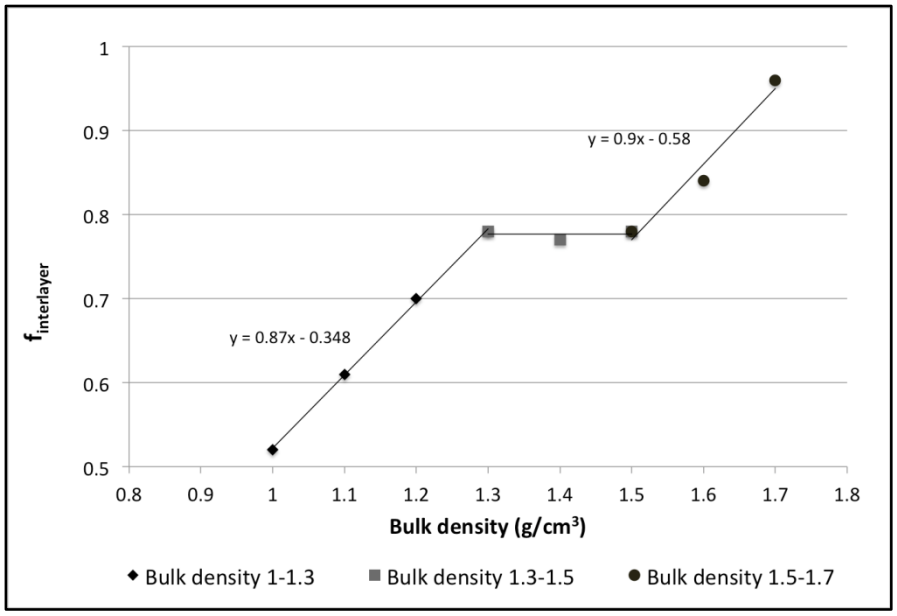

Figure 3.3 Fraction of interlayer pores as a function of bulk density given in Bourg et al. (2006).

Even though Eqns. 3.22 and 3.23 were specifically developed for montmorillonite, they were still developed for uncharged inorganic species and their performance have not been assessed for aqueous diffusion of uncharged organic species in clays.

Models Obtained from Studies of Organic Solute Diffusion in Clayey Soils

Field studies of back diffusion of organic solutes in clayey soils such as those by Ball et al. (1997) and Parker et al. (2004) did not use any of the methods discussed above for estimating relative diffusivity. Rather, Parker et al. (1994) provided a table of data relating porosity and relative diffusivity based on literature measurements, to support a value of 0.34 (Parker, 1996) and 0.4 (Parker et al., 2004) for clayey soils with porosities of

0.34 and 0.43, respectively. Based on these data, Figure 3.4 and Equation 3.26 were developed, to allow the calculation of relative diffusivities from a value of porosity. Ball et al. (1997) used a relative diffusivity of 0.7 for his modelling of concentration profile in the Dover Air Force Base (AFB) aquitard, where the porosity was 0.55, whereas Johnson et al. (1989) took 0.25 as the relative diffusivity in the aquitard in Sarnia, Ontario whose porosity was 0.37.

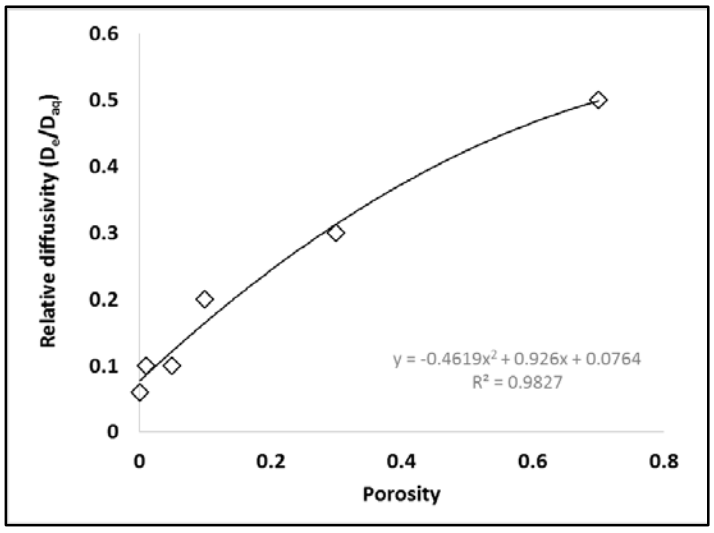

Figure 3.4 Correlation between porosity and relative diffusivity developed from data provided by Parker et al. (2004).

$$\frac{D_e}{D_{aq}} = -0.4619\varepsilon^2 + 0.926\varepsilon + 0.0764 \qquad \text{(Equation 3.26)}$$

Alternatively, a method to estimate the diffusion coefficient of organic solutes in clayey soils may be developed based on the experimental data reported by Grathwohl (1998) was used. Table 3.4 summarizes the measured effective diffusion coefficients of TCE in various low permeability soils, and Figure 3.5 illustrates the log-linear plot of those data for soils with clays content higher than 25%. Fitting a function to these data gives:

$$\log\left(\frac{D_e}{D_{aq}}\right) = 2.2517\rho_b - 4.3364 \qquad \text{(Equation 3.27)}$$

Table 3.4 Soil properties and measured diffusion coefficients from study of Grathwohl (1998).

Porosity	Silt (%)	Clay(%)	Dry Density (g/cm^3)	D_e (x 10^6 cm^2/sec)
0.33	92	6	1.78	1.25
0.41	48	41	1.56	1.37
0.45	47	52	1.46	0.88
0.46	44	55	1.43	0.72
0.55	12	87	1.19	0.21

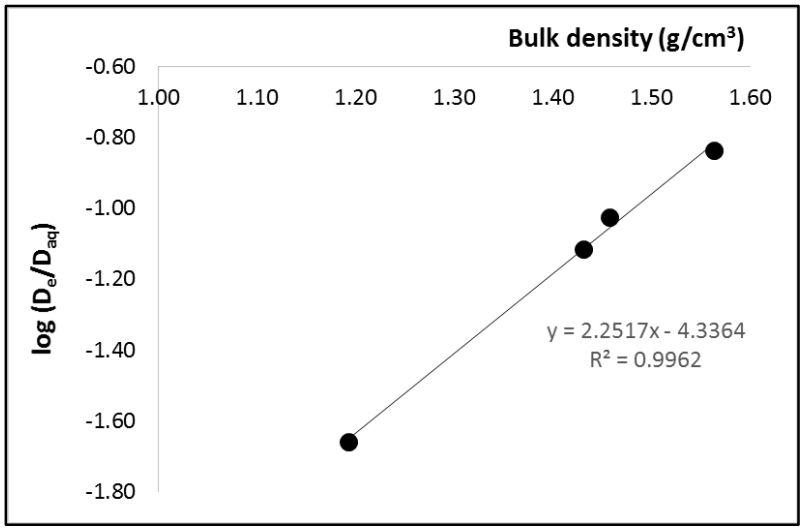

Figure 3.5 Relative diffusivity of TCE in clayey soils as a function of bulk density. Data from Grathwohl (1998).

Evaluation of Estimation Methods

In order to evaluate their performance for estimating the effective diffusion coefficient for organic solutes in saturated clayey soils, values of the relative diffusivity were calculated with all the models, correlations, and values listed in Table 3.3 and compared with values of relative diffusivity compiled in Table 3.2. The measurements of Sawatsky et al. (1997) were not used, due to the difference in orders of magnitude of their reported values relative to the others.

The average relative errors for the various methods are given in Table 3.5. Among the models developed for diffusion in the gas phase or aqueous diffusion of inorganic species in sandy soils, Penman's (1940) and Millington and Quirk's (1960, 1961) models produced the lowest overall percent relative error (110%) whereas Sallam's model's estimates are the worst (193% relative error). If the experimental results are divided into two categories, soils with a clay content lower than 25% versus those with a clay content higher than 25%, the relative errors change dramatically. For soils with a low clay content (<25%), the percent relative error range decreased to 28 – 92%, with Marshall's model having the least amount of error. However, for soils with a high clay content, the smallest percent relative error for these established models is 130% for the Penman model. These results support the observation of Olesen et al. (1999) that these estimation techniques generally give poor estimates for soil media containing more than 25% clay. So, these results confirmed the inapplicability of these models for diffusion in saturated clay soils.

The other models in Table 3.3 have not been assessed for their ability to estimate relative diffusivity of organic solutes in clayey soils. The results in Table 3.5 indicate that the relative diffusivity was overestimated on using methods based on field studies to determine the diffusion coefficient of organic solutes. In most cases, the relative average error is substantially higher when the clay content of the soil is above 25%. Among these field studies, the value used by Johnson et al. (1989) gave the best estimate (101% relative error). The correlation based on Grathwohl's data from experimental measurements of the diffusion coefficient of TCE (Equation 3.27) did not show a significant improvement over the value used by Johnson et al. (1989). On the other hand, the log-linear fit to literature data for HTO (Equation 3.21) and the linear fit to Bourg et al. (2006)'s method (Equations

3.22-3.25) provided improved estimates. The error for the log-linear relationship decreased to an underestimation of 63% in high clay content soils. Bourg et al.'s correlation (2006) yielded an underestimation of 16% of relative diffusivity in soils with a high clay content. Consequently, this method appears to be the most accurate for estimating effective diffusion coefficients for organic solutes in clayey soils.

Table 3.5 Percent average relative error for calculating relative diffusivity, D_e/D_{aq}.

Methods		Average Percent Relative Error			
		Overall	**Soil clay content <25% clay**	**Soil clay content >25% clay**	**On average**
Models developed for gas/inorganic species diffusion in unsaturated sandy soils	Penman (1940)	110	40	130	overestimate
	Marshall (1959)	109	28	132	overestimate
	Millington and Quirk (1960; 1961)	140	52	165	overestimate
	Sallam et al. (1984)	193	92	221	overestimate
Models used in field studies of organic diffusion in clayey soils	Johnson et al. (1989)	89	47	101	overestimate
	Parker et al. (1994)	189	212	106	overestimate
	Ball et al. (1997)	430	311	464	overestimate
Experimental fit to TCE diffusion data	Grathwohl (1998)	55	45	92	overestimate
Models developed for HTO diffusion in clay soils	Log-linear fit to data in Figure 3.2	67	82	63	underestimate
	Linear fits to Bourg et al. (2006)	23	48	16	underestimate

Diffusion is regarded as the mechanism responsible for transport into low permeable layers. The evaluation of estimation methods using available data in the literature suggests that these methods tend to overestimate the relative diffusivity, especially in soils with high clay content. Methods developed for tritiated water yield the best estimates for organic solutes, but these are not the methods that have been used in field

studies of back diffusion. The comparison of estimation methods and literature data suggests that the amount of mass accumulation in low permeability zones attributable to diffusion may be overestimated by these relationships. However, the review of the literature presented here also indicates that there are a limited number of measurements available for the effective diffusion coefficient of chlorinated organic solutes in saturated clayey soils, on which to base a hypothesis. Thus, measurements were made of the diffusion coefficient of both an organic solute and a surfactant, as components of DNAPL waste.

3.2. Materials and Methods

To avoid complications associated with sorption, measurements were made using a steady-state technique. Diffusion of a nonsorbing solute into low permeability layers can be modeled as diffusion in a plane sheet (Figure 3.6). At time t = 0, the porous medium is free of solute ($C_1 = 0$, $x > 0$, $t = 0$). The concentration at the boundary at the source is at a constant concentration for times greater than t = 0 ($C = C_o$, $x = 0$, $t > 0$) and the concentration at the other boundary of the plane sheet is zero to maximize the diffusive flux ($C = C_2 = 0$, $x = d$, $t > 0$). Under this constant concentration gradient, the amount of the nonsorbing substance (M) passed through the plane sheet per unit area (and left the plane sheet at x = d) can be determined to be (Crank, 1975, Grathwohl, 1998):

$$M = C_o d \left(\frac{D_e t}{d^2} - \frac{1}{6} - \frac{2}{\pi^2} \sum_{n=1}^{\infty} \frac{(-1)^n}{n^2} exp \left[\frac{-n^2 \pi^2 D_e t}{d^2} \right] \right) \qquad \text{(Equation 3.28)}$$

where d is the thickness of the plane sheet.

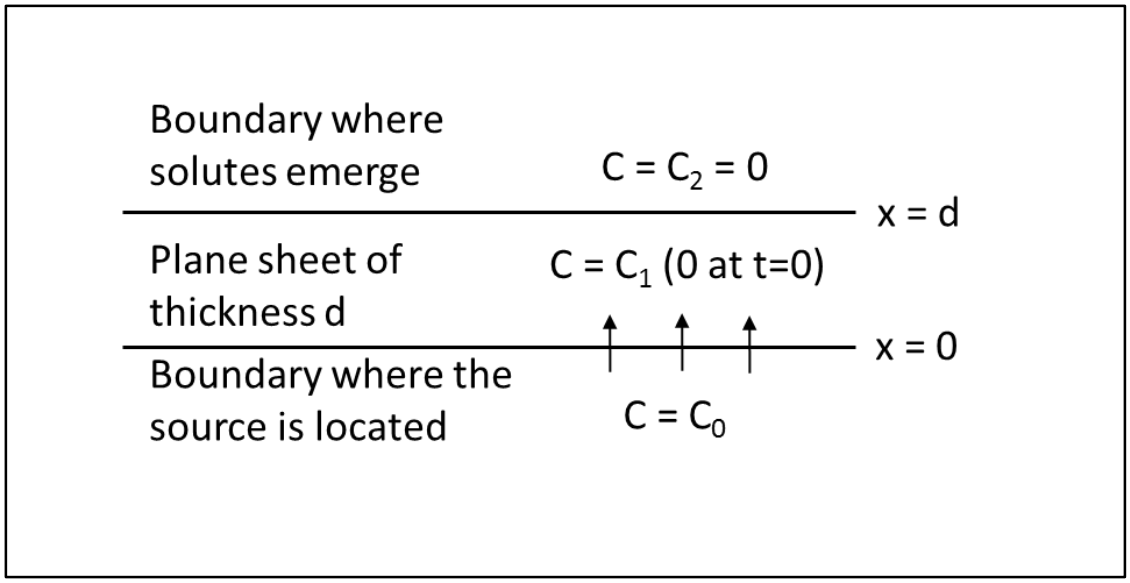

Figure 3.6 Diffusion through plane sheet with boundaries where the source is at the bottom of the plane.

As time approaches infinity, the exponential term in Equation 3.28 goes to zero. Relationship between the cumulative mass that has exited the plane sheet per unit area (M) and time (t) becomes linear:

$$M = \frac{C_o D_e}{d} t - \frac{C_o d}{6} \qquad \text{(Equation 3.29)}$$

Since steady-state is achieved as time approaches to infinity, the diffusion coefficient obtained from Equation 3.30 is the effective diffusion coefficient, i.e. the diffusion coefficient at steady-state. The y-intercept of Equation 3.29 ($C_o d/6$) is the "lag-time". If the solute sorb, then the "lag-time" is increased based on the degree of sorption. The derivative of M with respect to t, i.e., the slope, can be reorganized to yield the effective diffusion coefficient:

$$D_e = \frac{d}{C_o} \frac{dM}{dt} \qquad \text{(Equation 3.30)}$$

The time-lag method has been used to determine the diffusion coefficients in a variety of systems, including gas diffusion in polymers (Barrer and Rideal, 1939; Michaels

and Bixler, 1961) and ion diffusion in clay soils (Muurinen, 1990; Oscarson, 1994; Boving and Grathwohl, 2001; García-Gutiérrez et al., 2004). Grathwohl (1998) successfully applied this method to systems including chlorinated solutes in low permeability solids (Table 3.4). He measured the diffusion of TCE and diffusion of iodide in natural soil samples containing 6-87% clay (Grathwohl, 1998; Boving and Grathwohl, 2001). Steady-state was reached in less than three weeks with a sample thickness of 1 cm. The percent relative error was 22% for soil with a porosity of 0.45, and 38% for soil with a porosity of 0.46. Based on this experience, the time lag method was used in these experiments.

3.2.1 Preparation of Soil Samples and Solute Solutions for Diffusion Measurements

Silica silt and clay minerals were used to prepare two different types of soil matrices for diffusion measurements. The first soil matrix was silica silt with a median diameter of 10 μm, and a SiO_2 content of 99.7% (U.S. Silica, Frederick, MD). The second soil matrix was a combination of silica silt and pure Na-montmorillonite clay (SWy-2, cation exchange capacity (CEC) is 76.4 meq/100 g) (Clay Minerals Society, Chantilly, VA) to represent the presence of reactive clay minerals in aquitard materials. The determination of the relative quantities of each was based on the quantities cited as occurring in aquitards and the swelling potential. Ball et al. (1997) reported a clay fraction of 17-35% in the aquitard at Dover AFB, and Murray and Quirk (1982) stated that soil mixtures with a clay content of less than 30% can accommodate volume changes within the pores of the matrix. To satisfy both criteria, 25% was chosen as the clay fraction for the silt-clay mixtures. To minimize particle segregation issues during packing and saturation, a well-graded soil mixture was constructed. Figure 3.7 shows the particle size distribution obtained with a hydrometer

(151H) based on ASTM D422-63 (2007). The median grain diameter was 5 μm, a bit smaller than the median diameter of 9 μm reported for the aquitard at Dover AFB (Ball et al., 1997).

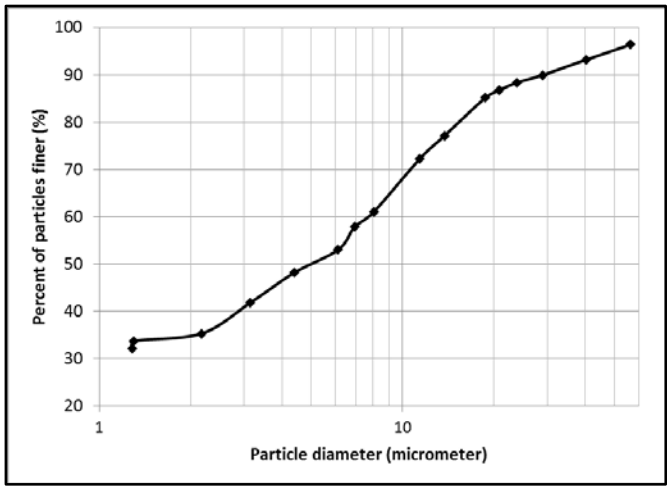

Figure 3.7 Particle size distribution of silt-clay mixture.

The soils were packed dry in a ring (I.D: 5 cm, height: 1 cm) in seven layers, compacting each layer with a 2.5 cm diameter wooden rod in accordance with a procedure outlined by Oliveira et al. (1996) for producing homogeneous packed columns. The dry bulk density was calculated from the mass of the soil packed in the ring (about 35 gram) and the volume of the ring (22.5 cm^2). The porosity of the samples was then determined from the bulk dry density assuming that the density of the solid was equal to 2.65 g/cm^3:

$$\rho_b = \rho_s(1 - \varepsilon) \qquad \text{(Equation 3.31)}$$

where ρ_b is dry bulk density (g/cm^3), ρ_s is the density of the solid (g/cm^3), and ε is porosity.

The ring then was placed on top of a reservoir which was filled with a 0.005 M $CaSO_4$ solution for saturation. A 0.005 M $CaSO_4$ solution was used rather than distilled water since distilled water is reported as problematic in hydraulic conductivity experiments

(ASTM D5856-95 [2007]). The silt in the ring stayed in contact with water for one day to allow for the spontaneous imbibition of water from the bottom of the sample to the top, and the change in the weight of the ring was recorded. Following that, the water level in the reservoir was raised to induce seepage through the porous medium to eliminate air that might be remaining. At the end of the second day, the weight of the ring was checked again, and since the change in mass was insignificant it was considered that saturation had been achieved.

Silt-clay mixtures were packed by the same method described for the silt, and then two different approaches were used for saturation. The first one entailed placing a stainless steel block with a weight about 0.5 kg on top of the soil to help ensure even swelling. After ten days of imbibition of water from the bottom, the change in the mass became negligible (change < 1%). Then, the portion of the soil that swelled beyond the top of the ring was scraped off, air dried and then weighed to calculate the porosity after expansion. Then, on the tenth day, the level of the reservoir was raised and maintained for another week to displace any remaining air. The second saturation method for silt-clay mixtures restricted the expansion of the soil even more. The soil mixture in the ring was placed on the reservoir filled with water while confined at the top, so the sample could not swell beyond the confines of the ring and the total volume could not change. As a result, the porosities of the samples treated in this manner were lower than the porosities of the silt-clay samples which were allowed to expand.

A summary of the experimental matrix is provided in Table 3.6. Diffusion experiments were conducted using four different solutes in these compacted and saturated soil samples. Iodide was used as an inorganic solute, produced by the dissolution of

potassium iodide (Sigma Aldrich, >99.5%) in Milli-Q water which was created by passing deionized, distilled water through a series of four Milli-Q filters and had a resistivity of 18.3 MΩ·cm. TCE (Fisher Scientific, >99.5%) was chosen as the chlorinated organic solute, as it is the solvent base of DNAPL waste from Hill AFB (Hsu, 2005) (Table 3.7). As surfactants are important components of DNAPL wastes and may diffuse at a different rate than chlorinated solutes based on their considerably larger molecular weights, measurements were also made of the rate of diffusion of an anionic surfactant, Aerosol OT (AOT) (anhydrous, Fisher Scientific) dissolved in Milli-Q water. AOT has a nonpolar tail and polar negatively-charged head, and a molecular weight of 456 g/mol; its structure is given in Figure 3.8. The experiments outlined above were conducted examining the diffusion in water. However, clayey soils in the subsurface are in contact with DNAPL waste for decades. Thus, they may become saturated with an organic solvent. To investigate the possible impact of this on the rate of diffusion, silt soil was packed into the stainless steel ring and saturated with pure PCE (Sigma Aldrich, HPLC grade, >99.9%). As the silt was air-dry initially, saturation with PCE appeared to occur within two days, as after that there was negligible mass change. However, in reality, it is unknown the extent to which the DNAPL waste permeates the clay. To imitate the situation in the field, a sample of the 75% silt and 25% clay mixture was compacted and saturated with water allowing it to freely expand, as explained previously. Then, this water-saturated soil mixture was put into a diffusion cell between a bottom and a top reservoir which were filled with PCE-based DNAPL waste (characteristics given in Table 3.7) and stayed there for 18 months. ^{13}C- labeled TCE (Cambridge Isotope Laboratory, MA, >98%) was used as the solute and added into the source reservoir instead of unlabeled TCE because the

PCE-based DNAPL waste contains TCE and it was necessary to be able to distinguish between the TCE already in the waste and the TCE diffusing through the soil.

Table 3.6 Experimental matrix for diffusion experiments.

Solute	Soil	Saturation liquid
Iodide	Silt	0.005 M $CaSO_4$
Iodide	Silt and clay-expanded	0.005 M $CaSO_4$
Iodide	Silt and clay-confined	0.005 M $CaSO_4$
TCE	Silt	0.005 M $CaSO_4$
TCE	Silt and clay-expanded	0.005 M $CaSO_4$
TCE	Silt and clay-confined	0.005 M $CaSO_4$
AOT	Silt	0.005 M $CaSO_4$
AOT	Silt and clay-expanded	0.005 M $CaSO_4$
AOT	Silt and clay-confined	0.005 M $CaSO_4$
^{13}C-labeled TCE	Silt	PCE
^{13}C-labeled TCE	Silt and clay-expanded	0.005 M $CaSO_4$*

*After saturation this sample was contacted with PCE-based DNAPL waste for 18 months.

Table 3.7 Characteristics of DNAPL wastes. Data from Hsu (2005).

	DNAPL Waste	
Source	Dry cleaner, Ann Arbor, MI	Operable Unit 2, Hill Air Force Base, UT
Dominant solvent	Tetrachloroethylene (PCE)	Trichloroethylene (TCE)
Density (g/mL)	1.60	1.30
Interfacial tension with water (dyn/cm)	2 to 3	2 to 3
Dominant surfactant content	nonionic (anionics << 1mM)	anionic
Contact angle at pH 7 (measured through water on quartz)	~30°	~30°

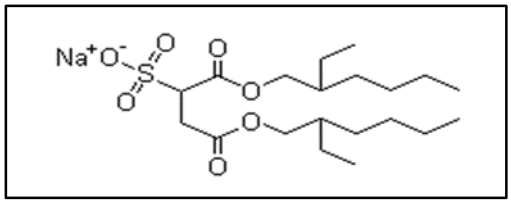

Figure 3.8 Structure of anionic surfactant, Aerosol OT (AOT).

3.2.2 Diffusion Experiments

3.2.2.a. Iodide Diffusion

The design of the diffusion cells was based on Grathwohl (1998) and Boving and Grathwohl (2001). The diffusion cell for iodide was constructed of Plexiglas and contained three main sections (Figure 3.9). The lower reservoir served as the source; the middle section consisted of a ring with a 5.0 cm internal diameter and height of 1 cm to hold the porous medium, and a top reservoir collected the material that had diffused through the porous medium. Each of the two reservoirs had a volume of about 350 cm^3. This volume was considered to be large enough to prevent significant concentration changes in the source and collection reservoirs during the experiments (Boving and Grathwohl, 2001), thus maintaining a constant concentration gradient across the sample. Stainless steel mesh (TWP, Berkeley, CA) with a pore size of 2 µm was placed on both the top and the bottom of the ring to keep the solid particles of the porous medium out of the reservoirs. The ring containing the compacted and saturated soil was placed on top of the source reservoir filled with a 0.1 M potassium iodide solution in Milli-Q water. The upper reservoir was filled with a 0.1 M potassium nitrate (Sigma Aldrich, >99%) solution, in order to provide a similar osmotic potential in both reservoirs and eliminate the transport of solutes due to osmotic potential gradients. The upper reservoir was placed on top of the ring and the three components of diffusion cell were assembled by tightening the screws. Every day, the

diffusion cell was rotated to minimize the development of concentration gradients within the reservoirs.

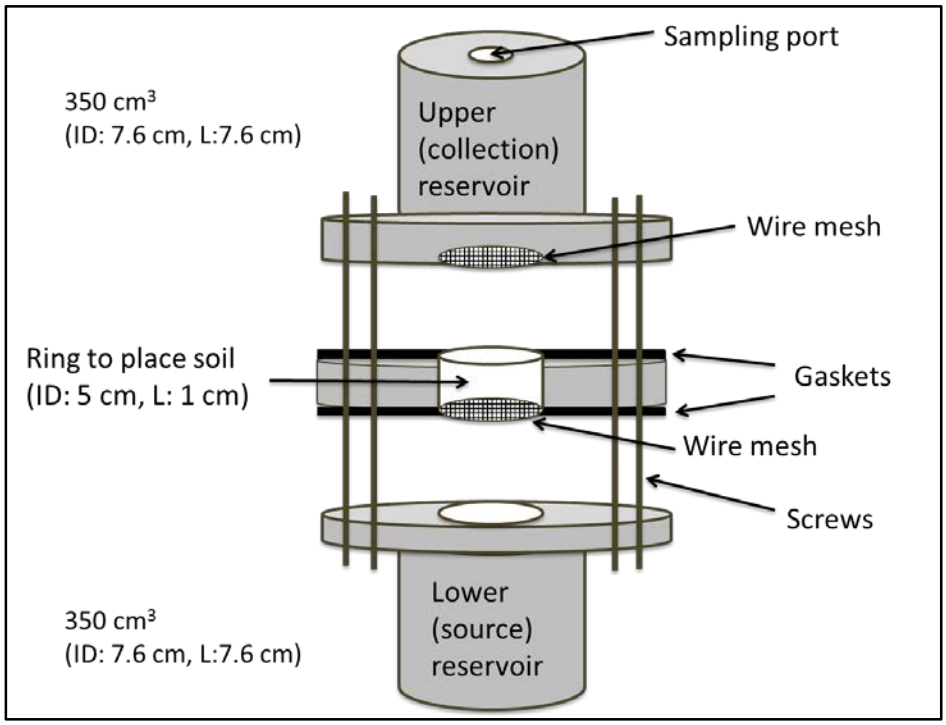

Figure 3.9 Plexiglas diffusion cell used for measuring iodide diffusion.

Iodide concentrations over time were measured in the upper collection reservoir using an iodide selective probe (Ionplus, Thermo Scientific, Beverly, MA) connected to an Orion Five Star Meter (Thermo Scientific, Beverly, MA). The probe was inserted into the collection reservoir and monitored until the reading was steady. After the reading, the probe was removed, rinsed and stored in a beaker containing Milli-Q water. The probe had the capability of measuring concentrations between 5.00×10^{-3} and 1.27×10^{5} mg/L. Calibration standards over the concentration range of 317 - 1269 mg/L were prepared from a 0.1 M iodide standard (Thermo Scientific, Beverly, MA) using Milli-Q water for dilution. The same standard solutions were used throughout the experiment, and the average error

for calibration standards was less than 5%. The iodide probe was recalibrated if the error between the standard solution and the reading exceeded 6%. The average calibration slope was -60 which fell within the recommended range of -54 to -60. After each run, the reference electrode filling solution was replenished. Although the instruction manual for the probe suggested using an iodide ionic strength adjuster (ISA) to avoid errors caused by the ionic strength of the sample, an ISA was not used because the ionic strength had already been adjusted using potassium nitrate.

The cumulative mass of iodide in the collection reservoir was calculated from the concentration measured by the iodide probe and the volume of the collection reservoir (350 cm^3). The cumulative mass was divided by the cross-sectional area of ring containing the soil and the cumulative mass per unit area was plotted as a function of time to obtain D_e using Equation 3.30.

3.2.2.b Chlorinated Organic Solute Diffusion

The experimental setup to measure TCE diffusion was also composed of three parts (Figure 3.10), but it was constructed out of stainless steel for greater chemical resistance. The volume of the source reservoir was approximately 10 mL, and it was filled with pure TCE. The aqueous concentration at the lower boundary was taken as the aqueous solubility of TCE. The collection reservoir (volume of 60 mL) was filled with 20 mL of water (e.g., 0.005 M $CaSO_4$ solution). Then, the ring where the compacted saturated soil resided was sandwiched in between the source and collection reservoirs. Air from a zero grade air tank (Metro Welding, Detroit, MI) was humidified with Milli-Q water, and the humidified air was bubbled through the collection reservoir at a flowrate of 0.5 mL/min (Figure 3.11). As

TCE is a volatile compound, it partitioned into the air, and the TCE that emerged from the collection reservoir was swept into a toluene (Sigma Aldrich, HPLC grade >99.9%) trap with a volume of 20 mL. The continuous removal of TCE maintained the concentration in the collection reservoir close to zero. The connections between the air tank, collection reservoir and the toluene trap were all Teflon tubing.

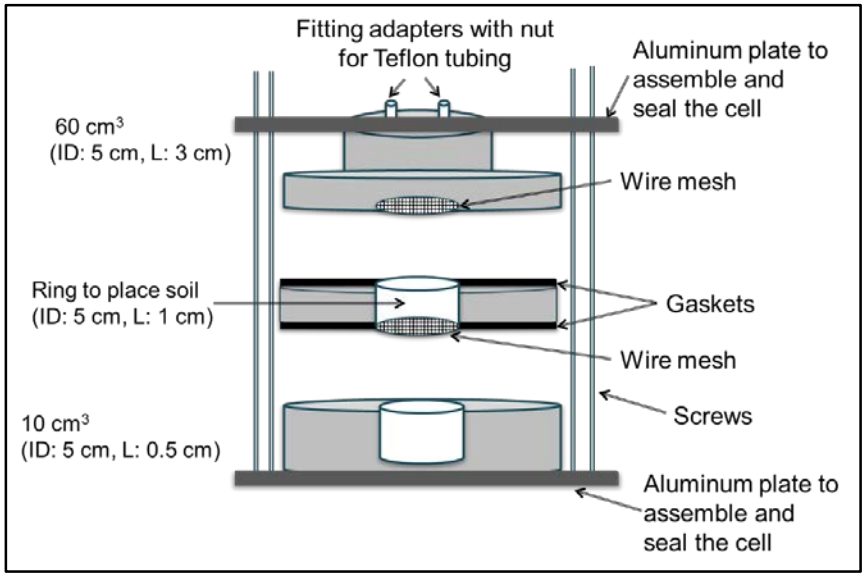

Figure 3.10 Stainless steel diffusion cell used to measure TCE diffusion.

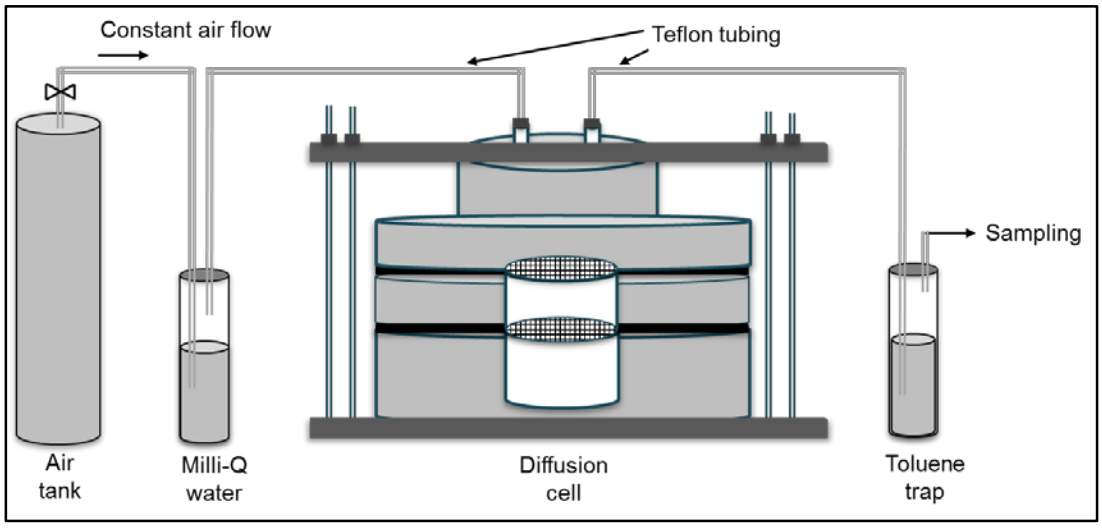

Figure 3.11 Experimental setup used to measure TCE diffusion (after Grathwohl, 1998).

0.5-mL samples were withdrawn from the toluene trap daily over a period of two to three weeks; they were stored in a refrigerator (around 4°C) until they were analyzed using a gas chromatograph (HP 5890) with an electron capture detector (ECD). A Phenomenex ZB-5 column (film thickness: 0.25 μm, ID: 0.25mm, L: 30m) was used as the stationary phase and N_2 was used as carrier gas. Other parameters for the analytic method are summarized in Table 3.8. To prepare the stock solution of TCE in toluene for preparation of calibration standards, toluene was added to a volumetric flask which was then weighed. Then, two or more drops of TCE were added using a 10 μL glass syringe. The flask with toluene and TCE was then reweighed and then the remaining volume was filled with toluene. The concentration of the stock solution was calculated from the weight and volume of the toluene. Concentrations in the range of 5 to 25 mg/L were used for calibration. In order to decrease the concentration of the stock solution to this range, samples were diluted from 10 to 100 times. As the volume in the toluene trap decreased over time due to sampling, the volume of toluene was adjusted by subtracting the volume of sample (0.5 mL) from the previous volume of toluene. The cumulative mass of TCE was calculated by multiplying the concentration and the modified volume.

Table 3.8 GC-ECD method parameters used for TCE detection.

Injection volume (μL)	1
Initial oven temperature (°C)	75
Temperature increase rate (°C/min)	15
Final oven temperature (°C)	135
Run time (min)	5
Detector temperature (°C)	275
Pressure (psi)	4

3.2.2.c Surfactant Diffusion

The Plexiglas set-up used for iodide diffusion was adapted for use in the experiments examining the diffusion of surfactants in the soils. The source reservoir was filled with a 10^{-3} M AOT solution made up in Milli-Q water. After that, the ring with the soil and the collection reservoir with Milli-Q water were placed on top. Two weeks after the start of the experiment, a 1-mL sample was taken from the collection reservoir every other day for four weeks so that the total volume of sample taken from the collection reservoir did not exceed 10% of the total volume of the reservoir (350 cm^3). The experiment was terminated when the concentration in the collection reservoir reached 10% of the concentration in the source reservoir.

The samples were analyzed using high-performance liquid chromatography (HPLC) (HP 1090, Hewlett-Packard, Palo Alto, CA). An Econosphere 3μm silica column (ID: 4.6 mm, L: 150 mm) was used as the stationary phase, and a mixture of Milli-Q water and acetonitrile (Fisher Scientific, HPLC grade, 99.9%) at a ratio of 20:80, respectively was used as the carrier liquid without a solvent program. An evaporative light scattering detector (ELSD) (Sedere SEDEX 75, Richard Scientific, Novato, CA) helped to quantify the concentration of AOT in the samples taken from the collection reservoir. Other parameters for the analytic method are given in Table 3.9. An analytic sequence was initialized once the baseline was stabilized. Calibration standards were made up over the range of 9 - 46 mg/L and run in the same sequence as the samples.

Table 3.9 HPLC-ELSD method parameters for AOT detection.

Injection volume (µL)	50
Flow rate (mL/min)	0.5
Run time (min)	5
Oven temperature (°C)	60
Detector temperature (°C)	40
Pressure (bar)	2.2
Gain	7

3.2.2.d Labeled Chlorinated Organic Solute Diffusion

The experimental setup used for measuring the diffusion rate of ^{13}C-labeled TCE was modified from the one used for diffusion of TCE in water-saturated soils (Figure 3.10). A fitting adapter and nut were added at the bottom of the source reservoir for the injection of the ^{13}C-labeled TCE (Figure 3.12). The collection reservoir was filled with 60 mL PCE or PCE-based DNAPL, and then 0.1 mL ^{13}C-labeled TCE was injected into the source reservoir to start the diffusion experiment. The initial concentration of ^{13}C-labeled TCE in PCE or PCE-based waste was 14600 mg/L and was considered to be high enough to remain constant over the duration of the experiment. The fitting adapters and nuts at the top of the collection reservoir were blocked with a piece of viton o-ring. One of the adapters was loosened to take a 0.1 mL sample from the collection reservoir and was retightened after sampling. Sampling continued until the concentration of ^{13}C-labeled TCE in the collection reservoir reached 10% of the concentration in the source reservoir.

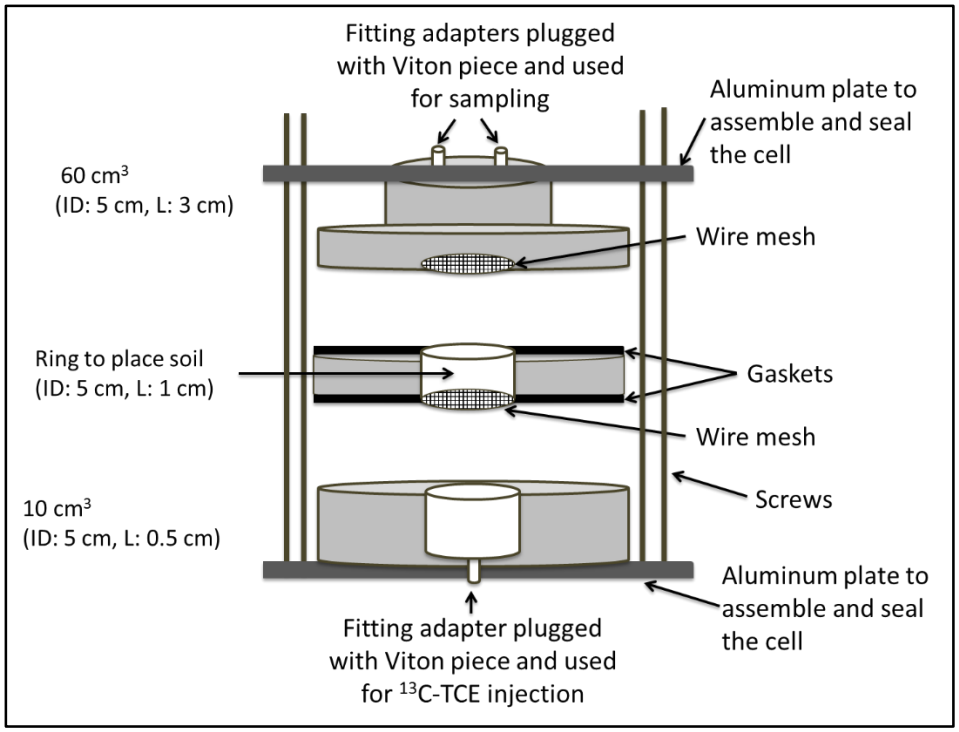

Figure 3.12 Stainless steel cell for measuring ^{13}C-labeled TCE diffusion, adapted from that shown in Figure 3.10.

The concentration of ^{13}C-labeled TCE was measured using a gas chromatograph (HP 5890) with a HP 624 column (thickness: 1.4µm, ID: 0.25 mm, L:35 m) and H_2 as the carrier gas. Other parameters for the analytic method are listed in Table 3.10. A three-minute solvent delay and a decrease in the voltage from 1694 down to 1247 mAV at the sixth minute were used to avoid damaging the detector in the case of liquid injection. A mass selective detector (HP 5972) was chosen to differentiate the TCE and ^{13}C-labeled TCE, based on a shift of the base peaks. The most abundant mass-to-charge ratios (m/z) of TCE were at 130, 132, and 134 whereas these values shifted to 131, 133, and 135 for ^{13}C-labeled TCE because of the increase in molecular weight of 1 g/mol. Ions at m/z values of 131, 133, and 135 were extracted and used for analysis of the concentration of ^{13}C-labeled TCE. A stock solution was prepared by adding 5 µL of ^{13}C-labeled TCE into 1 mL

of PCE. Then, calibration standards were prepared over the range of 146 – 1168 mg/L by diluting this stock solution with PCE.

Table 3.10 GC-MS method parameters for ^{13}C-labeled TCE detection.

Injection volume (µL)	1
Initial oven temperature (°C)	45
Temperature increase rate (°C/min)	35
Final oven temperature (°C)	145
Run time (min)	7.9
Detector temperature (°C)	245
Pressure (psi)	12

3.3. Results and Discussions

3.3.1. Iodide Diffusion

The main goal of the iodide experiments was to examine the applicability of estimation methods for clayey soils and to serve as a comparison for the measurements of diffusion of TCE. Figure 3.13 a, b, and c show plots of the cumulative mass of iodide that diffused through the silt, expanded silt-clay mixture and confined silt-clay mixture, respectively as a function of time. Table 3.11 summarizes the average mass flux, i.e. cumulative mass change per unit area over time, with the corresponding effective diffusion coefficients. The average effective diffusion coefficient of iodide was determined to be $2.00 \times 10^{-6} \pm 6.04 \times 10^{-8}$ cm^2/sec for silt, and $1.91 \times 10^{-6} \pm 5.39 \times 10^{-8}$ cm^2/sec for the silt-clay mixture that was allowed to expand during saturation (Table 3.12). The relative standard deviation was smaller than 5%, indicating reproducible results. These results are not significantly different (p-value > 0.15 at 95% confidence level) which suggests that the presence of 25% clay in and of itself did not reduce the diffusion rate of iodide significantly. However, in the case of the silt-clay mixture that was not allowed to expand

freely, the effective diffusion coefficient of iodide decreased significantly (p-value < 0.15) to 1.02 x 10^{-6} cm^2/sec. Since the silt and confined silt-clay mixture had the same porosity of 0.44, it is apparent that clay content affected the diffusion rate substantially. Thus, estimating the diffusion coefficient based on the porosity would fail to predict the difference. Furthermore, the silt-clay mixtures have the same clay content, yet the diffusion coefficient was reduced in the confined sample, due to the lower porosity of the confined sample ($\varepsilon = 0.43$) compared to the porosity of the expanded mixture ($\varepsilon = 0.66$). Therefore, neither clay percentage nor porosity alone is sufficient to describe the diffusive characteristics of a clayey soil.

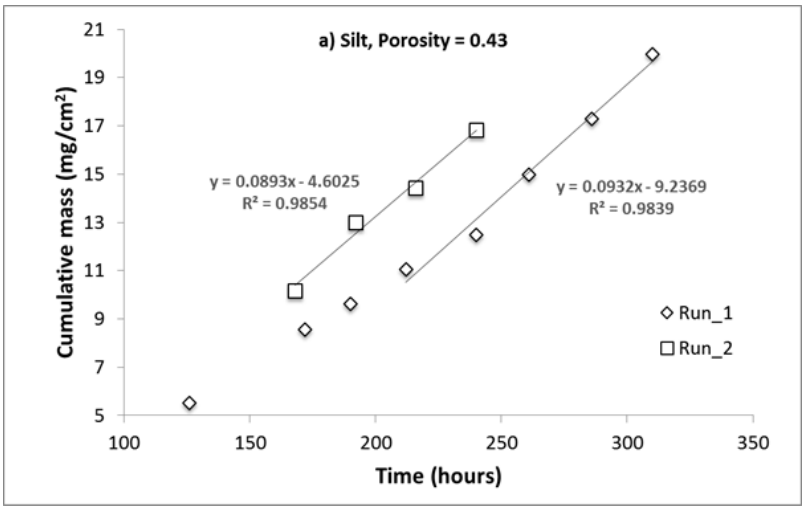

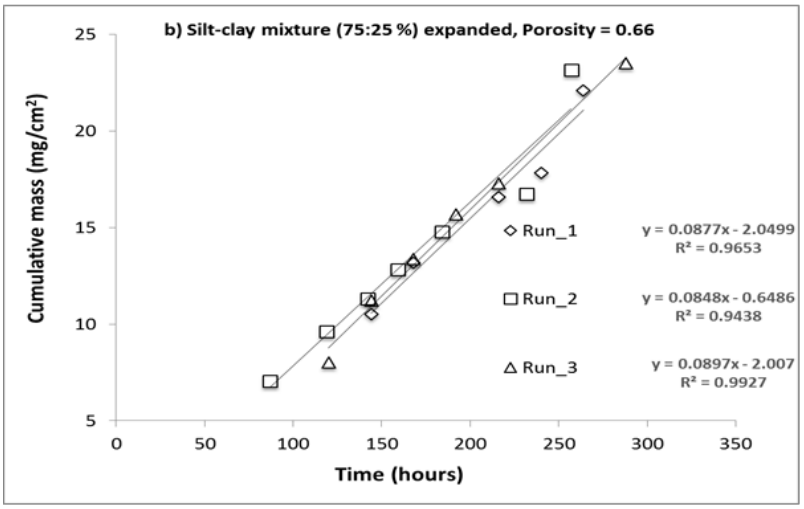

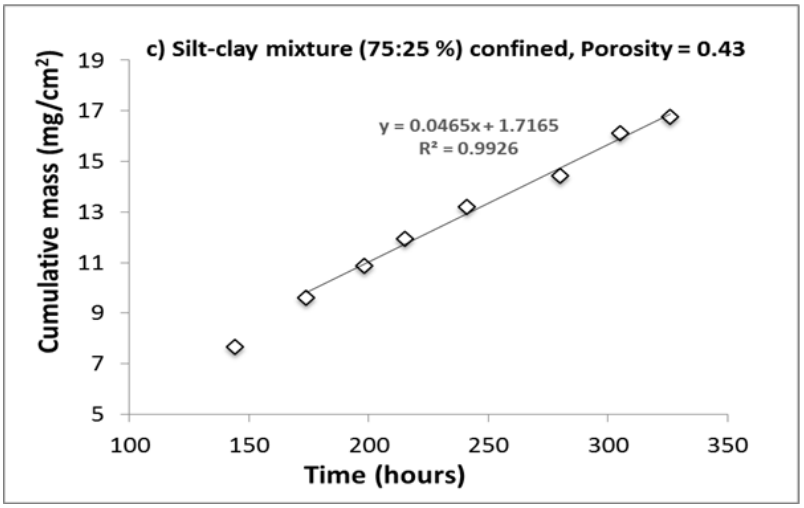

Figure 3.13 Cumulative mass per unit area vs time for iodide diffusion through a) silt, b) expanded silt-clay mixture, c) confined silt-clay mixture.

Table 3.11 Summary of slopes obtained from experimental data and calculated effective diffusion coefficients for iodide.

Porous medium	Porosity	Best fit mass flux (dM/dt) (mg/cm^2·hour)	D_e (x 10^6 cm^2/sec)
Silt	0.44	0.0932	2.04
Silt	0.42	0.0893	1.95
Silt and clay mixture, expanded	0.69	0.0877	1.92
Silt and clay mixture, expanded	0.64	0.0848	1.86
Silt and clay mixture, expanded	0.65	0.0897	1.96
Silt and clay mixture, confined	0.43	0.0465	1.02

D_e calculated using Equation 3.30, assuming that C_o = 12690 mg/L (0.1 M KI) and d = 1 cm.

Table 3.12 Average effective diffusion coefficients for iodide in different soils.

Porous medium	Average porosity	Average D_e (x 10^6 cm^2/sec)	Standard deviation (x 10^8 cm^2/sec)	Relative standard deviation (%)	Average relative diffusivity (D_e/D_{aq})
Silt	0.43	2.00	6.04	3.0	0.12
Silt and clay mixture, expanded	0.66	1.91	5.39	2.8	0.12
Silt and clay mixture, confined	0.43	1.02	NA	NA	0.06

Relative standard deviation = standard deviation/average, D_{aq} =18.6 x 10^{-6} cm^2/sec (Robinson and Stokes [1955]), NA: not applicable since single experimental value

Effective diffusion coefficients can be estimated by using the relations summarized in Table 3.3 (Table 3.13). The methods developed for unsaturated sandy soils (Penman, 1940; Marshall, 1959; Millington and Quirk, 1960; 1961; Sallam et al., 1984) have been reported to overestimate the relative diffusivity in clayey soils and the same behavior was observed in the case of the measurements here, with a relative error of > 350% between the measured and estimated values. Equations 3.21 and 3.22, which were suggested as providing more accurate estimates for clayey soils, performed better in estimating the relative diffusivity of iodide. The log-linear fit to the literature results for tritiated water estimated the relative diffusivity of iodide both in expanded and confined in silt-clay

mixtures with the smallest relative error (18% overestimation and 33% underestimation, respectively). Since the general tendency of the methods is to overestimate the diffusion coefficients, it could not be evaluated whether the fact that the measured diffusion coefficients are lower than the estimated values is due to anion exclusion.

Table 3.13 Comparison of relative diffusivities for iodide measured in this study and estimated by methods summarized in Table 3.3.

Models	Average percent relative error (%)		
	Silt	Silt-clay expanded	Silt-clay confined
Penman (1940)	474 (0.66)	461 (0.66)	958 (0.66)
Marshall (1959)	145 (0.28)	355 (0.54)	352 (0.28)
Millington and Quirk (1960, 1961)	182 (0.32)	388 (0.57)	420 (0.32)
Sallam (1984)	243 (0.40)	438 (0.63)	534 (0.40)
Johnson et al. (1989)	117 (0.25)	112 (0.25)	301 (0.25)
Parker et al. (1994) (Equation 3.26)	238 (0.39)	313 (0.49)	524 (0.39)
Ball et al. (1997)	508 (0.70)	495 (0.70)	1022 (0.70)
Grathwohl (1998) (Equation 3.27)	1 (0.12)	96* (0.005)	1 (0.12)
Log-linear fit to data (Equation 3.21)	64* (0.04)	18 (0.14)	33* (0.04)
Bourg et al. (2006) (Equation 3.22)	1* (0.11)	48 (0.17)	82 (0.11)

*Underestimation.
Numbers in parentheses are relative diffusivity estimated by the method.

3.3.2. TCE Diffusion

A goal of the diffusion measurements of a chlorinated organic solvent was to ascertain whether the few measurements in the literature were reasonable. Additionally, the iodide diffusion experiments elucidated the impact of porosity and clay content, showing that an estimate based on porosity was insufficient to predict relative diffusivity in soil mixtures containing clay. So, another goal of the organic diffusion experiments was to evaluate if the estimation methods outlined in the background could accurately predict

the diffusion coefficients in case of an organic solute. The third goal was to estimate how much mass could conceivably accumulate in a clay lens through diffusion.

The mass flux for TCE using the setup shown in Figure 3.10 was observed. Based on the slope of the linear part of the graphs (Figures. 3.14 a, b, and c), the aqueous solubility of TCE, and the thickness of the soil sample, effective diffusion coefficients in silt and silt-clay mixtures were calculated (Table 3.14 and Table 3.15). The effective diffusion coefficients in silt and expanded silt-clay mixture were $1.31 \times 10^{-6} \pm 5.50 \times 10^{-8}$ cm^2/sec and $1.30 \times 10^{-6} \pm 1.49 \times 10^{-8}$ cm^2/sec, respectively, not statistically different (*p*-value > 0.15) from the results for the diffusion of iodide. Furthermore, the effective diffusion coefficient in the confined silt-clay mixture was found to be reduced significantly ($0.70 \times 10^{-6} \pm 6.19 \times 10^{-8}$ cm^2/sec). The relative standard deviations are slightly higher than those obtained in the case of iodide but still around 10%.

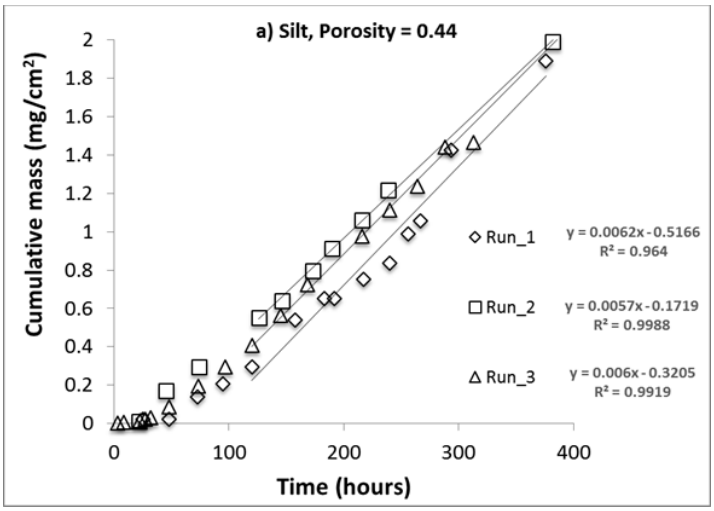

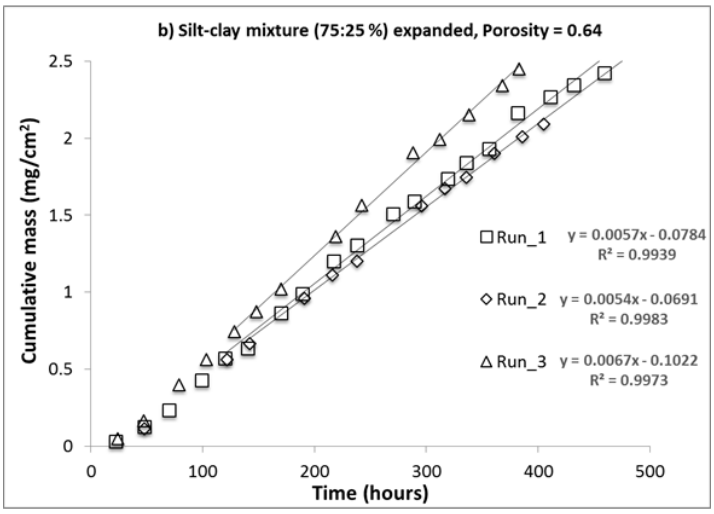

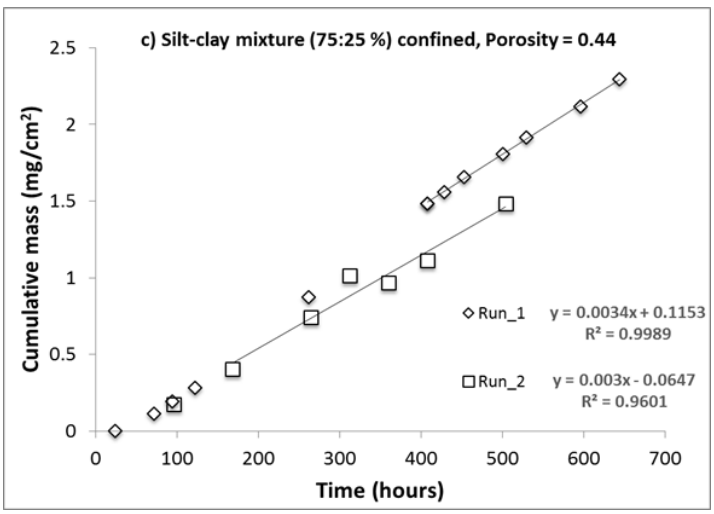

Figure 3.14 Cumulative mass per unit area vs time for TCE diffusion through a) silt, b) expanded silt-clay mixture, c) confined silt-clay mixture.

Table 3.14 Summary of slopes obtained from experimental data and calculated effective diffusion coefficients for TCE.

Porous medium	Porosity	Best fit mass flux (dM/dt) (mg/cm^2·hour)	D_e (x 10^6 cm^2/sec)
Silt	0.45	0.0062	1.36
Silt	0.45	0.0057	1.25
Silt	0.43	0.0060	1.31
Silt and clay mixture, expanded	0.68	0.0057	1.25
Silt and clay mixture, expanded	0.64	0.0054	1.18
Silt and clay mixture, expanded	0.60	0.0067	1.47
Silt and clay mixture, confined	0.44	0.0034	0.74
Silt and clay mixture, confined	0.43	0.0030	0.66

D_e calculated using Equation 3.30, assuming that C_o = 1270 mg/L (the solubility limit for TCE as measured by Grathwohl, 1998) and d = 1 cm.

Table 3.15 Average effective diffusion coefficients for TCE in different soils.

Porous medium	Average porosity	Average D_e (x 10^6 cm^2/sec)	Standard deviation (x 10^8 cm^2/sec)	Relative standard deviation (%)	Average relative diffusivity (D_e/D_{aq})
Silt	0.44	1.31	5.50	4.2	0.14
Silt and clay mixture, expanded	0.64	1.30	1.49	11.5	0.14
Silt and clay mixture, confined	0.44	0.70	6.19	8.8	0.07

Relative standard deviation: standard deviation/average, D_{aq} = 9.4x10^{-6} cm^2/sec (estimated using method of Hayduk and Laudie [1974]).

Among the studies summarized in Table 3.2, only three of them measured the effective diffusion coefficient of TCE in the laboratory, and the results seem to agree reasonably well with one another and with those here. For example, Khandelwal et al. (1998) measured the value to be 1.27 x 10^{-6} cm^2/sec in a soil containing 43% silt and 6% bentonite. Additionally, Itakura et al. (2003) determined the effective diffusion coefficient to be 0.83 x 10^{-6} cm^2/sec and 0.91 x 10^{-6} cm^2/sec in soils containing 51% and 95% silt, respectively. Using a similar experimental setup to the one employed in these studies, Grathwohl (1998) measured an effective diffusion coefficient of TCE ranging from 1.37

and 0.20 x 10^{-6} cm^2/sec for samples whose clay content varied from 6 to 87% (Table 3.4) in agreement with the data reported in this study.

On the other hand, Myrand et al. (1992) determined the apparent diffusion coefficient using a nonsteady-state method and the retardation factor for TCE in clayey soils using batch experiments. The effective diffusion coefficient calculated using Equation 3.30 was 3.50 x 10^{-6} cm^2/sec, higher than the value obtained here (0.7 x 10^{-6} cm^2/sec) as well as higher than the value reported by Grathwohl (1998) (1.37 x 10^{-6} cm^2/sec) for soil of a similar clay content and porosity. This discrepancy may stem from the fact that the effective diffusion coefficient in Myrand et al. (1992) was determined from the apparent diffusion coefficient. To do so requires a measure of the retardation coefficient, which, in turn, entails an assumption of equilibrium and a particular model for the sorption isotherm. The lack of agreement highlights the discrepancies that may ensue when comparing nonsteady-state and steady-state measurements in systems where sorption occur.

Table 3.16 shows that the models originally proposed for solute transport for unsaturated sandy soils (Penman, 1940; Marshall, 1959; Millington and Quirk, 1960,1961; Sallam et al., 1984) overestimate the relative diffusivities with a relative error >270%, similar to the trend for iodide diffusion. The models derived for clayey soils overestimate the relative diffusivity with an average relative error range of 9-52% except the log-linear fit (Equation 3.21) which underestimated the relative diffusivity of TCE by 41%. The model developed from the experimental data of Grathwohl (1998) (Equation 3.27) performed the best for the confined silt-clay mixture (36% overestimation) whereas it performed poorly for the expanded silt-clay mixture (95% underestimation). The relative

diffusivities estimated based on the field studies of organic solute diffusion in saturated clay soils (Johnson et al., 1989; Parker et al., 1994; Ball et al., 1997) resulted in an average overestimation of at least 80%. Thus, overall, the best estimates for the relative diffusivity of TCE in clayey soils were achieved using the correlations developed based on data for tritiated water. It can be concluded that, in situations where the clay content of the soil was more than 25%, models which estimate relative diffusivity as an exponential function of porosity failed to estimate the effective diffusion coefficient. On the contrary, the models proposed herein which predict effective diffusion coefficient from a linear or log-linear relation with bulk density, i.e. porosity, worked better.

Table 3.16 Comparison of relative diffusivities for TCE measured in this study and estimated by methods summarized in Table 3.3.

Model	Average percent relative error (%)		
	Silt	Silt-clay expanded	Silt-clay confined
Penman (1940)	374 (0.66)	377 (0.66)	786 (0.66)
Marshall (1959)	109 (0.29)	270 (0.51)	292 (0.29)
Millington and Quirk (1960, 1961)	140 (0.33)	299 (0.55)	349 (0.33)
Sallam (1984)	191 (0.41)	343 (0.61)	444 (0.41)
Johnson et al. (1989)	79 (0.25)	81 (0.25)	236 (0.25)
Parker et al. (1994) (Equation 3.26)	183 (0.39)	247 (0.48)	430 (0.39)
Ball et al. (1997)	402 (0.7)	406 (0.7)	840 (0.7)
Grathwohl (1998) (Equation 3.27)	27* (0.10)	95* (0.006)	36 (0.10)
Log-linear fit to data (Equation 3.21)	68* (0.04)	9* (0.13)	41* (0.04)
Bourg et al. (2006) (Equation 3.22)	19* (0.11)	20 (0.17)	52 (0.11)

*Underestimation.
Numbers in parentheses are relative diffusivity estimated by the model.

3.3.3. AOT Diffusion

DNAPL wastes are comprised of both chlorinated solvents and surfactants. However, surfactants are considerably larger molecules and may be comprised of both

charged and uncharged moieties. The relations to estimate the aqueous diffusion coefficient have not been confirmed rigorously for larger molecules, but based on Equations 3.14 and 3.15 the aqueous diffusion coefficient of AOT is expected to be around 2-3 times smaller than that of TCE. Figure 3.15 a, b, and c show the experimental results obtained here and summarized in Table 3.17, with the average effective diffusion coefficients and standard deviations given in Table 3.18. The diffusion coefficients were determined to be $0.65 \times 10^{-6} \pm 9.30 \times 10^{-8}$ cm^2/sec in silt and $0.41 \times 10^{-6} \pm 18.60 \times 10^{-8}$ cm^2/sec in the expanded silt-clay mixture and 0.23×10^{-6} cm^2/sec in the confined silt-clay mixture respectively. The results for silt and expanded silt-clay sample were not significantly different (p-value<0.15), probably due to the large standard deviation for the expanded silt-clay sample. On the other hand, the diffusion coefficients in the silt and confined silt-clay samples were found to be statistically different. Moreover, the effective diffusion coefficient of AOT is two times smaller than that of TCE in the silt, and three times smaller than that in the confined silt-clay mixture, which is essentially equivalent to the reduction in the aqueous diffusion coefficient. Thus, no additional reduction in the relative diffusivity was seen for AOT, despite its larger size or negatively charged hydrophilic moiety.

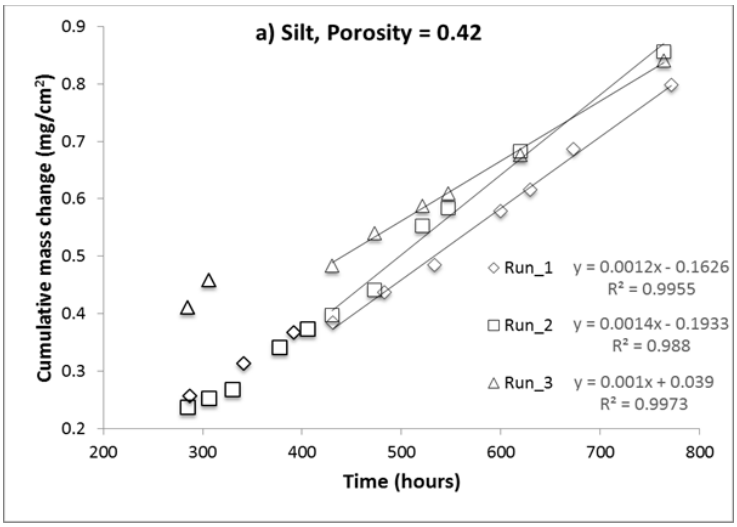

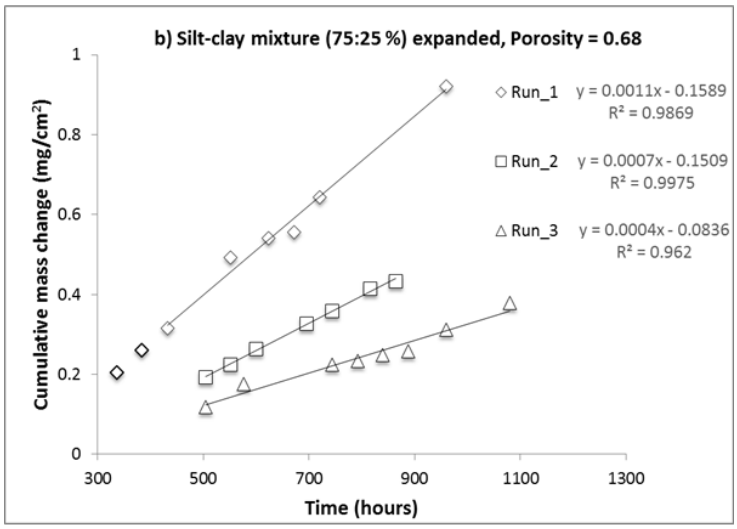

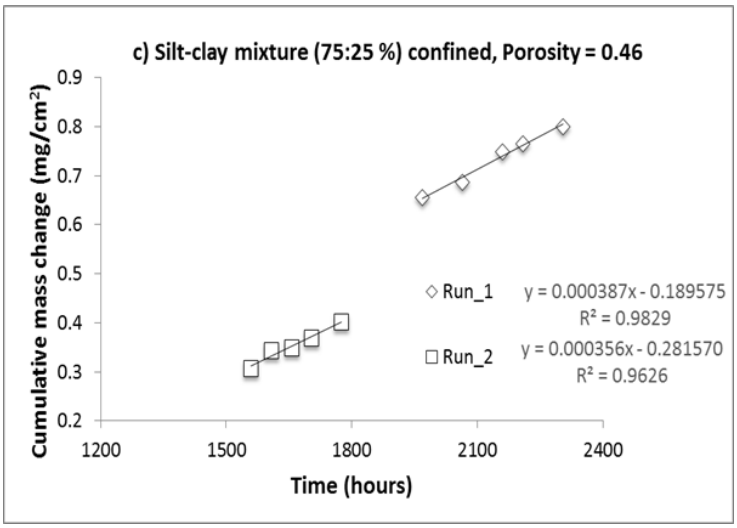

Figure 3.15 Cumulative mass per unit area vs time for AOT diffusion through a) silt, b) expanded silt-clay mixture, c) confined silt-clay mixture.

Table 3.17 Summary of slopes obtained from experimental data and calculated effective diffusion coefficients for AOT.

Porous medium	Porosity	Best fit mass flux (dM/dt) (mg/cm^2.hour)	D_e (x 10^6 cm^2/sec)
Silt	0.41	0.0011	0.67
Silt	0.43	0.0012	0.73
Silt	0.42	0.0009	0.55
Silt and clay mixture, expanded	0.62	0.0010	0.61
Silt and clay mixture, expanded	0.73	0.0006	0.36
Silt and clay mixture, expanded	0.69	0.0004	0.24
Silt and clay mixture, confined	0.47	3.87×10^{-4}	0.24
Silt and clay mixture, confined	0.44	3.56×10^{-4}	0.22

C_o= 456 mg/L (1 mM) AOT in Milli-Q water, d (thickness of the sample) = 1 cm (Equation 3.30).

Table 3.18 Average effective diffusion coefficients for AOT in different soils with standard deviation and relative standard error.

Porous medium	Average porosity	Average D_e (x 10^6 cm^2/sec)	Standard deviation (x 10^8 cm^2/sec)	Relative standard deviation (%)	Average relative diffusivity (D_e/D_{aq})
Silt	0.42	0.65	9.3	14.3	0.17
Silt and clay mixture, expanded	0.68	0.41	18.6	45.8	0.11
Silt and clay mixture confined	0.46	0.23	1.3	5.9	0.06

Relative standard deviation: standard deviation/average, $D_{aq} = 3.8 \times 10^{-6}$ cm^2/sec (estimated using method of Hayduk and Laudie [1974]).

Given the observation that the reduction in the effective diffusion coefficient could be attributed to the reduction in the aqueous diffusion coefficient, the same conclusions as to the best estimation methods were drawn for AOT as for TCE. For the silt soil, the correlation given by Bourg et al (2006) gave the best agreement whereas for the silt-clay mixtures, the linear fit of literature data (Equation 3.21) performed the best with a relative error of 14% for the confined silt-clay mixture (Table 3.19).

Table 3.19 Comparison of relative diffusivities for AOT measured in this study and estimated by methods summarized in Table 3.3.

Methods	Relative percent average error (%)		
	Silt	Silt-clay expanded	Silt-clay confined
Penman (1940)	282 (0.66)	505 (0.66)	998 (0.66)
Marshall (1959)	57 (0.27)	414 (0.56)	419 (0.31)
Millington and Quirk (1960, 1961)	82 (0.31)	448 (0.60)	491 (0.36)
Sallam (1984)	123 (0.39)	500 (0.65)	608 (0.43)
Johnson et al. (1989)	45 (0.25)	129 (0.25)	316 (0.25)
Parker et al. (1994) (Equation 3.26)	122 (0.38)	352 (0.49)	573 (0.40)
Ball et al. (1997)	305 (0.70)	542 (0.70)	1065 (0.70)
Grathwohl (1998) (Equation 3.27)	23* (0.13)	97* (0.004)	28 (0.08)
Log-linear fit to data (Equation 3.21)	76* (0.04)	49 (0.16)	14* (0.05)
Bourg et al. (2006) (Equation 3.22)	34* (0.11)	67 (0.18)	89 (0.11)

*Underestimation.
Numbers in parentheses are relative diffusivity estimated by the method.

3.3.4. ^{13}C-labeled TCE Diffusion

To more closely emulate the conditions in the field, a water-saturated silt-clay sample was contacted with PCE-based DNAPL for 18 months. To differentiate between the diffusion of TCE through the waste and TCE already present in the PCE-based DNAPL waste, ^{13}C-labeled TCE was used. For comparison, the diffusion coefficient of ^{13}C-labeled TCE through silt saturated with PCE was measured. As diffusion in a liquid phase is a function of the interactions between the solvent and the solute, the diffusion coefficient of TCE in PCE can be estimated by setting the association factor in Equation 3.14 equal to one (designating an unassociated nonpolar solvent), 165 g/mol as the molecular weight of the solvent, and 0.93 cP as the viscosity of the solvent (Riddick et al., 1986). Using these parameter values, the diffusion coefficient of TCE in PCE was estimated to be 19.0 x 10^{-6} cm^2/sec (Wilke and Chang, 1955) and 10.3 x 10^{-6} cm^2/sec (Hayduk and Minhas, 1982) which are 88% and 9% higher than the diffusion coefficient of TCE in water, respectively.

The effective diffusion coefficient of TCE in silt saturated with PCE through silt was measured to be 1.39 x 10^{-6} cm^2/sec (Figure 3.16.a, Table 3.20), only 6% higher than the effective diffusion coefficient of TCE in the same silt saturated with water (1.31 x 10^{-6} cm^2/sec, Table 3.15). However, this difference was not statistically significant (*p*-value > 0.15). If the impact of the porous medium on diffusion can be considered to be the same in both cases, the ratio of the effective diffusion coefficients of TCE in water versus that in PCE can be assumed to be equal to the ratio of the bulk diffusion coefficients in the different liquid phases. The measurements reported here agree with that supposition as the effective diffusion coefficient of TCE in PCE was calculated to be 9% or 88% higher than the effective diffusion coefficient of TCE in water. Thus, the increase of 6% could be attributable to the difference in the diffusion coefficient in the different bulk liquids.

The results reported in Section 3.3.2 showed that the effective diffusion coefficients of TCE in silt and in the expanded silt-clay mixture were very similar. Also, diffusion through silt soil saturated with PCE versus saturated with water did not affect the effective diffusion rate of ^{13}C-TCE significantly. If the situation with PCE-based waste in contact with an expanded silt-clay mixture analogous to these cases, then it might be anticipated that the effective diffusion coefficient of ^{13}C-TCE through the expanded silt-clay mixture contacted with PCE waste would be similar to the effective diffusion coefficient of ^{13}C-TCE in silt. On the contrary, the diffusion coefficient of ^{13}C-TCE was 1.14 x 10^{-8} cm^2/sec (Table 3.21), more than two orders of magnitude lower. Therefore, it appeared that in case of diffusion from a real DNAPL waste in a saturated soil matrix, the diffusion rate of the chlorinated solute could be substantially slower than that of a clean system involving a single solute in water-saturated soil.

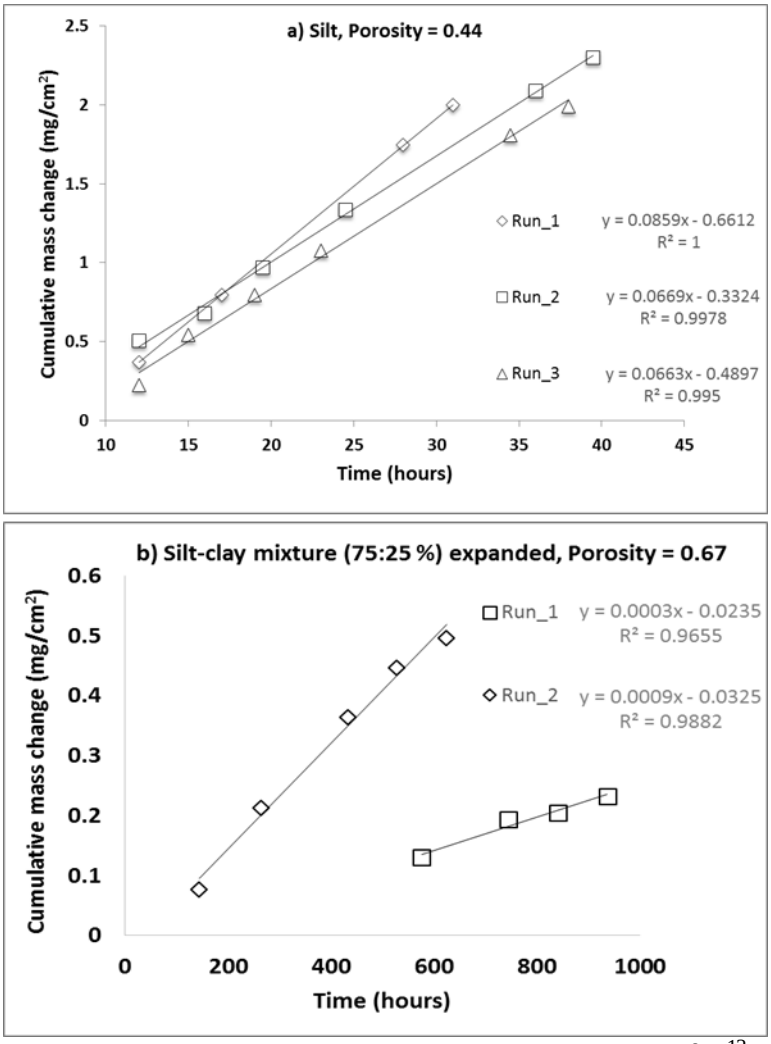

Figure 3.16 Cumulative mass change per unit area vs time for ^{13}C-labeled TCE diffusion through a) silt saturated with PCE, b) expanded silt-clay mixture in contact with PCE-based DNAPL waste for 18 months.

Table 3.20 Summary of slopes obtained from experimental data and calculated effective diffusion coefficients for ^{13}C-labeled TCE.

Porous medium	Porosity	Best fit mass flux (dM/dt) (mg/cm²·hour)	D_e (cm²/sec)
Silt, saturated with PCE	0.45	0.0859	1.63×10^{-6}
Silt, saturated with PCE	0.44	0.0669	1.27×10^{-6}
Silt, saturated with PCE	0.41	0.0663	1.26×10^{-6}
Silt and clay mixture, expanded, contacted with PCE-based DNAPL waste for 18 months	0.68	0.0003	0.57×10^{-8}
Silt and clay mixture, expanded, contacted with PCE-based DNAPL waste for 18 months	0.65	0.0009	1.71×10^{-8}

C_o = 14600 mg/L ^{13}C-labeled TCE in PCE, d (thickness of the sample) = 1 cm in Equation 3.30.

Table 3.21 Average effective diffusion coefficients for ^{13}C-labeled TCE in different soils with standard deviation and relative standard deviation.

Porous medium	Average porosity	Average D_e (cm^2/sec)	Standard deviation ($x\ 10^8\ cm^2/sec$)	Relative standard deviation (%)	Average relative diffusivity (D_e/D_{aq})
Silt, saturated with PCE	0.44	1.39×10^{-6}	21.2	15.3	0.13
Silt and clay mixture, expanded, contacted with PCE-based DNAPL waste for 18 months	0.67	1.14×10^{-8}	0.81	70.7	0.001*

Relative standard deviation = standard deviation/average.
*Relative to diffusion coefficient of TCE in water.

3.4. Conclusions

The definition of the effective diffusion coefficient varies between studies, depending on how the porosity, tortuosity and sorption are handled. Unless the study explicitly explains how these terms are defined, the comparison and evaluation of data among studies can be challenging. Eight of the eleven studies summarized in Table 3.2 utilized nonsteady state experiments which gives an apparent diffusion coefficient. In the cases where nonsteady state experiments were conducted, the effective diffusion coefficient for the soil-solute couple was calculated from the apparent diffusion coefficient and the reported retardation factor. However, the studies can be difficult to compare as the retardation factors are then determined in batch experiments with an assumed isotherm form.

Diffusion rates are essential to calculate the rates of transport into and out aquitards and the mass storage therein. In models of subsurface transport looking at the impact of aquitards, the effective diffusion coefficient is usually estimated because there are very few measured values. The estimation methods suggest an exponential dependence of the relative diffusivity on the porosity of soil, but they were not developed originally for

organic solute diffusion in saturated clayey media. The results reported here for TCE and iodide show the results grossly overestimate the diffusion coefficient, especially in soils with a clay content higher than 25%. Similarly, it was found that the relative diffusivities of TCE based on field studies provide an overestimate of the values measured here. Two other estimation methods were also explored: a log-linear relationship developed by fitting experimental data for the diffusion of tritiated water in clay soils and a theoretical relation by Bourg et al. (2006) developed for clay soils considering clay variables such as the fraction of interlayer space. Both of these estimation methods performed better in estimating relative diffusivities of TCE and iodide.

The diffusion coefficient of an anionic surfactant (AOT) was also measured because it is known that field wastes contain surfactants. It appeared that reductions in the effective diffusion coefficient and aqueous diffusion coefficient were to a similar degree, so no additional decrease in relative diffusivity for AOT was observed despite its larger size. Log-linear relation developed from literature experimental data for tritiated water and the theoretical relation developed by Bourg et al. (2006) gave the best estimates for AOT, similar to the results for iodide and TCE.

In order to evaluate diffusion of a chlorinated solvent in a clayey soil in a situation more reflective of the field, ^{13}C-labeled TCE diffusion was measured in a silt-clay mixture that had been in contact with a PCE-based DNAPL waste from a field site for 18 months. In this system, the effective diffusion coefficient was almost two orders of magnitude lower than that for pure TCE through water, suggesting that diffusion at a field site from a waste matrix may be much slower than diffusion of a chlorinated solute from a pure solvent.

3.5. Implications of the Diffusion Measurements

The diffusion coefficient of TCE observed in the field (3.25 x 10^{-6} cm^2/sec) has been reported as 1.7 times higher than the diffusion coefficient of TCE estimated based on the relative diffusivity of chloride (1.95 x 10^{-6} cm^2/sec, Johnson et al., 1989). The average effective diffusion coefficient of TCE measured here was 1.30 x 10^{-6} cm^2/sec for an unconfined saturated silt-clay mixture (75% silt and 25% clay) and 0.7 x 10^{-6} cm^2/sec for a confined saturated silt-clay mixture. These values are in agreement with those reported by Grathwohl (1998) and others (Khandelwal et al, 1998; Itakura et al., 2003). The diffusion coefficient for the expanded silt-clay sample contacted with field DNAPL waste was 1.14 x 10^{-8} cm^2/sec which is considerably lower than previously reported values. The diffusion coefficients for TCE measured here are almost four times lower than the ones estimated by Parker et al.(1994)'s method (Table 3.3), and five times lower than the observed diffusion coefficients reported in Johnson et al. (1989). The fact that the measured diffusion coefficients are all lower than the estimates magnifies the reported discrepancy between the observed values and what can be attributed to diffusion.

In order to assess the impact of this discrepancy between measured and field observed diffusion coefficients on mass storage, the diffusion of TCE from a DNAPL waste pool into an aquitard was modeled as diffusion into a plane sheet (Figure 3.17). The amount of mass accumulated over 30 years into a 5-m thick aquitard was estimated by (Crank, 1975):

$$\frac{M_t}{M_\infty} = 1 - \frac{8}{\pi}\sum_{n=0}^{\infty}\frac{1}{(2n+1)}\exp\{-D_e(2n+1)^2\pi^2\, t/d^2\} \quad \text{(Equation 3.32)}$$

where M_t is the total amount of diffusing substance which has entered the sheet per unit area during time t, and M_∞ is defined by:

$$M_\infty = d\left\{\frac{1}{2}(C_0 + C_2) - C_1\right\} \qquad \text{(Equation 3.33)}$$

where C_o = the concentration at x = 0; C_2 = concentration at x = d; C_1 = the concentration in the plane at t = 0, assumed to be uniform.

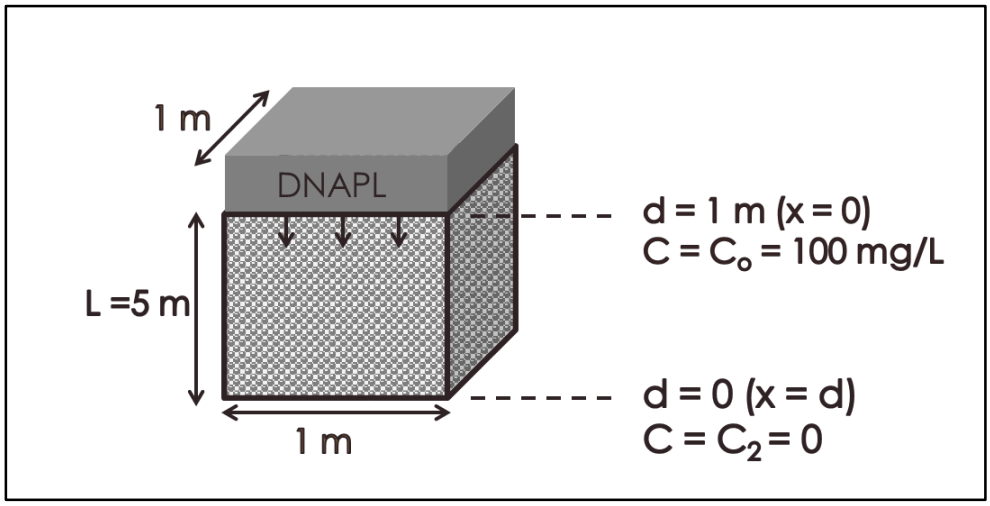

Figure 3.17 DNAPL pool on a unit area of a hypothetical aquitard.

The concentration at x = 0 was set equal to 100 mg/L as the aqueous phase concentration of TCE for water equilibrated with a PCE-based DNAPL waste was measured to be 59±25 mg/L (Dou et al., 2008). Calculations of mass accumulation were made using three values for the effective diffusion coefficient of TCE: 0.7 x 10^{-6} cm^2/sec (as measured in this study for the confined silt-clay mixture), 1.14 x 10^{-8} cm^2/sec (the measured diffusion coefficient of ^{13}C-TCE in expanded silt-clay mixture contacted with PCE-based DNAPL waste) and 3.25 x 10^{-6} cm^2/sec (the diffusion coefficient for TCE based on the field study by Johnson et al. [1989]). The calculations, summarized in Table 3.22, show that using the measured value of the effective diffusion coefficient for the confined silt-clay mixture results in a halving of the estimate of the mass storage in the aquitard. Using the slower diffusion rate of TCE through a silt-clay mixture contacted with DNAPL

waste, the estimated mass that accumulated in the aquitard was 17 times smaller than the field observation. Given that it is thought that the observed diffusion coefficients already underpredicted the mass stored in the aquitard, these results suggest that transport rates in the field cannot be attributed to diffusion into a competent clay layer alone and it is necessary to consider other conceptualizations of transport.

Table 3.22 Mass of TCE accumulated in a hypothetical aquitard after 30 years of diffusion using measured and observed diffusion coefficients.

	D_e (cm^2/sec)	Mass (g)
Measured in this study (in expanded silt-clay mixture contacted with DNAPL waste)	1.14 x 10-8	3.7
Measured in this study (in confined silt-clay mixture)	0.70×10^{-6}	29.0
Observed in the field by Johnson et al. (1989)	3.25×10^{-6}	62.6

Chapter 4
Determination of Structural Modifications in Clay Soils due to Contact with Chlorinated DNAPLs

Measured diffusion coefficients suggest that the simple diffusion into a competent clay layer alone fails to explain the higher than expected mass storage in low permeable layers. One hypothesis that might explain enhanced transport into aquitards is the modification of the clayey soils' structure. Data from field sites suggest that aquitards at hazardous waste sites may contain up to 70% clay including considerable amounts of smectites, which change their structure with water content. Additionally, the documented existence of subsurface DNAPL pools is evidence of direct contact between the aquitard and DNAPL waste. Thus, the impact of waste DNAPLs on the structure of clayey soils needs to be examined. If waste DNAPLs can cause the contraction of the structure of the clayey soil and the formation of cracks, higher transport rates into the aquitards might result. Parts of this chapter have been published as "Impact DNAPL contact on the Structure of Smectitic Clay Materials" in *Chemosphere* (2014, 95, 182-187).

4.1 Background

As reviewed in Chapter 2, the distance between two adjacent layers of smectite clay minerals, i.e. basal spacing, varies based on water content. The basal spacing of an air-dry smectitic clay increases from 12 Å (for Na-montmorillonite or 15 Å for Ca-montmorillonite) to around 19 Å after full hydration. In addition to basal spacing changes

in contact with water, the thickness of interlayer space changes in montmorillonite clays may occur in contact with aqueous solutions of organic solvents. Brindley et al. (1969) equilibrated Ca-montmorillonite with solutions of several organic solvents. The general conclusion was that dilute solutions of organic solvents increased the basal spacing of smectites to the same degree as water, whereas their concentrated solutions expanded the structure less. For example, ethanol solutions more concentrated than 35% or methanol solutions more concentrated than 47% increased the basal spacing of calcium montmorillonite to about 17 Å where more dilute solutions increased the basal spacing to above 19 Å, similar to the basal spacing with water. Even though n-propanol belongs to the same chemical group as these organics, the basal spacing of dry clay increased to 18 Å in a solution of propanol more concentrated than 8%; below this volume percent the basal spacing increased to above 19 Å. Like propanol, diol-group organic liquids did not cause as much swelling (measured basal spacing 17-18 Å) as water (measured basal spacing higher than 19 Å) when the solution's organic liquid content was higher than 8%. Consistent with this finding, Brown and Thomas (1987) reported that bentonite clays in dilute water-acetone or water-ethanol solutions had a basal spacing of 19-20 Å, equivalent to the basal spacing of bentonite in contact with water. The basal spacing increased less (up to 16 Å) compared to that with water when the solution percentage of acetone exceeded 50% or the percentage of ethanol exceeded 75%. Most of the work has been performed using miscible organic solvents. However, more recently, a study by Matthieu et al. (2013) found that the basal spacing of Na-montmorillonite in contact with an aqueous solution saturated with TCE was 18.2 Å, similar to the value reported with water.

In addition to the basal spacing changes observed with concentrated aqueous solutions of organic solvents, the impact of pure solvents has also been addressed by several studies. Barshad (1952) measured the basal spacing of dry Ca and Na-montmorillonite contacted with a variety of organic liquids and found that the organic liquids could not expand the structure of clay as much as water. The degree of swelling was hypothesized to be related to the dielectric constant of the organic liquid. Following this study, the relation between the basal spacing of clay and the dielectric constant of the solvent was analyzed further but no general correlation was derived (Olejnik et al. 1974; Berkheiser and Mortland, 1975; Murray and Quirk, 1982).

The measurements previously made emphasized water-miscible compounds, such as alcohols and acetone, and comparatively few utilized chlorinated solvents, the organic compounds often of concern in at hazardous waste sites. Middleton and Cherry (1996) provide a summary of historic measurements of basal spacing for clay minerals in contact with organic liquids. Greene-Kelly (1955) measured a basal spacing of 12.5 Å for Na-montmorillonite in contact with chlorobenzene; similarly, Berkheiser and Mortland (1975) reported that the basal spacing for Ca-montmorillonite and Na-montmorillonite contacted dry with 1,2-dichloroethane was 14.7 Å and 12.6-13.0 Å, respectively, and Griffin et al. (1984) reported a value of 13.8 Å for carbon tetrachloride. Thus, these organic liquids did not appear to increase the basal spacing above that with air.

Although the literature about the basal spacing values for initially air-dry montmorillonite clays contacted with organic liquids provide some insight, in the context of the field, it is more important to understand basal structure changes that may occur when the clay is already saturated with water since chlorinated organic solvent wastes pool on

top of water-saturated clay layers and lenses. It appears that there is only a single reported measurement of a water-saturated smectitic clay in contact with a chlorinated organic liquid phase: Griffin et al. (1984) obtained a value of 20.5 Å for the basal spacing of water-saturated bentonite in contact with carbon tetrachloride, similar to the value of 20.1 Å reported in the same study for contact with water. This measurement suggests that the pure solvent was not able to displace water and cause a contraction of the basal spacing in water-saturated cases.

In addition to the paucity of basal spacing measurements of water saturated clays with pure chlorinated organic liquids, there are no reported measurements with actual chlorinated solvent wastes or mixtures simulating such wastes. Solvents found at hazardous waste sites are not pure. Surfactants are a critical component of the waste because they can change not only the wettability of mineral surfaces, but also the structure of clay. For example, contacting a Na-smectite with an aqueous solution of hexadecyltriammonium bromide increased the basal spacing from about 20 Å to as high as 40 Å (Lee and Kim, 2002), with the organic cations serving as "pillars" in the interlayer spacing. It may be thought that only cationic surfactants may sorb and expand the interlayer spacing, due to the predominantly negative charge of clay surfaces, but Shen (2001) showed that nonionic linear alcohol ethoxylates could also sorb and increase the basal spacing of dry bentonite from 11 Å up to 17 Å.

The significance of the modification in the structure of clays is that such changes have been linked to increases in transport. Laboratory measurements have shown increases in hydraulic conductivity of two to three (Anderson et al., 1985), three to four (Li et al., 1996) and one to five orders of magnitude (Brown and Thomas, 1984) depending on the

organic liquid, clay type and percent clay. The increase is attributed to the formation of cracks or channels due to the contraction of the clay structure resulting from the contact with organic solvents. However, such studies generally use substantial hydraulic gradients (up to 360 m/m [Anderson et al., 1985]) to drive the organic liquids through the low permeability materials. These gradients far exceed those which are generated by pools of DNAPL on top of low permeability layers; for example, Oolman et al. (1995) reported a depth of DNAPL of two meters at Hill AFB, UT, and typical pool depths are probably considerably less. If the forcing of the DNAPL into these geologic materials under a substantial gradient resulted in the cracking, then the ensuing changes in hydraulic conductivity may not reflect field processes.

Although cracking of clay soils due to contact with organic solvents under low heads is still speculative, cracking induced by desiccation and its impact on hydraulic conductivity is well-documented. Increase in hydraulic conductivity as a result of desiccations cracks were determined to be from 12-34 times (Rayhani et al., 2007) up to 100-1000 times (Omidi et al., 1996). Numerous studies have focused on the characterization and quantification of cracks, analyzing the number of intersections, number of segments, and area of cracks per unit surface area (Table 4.1). The investigations of crack patterns reveal that cracks form quadrangles with "T" or "+" shape intersection (Tang et al., 2012), squares (Tang et al., 2011), orthogonal squares (Velde, 1999) or pentagons and quadrangles (Li and Zhang, 2010). Velde (1999) studied more than 22 soils samples with clay contents of 17-100% and found that the segment to intersection ratio was in a range of 1.5 to 2 where 1.5 represents intersecting hexagons and 2 represents intersecting squares. Tang et al. (2012) stated when the segment to

intersection ratio increased from 1.5 to 2, "T"-shaped intersections turned to "+"-shapes intersections. Desiccation cracks may be less than 2-3 mm wide, whereas aperture sizes greater than 10 mm extending through an entire clay layer with a thickness of 6 m were also reported (Morris et al., 1992). Cracks observed during the permeation of organic solvents in clay soils around 5 mm (McCaulou and Huling, 1999) and 1 cm (Abdul et al., 1989).

Table 4.1 Parameters and properties of desiccation cracks summarized from the literature.

Segment / Intersection Ratio	Crack area / Surface Area (%)	# Polygon / Area (cm^{-2})	Aperture Width (mm)	Aperture Length (mm)	Reference
1.49 – 1.61	9.3 – 24.2	-	-	-	Tang et al. (2008)
-	-	0.075 (max)	0.49 (average)	31.6 (average)	Li and Zhang, (2010)
-	14 (max)	-	2 (max)	-	Tang et al. (2011)
1.9*	19.3	0.53	2.2	17	Tang et al. (2012)

*Calculated from data provided in Tang et al. 2012.

This chapter aims to evaluate the changes in clay structure by investigating basal spacing of clay minerals saturated with water and contacted with pure organic solvents, and chlorinated solvent wastes from the field. Furthermore, changes at the macro scale were observed and crack properties quantified such as length, aperture size, number of intersections and segments per unit area.

4.2 Materials and Methods

Basal spacing measurements were made for three smectitic clays: two montmorillonites, one with Na as the major cation (SWy-2), and the other with Ca as the

major cation (STx-1), obtained from the Clay Minerals Society Source Clays Repository (Chantilly, VA). Information about the cation exchange capacity of these clay minerals can be found in Table 4.2. These clays were used as received. The third was a commercial Wyoming Na-bentonite (Southwestern Materials, Austin, TX), processed by grinding with a mortar and pestle, and then sieving using a 106 μm sieve. Hydrometer test indicated 96% of the material is <2 μm, and mineralogical analysis showed Na-montmorillonite to be the primary mineral (>90%).

Table 4.2 Properties of pure clays used in this study.

Clay	CEC (meq/ 100g)
Sodium montmorillonite (SWy-1, major cations: Na and Ca)	76.4
Texas montmorillonite (STx-1, major cation: Ca)	84.4

Data from Olphen and Fripiat (1979).

Although the principal organic solvents of concern in this study were chlorinated solvents, additional organic solvents were included to obtain a range of chemical properties, in terms of both solubility and dielectric constant (Table 4.3). In addition, two DNAPL wastes were examined. Characteristics of these wastes are described in Hsu (2005) and are summarized in Table 3.7. One of these wastes was a dry cleaning PCE waste, obtained from a waste storage tank of a dry cleaner (Ann Arbor, MI). This liquid was still transparent, but less clear than and with a density slightly less than that of pure PCE. Its interfacial tension was markedly less than that for pure PCE: 2-3 dyn/cm, rather than 47.5 dyn/cm (Demond and Lindner, 1993). Based on chemical analyses reported in Hsu (2005), it is believed that this waste contained anionic surfactants at a concentration below 1 mM, and that nonionic surfactants were the dominant surface-active species. The

other DNAPL waste was a degreasing TCE waste obtained from Operable Unit 2 at Hill AFB (UT). Its appearance was black and opaque, with a density of 1.3 g/mL. The interfacial tension of this waste was also about an order of magnitude less than its pure counterpart, but the reduction was attributed to the presence of predominantly anionic surfactants (Hsu, 2005). Neither of these wastes caused quartz to become organic-wet in the presence of water at neutral pH; the measured contact angle (measured through water) was approximately 30° (Table 3.7).

Table 4.3 Organic solvents used for basal spacing measurements and their relevant properties.

Solvent	Chemical formula	Supplier	Purity	Solubility (mg/L)	Density (g/cm^3)	Dielectric constant
Acetone	$(CH_3)_2CO$	Sigma Aldrich	>99.9%	Infinitely	0.78	20.9
Aniline	$C_6H_5NH_2$	Sigma Aldrich	>99.5%	33800	1.02	6.71
Butanol	C_4H_9OH	Sigma Aldrich	>99%	74500	0.81	20.45
2-Chloroaniline	$ClC_6H_4NH_2$	Sigma Aldrich	>99.5%	8760	1.21	13.4
1,2-Dichlorobenzene	$C_6H_4Cl_2$	Sigma Aldrich	99%	156	1.3	9.9
Ethanol	C_2H_6O	Sigma Aldrich	>99%	Infinitely	0.79	24.55
Nitrobenzene	$C_6H_5NO_2$	Acros Organics	>99%	1900	1.2	34.8
1,1,2-Trichloroethane	$C_2H_3Cl_3$	Acros Organics	98%	4400	1.43	7.29
Tetrachloroethylene	C_2Cl_4	Sigma Aldrich	>99.9%	150	1.61	2.28
1,2,4-Trichlorobenzene	$C_6H_3Cl_3$	Sigma Aldrich	>99%	-	1.45	-
Trichloroethylene	C_2HCl_3	Fisher Scientific	>99.5%	1370	1.45	3.42

Data from Riddick et al. (1986).

Four sets of measurements were performed using air-dry clays (i.e., exposed to air at 30% relative humidity at room temperature) involving the addition of water (a 0.005 M $CaSO_4$ solution), the addition of pure organic liquids, and the addition of field wastes. For

the wet specimens, oriented samples were prepared by a smear mount method as suggested in the literature (Moore and Reynolds, 1997; Brindley and Brown, 1980). The samples were prepared by packing 0.2 g of air-dry (at 30% relative humidity) clay in a glass sample holder 0.5 mm deep (Rigaku, The Woodlands, TX). The surface was then smoothed by passing the edge of a glass slide over it. Water-wetted samples were prepared by packing 0.2 g of air-dry clay onto the glass slide and then storing the glass slide in a plastic container in contact with a 0.005 M $CaSO_4$ solution for one day. The next day, the surface of the wet sample was smoothed using a glass slide.

The analysis of the solvent wet samples required an airtight sample holder due to the hazardous nature of the solvents used in this study. Therefore, a special airtight sample holder made out of aluminum covered by a beryllium membrane was used (Rigaku, The Woodlands, TX). The beryllium membrane is reported to have no peaks under 38^o (Lexa, 1998) so it is not expected to interfere with the clay's diffraction peaks that are reported at 2θ angles lower than 20^o (Brindley and Brown, 1980). On the contrary, Lerz and Kramer (1966) found an interference with a greater impact at smaller 2θ angles. The issue encountered with the beryllium membrane was that the characteristic peak was not observed in the diffraction patterns. This phenomenon might have arisen due to an unavoidable air gap between the membrane and sample surface during sample preparation. Thus, Kapton® film was used instead which is compatible with chlorinated solvents and does create any peak interference. It is also transparent so it permits the observation of any possible air gap between the sample surface and film.

The organic liquid-saturated samples were prepared by packing air-dry clay into an aluminum air-tight sample holder (Rigaku, Woddlands, TX) with a Kapton® film in the

cover of the sample holder, followed by the addition of the solvent to the clay. To assess whether the variation in sample holders and covers caused any differences in the XRD measurements, some measurements of air-dry and water-saturated clays were also made using the aluminum sample holder and Kapton® film, and no appreciable differences were observed. For the samples that were scanned covered by Kapton® film, the film was scanned under the same conditions as the sample so that the resulting pattern could be categorized as part of the background. The standard equilibration time for measurements with air-dry clays was fifteen minutes. Some additional samples were run at extended times (up to one month) and no differences were observed in the basal spacing measurements. The lack of dependence on time is consistent with the observation of Amarasinghe et al. (2009) who found that organic solvents can enter the interlayer space of air-dry Na-montmorillonite almost immediately.

Changes in the basal spacing were measured using an x-ray diffractometer (XRD) (Rigaku, The Woodlands, TX), equipped with a rotary anode source (Cu) with a 12 kW X-ray generator and graphite monochromator and two wide angle horizontal goniometers (2^o – 138^o). Initially, the samples were scanned at an incident angle range of 2-65^o with a step size of 0.02^o and a counting time of 2 seconds. After the location of the (001) peak was determined, samples were scanned in a continuous mode within the 2-10° 2θ range at a speed of 2° per minute. JADE (Version 10; Materials Data, Livermore, CA) was used for the data analysis. A background curve was fitted automatically by the software. After determining the portion of the profile attributable to background, the PseudoVoigt profile function was then used to fit the profiles to determine the location of the peaks.

In addition, samples were prepared with water-saturated clays in both vials and in beakers in order to measure the basal spacing and observe structural changes at the macro scale. Two vials were prepared by placing 0.5 to 1.0 grams of montmorillonite in 20-mL glass vials. Then about 10 mL of a 0.005 M $CaSO_4$ solution were added; the vials were then shaken and allowed to equilibrate for two days. After equilibration with water, about 10 mL of pure TCE was added to one of the vials, and 10 mL of PCE-based DNAPL waste added to the other one. The vials were rotated for seven days and then left to sit for another 49 days. Photographs were taken over time to record visual changes; samples were also taken at 18 days and 180 days and analyzed by XRD.

To investigate the impact of extended periods of equilibration under conditions that more closely simulate the subsurface, layered systems were constructed in three 1-liter borosilicate glass beakers (Figure 4.1). These systems consisted of a saturated layer of sand about 3 cm thick, a saturated layer of clay about 0.5 cm thick on top of the sand, and a layer of organic liquid about 2.5 cm thick on top of the clay. The method used to pack the sand layer was similar to the one developed by Oliviera et al. (1996) involving sprinkling sand into ponded water, followed by compaction. The clay layer was constructed of the commercial Na-bentonite clay. To pack the clay into a layer, an optimum consistency needed to be achieved. For this clay, it appeared that a ratio of 5 mL of 0.005 M $CaSO_4$ solution to 10 g of clay (close to the plastic limit of 52 wt%) gave a consistency that allowed the clay to be packed. Following packing, 100 mL of 0.005 M $CaSO_4$ solution were ponded on top of the clay and the system was left sitting for two weeks to saturate the clay; this time frame was consistent with the observed termination of expansion and the saturation times used in other studies (Nowak, 1984; Miyahara et al.,

1991). As the clay layer absorbed water, it expanded to about three times its original height; consequently some of the clay was removed in order to adjust its thickness to about 0.5 cm. Then, a 2.5-cm layer of either pure PCE, TCE-based DNAPL waste or PCE-based DNAPL waste was ponded on top of the clay layer in each beaker. The beakers were covered to minimize evaporation and left to sit at ambient conditions for up to 300 days or more. Photographs were taken over time and analyzed using the image analysis software, ImageJ. Clay samples were removed, placed in the air-tight sample holder and the basal spacing analyzed using XRD.

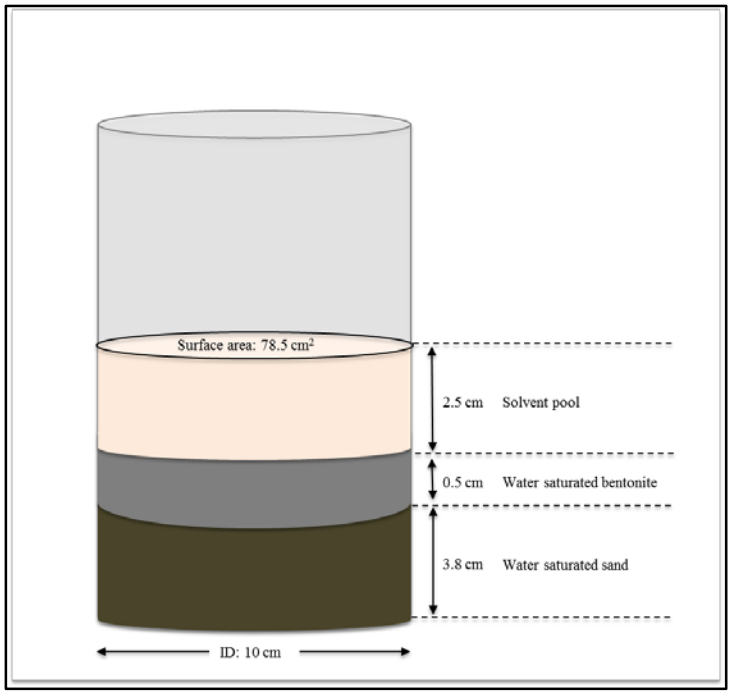

Figure 4.1 Diagram of the layered clay and sand system prepared in beakers.

4.3 Results and Discussions

Figure 4.2 shows the measured basal spacings of air dry (30% relative humidity) Ca- and Na-montmorillonite contacted with water or contacted with pure organic liquids.

Contact of the air-dry samples with water increased their basal spacing, with the basal spacings reported here consistent with values reported in the literature (Barshad, 1952; Brindley et al., 1969; Brindley and Brown, 1980; Brown and Thomas, 1987; Li et al, 1996). For air-dry Ca and Na-montmorillonite contacted with organic liquids, the data show that the basal spacings are generally closer to those for an air-dry state than to those for a water-saturated state. The measurements reported here for the chlorinated solvents show that the basal spacings in contact with such compounds are consistent with those for nonchlorinated organic solvents with similar dielectric constants. Greater basal spacings were measured for acetone and ethanol. However, the difference does not seem to be a function of the dielectric constant, as nitrobenzene has a larger dielectric constant than acetone and ethanol, but yields a smaller basal spacing.

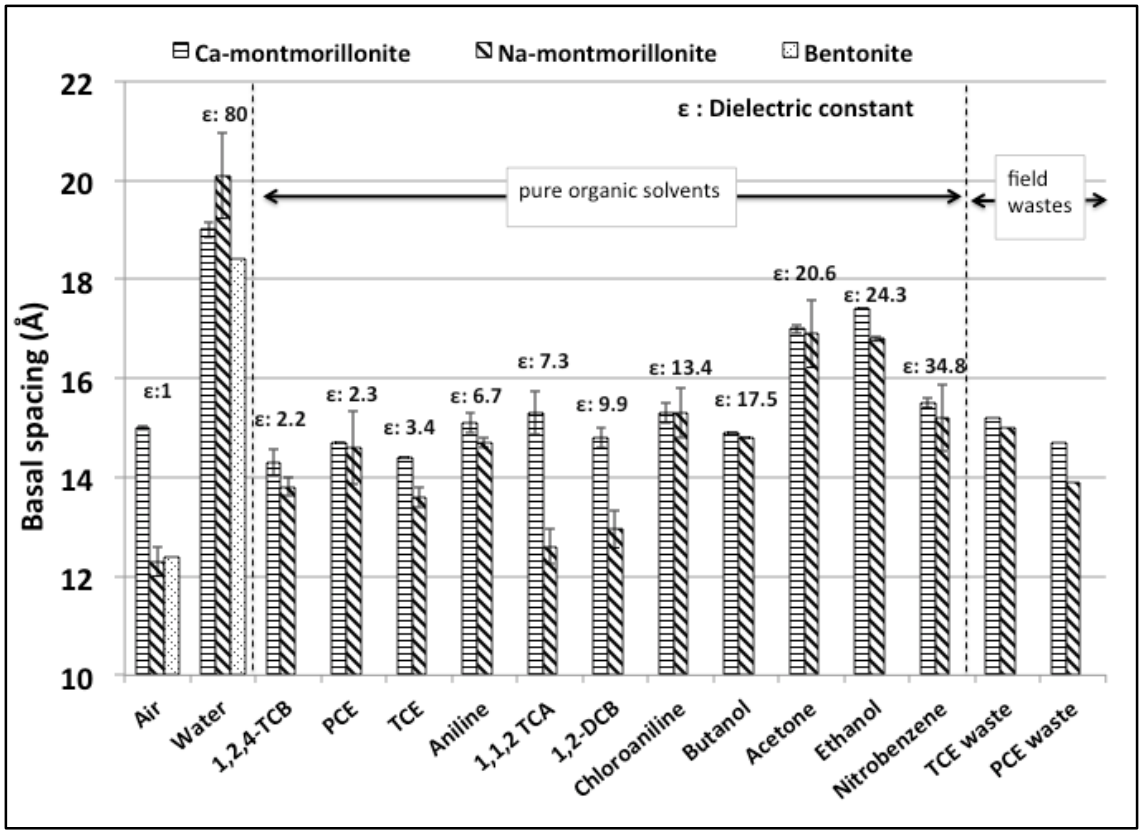

Figure 4.2 Basal spacing of smectites in contact with air, pure organic liquids and field wastes. Error bars represent the standard deviations. Water is 0.005 M $CaSO_4$ solution; air dry is at room relative humidity (30%); characteristics of the organic liquids and field wastes are given in Table 4.3 and Table 3.7, respectively.

Figure 4.3 compares the results from this study with basal spacing measurements for organic liquids reported in the literature (MacEwan, 1948; Greene-Kelly, 1955; Berkheiser and Mortland, 1975; Griffin et al., 1984). The data presented in this figure corroborates the observation based on the data from this study, that basal spacings obtained with chlorinated compounds are consistent with those for nonchlorinated compounds with similar dielectric constants. Furthermore, it suggests that the impact of organic compounds on basal spacing may be more directly correlated with solubility, as those compounds that are completely miscible in water caused some expansion of the clay structure relative to the air-dry state, regardless of the dielectric constant. The relative impact of the parameters

of solubility versus dielectric constant can be seen in particular in the case of pyridine versus nitrobenzene: pyridine is miscible in water and has a dielectric constant of 12.91 and the basal spacing of Ca-montmorillonite in contact with pyridine is 20.3 Å (Berkheiser and Mortland, 1975), whereas nitrobenzene has a solubility of 1900 mg/L and a dielectric constant of 34.78, and the basal spacing of Ca-montmorillonite in contact with nitrobenzene is 15.0 Å (Berkheiser and Mortland, 1975).

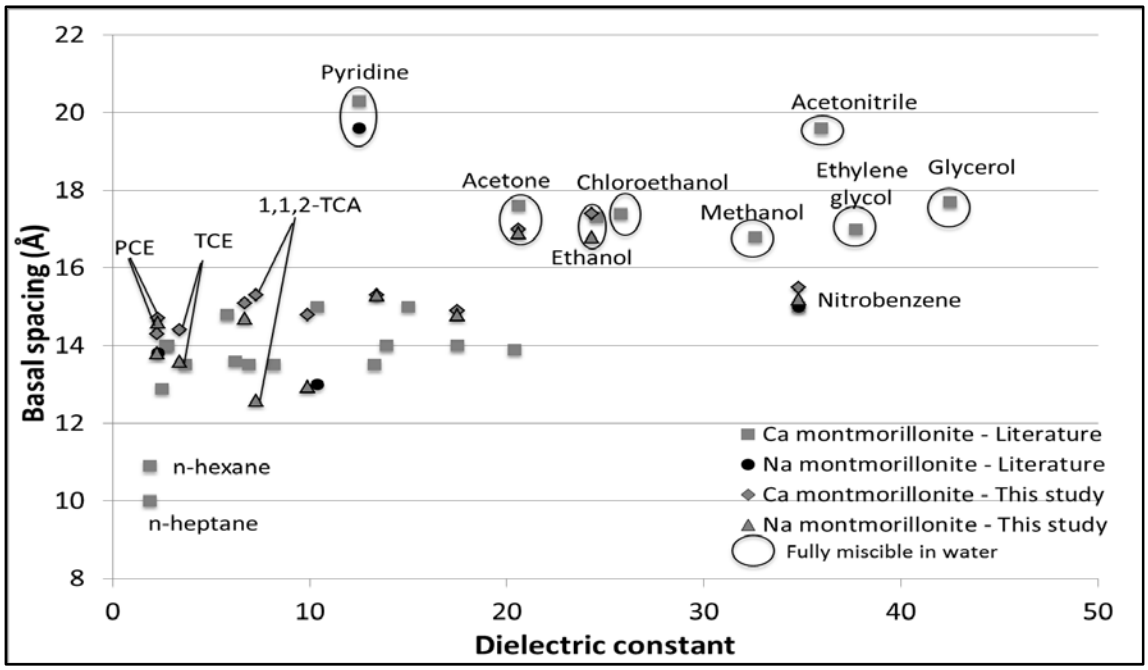

Figure 4.3 Comparison of basal spacings for air-dry montmorillonite contacted with pure organic liquids measured in this study with those reported in the literature (MacEwan, 1948; Greene-Kelly, 1955; Berkheiser and Mortland, 1975; Griffin et al., 1984).

The basal spacings for air-dry Ca-montmorillonite in contact with the TCE-based waste and the PCE-based waste were 15.2 ± 0.01 Å and 14.7± 0.7 Å, respectively, similar to those for the clays in contact with their pure solvent counterparts of 14.4 and 14.7 Å (Figure 4.2). Analogous behavior was observed for Na-montmorillonite: the basal spacing for Na-montmorillonite was 15.0 Å and 13.9 Å in contact with the TCE- and PCE-based

DNAPLs, respectively, whereas the basal spacing of Na-montmorillonite in contact with pure TCE and PCE was 13.6 $\pm$ 0.2 and 14.6 $\pm$ 0.7 Å respectively. Thus, it appears that the DNAPL wastes have an impact on the basal spacing of air-dry clays similar to that of their pure solvent counterparts.

At the contaminated sites, however, waste DNAPLs contact water-saturated clays. To investigate whether contact with chlorinated organic liquids can cause a change in the basal spacing of water-saturated clays, additional XRD measurements were conducted with clay samples taken from the vials and beakers in which the clays were saturated with a 0.005 M $CaSO_4$ aqueous solution and then contacted with pure chlorinated solvents or DNAPL wastes. The basal spacings for these systems are shown in Table 4.4. The basal spacings for water-saturated clay in contact with pure TCE for 56 days in a vial were 17.9 Å and 18.8 Å, respectively for Ca- and Na-montmorillonite, similar to the measured basal spacings in contact with just water (Figure 4.2). The bentonite sample extracted from the layered beaker system in contact with pure PCE for 319 days had a basal spacing of 19.5 Å. Thus, if the clays were initially saturated with water, even extended contact with pure chlorinated solvents did not appear to alter the clays' basal spacing appreciably from the values obtained from contact with just water.

Table 4.4 also presents basal spacing measurements for water-saturated montmorillonites in contact with PCE-based DNAPL waste in a vial at 18 and 180 days. These measurements show that at even 18 days, the intraparticle structure of Na-montmorillonite has started changing, yielding two peaks in the XRD profile (Figure 4.4.a). The peak with the higher intensity represents layers with a basal spacing of 20.9 Å, so the space between those layers still contain water. However, the other peak indicates the

existence of regions with a basal spacing of 14.0 Å, locations where the spacing has contracted from 20.9 Å to 14.0 Å. Figure 4.4.b and Figure 4.4.c show XRD profiles obtained from samples of Na-bentonite taken from a beaker in which water-saturated bentonite was in contact with TCE-based DNAPL waste for 105 days. These profiles show a shift in the basal spacing of the clay, with a greater shift occurring in the surficial sample (Figure 4.4.b) than in the one from below the surface (Figure 4.4.c). Therefore, these profiles suggest that the structure of water-saturated sodium smectites can contract due to contact with DNAPL wastes, shifting from a basal spacing indicative of contact with water to one indicative of contact with a low-solubility organic liquid.

Table 4.4 Basal spacings of water-saturated smectites contacted with pure chlorinated solvents or DNAPL waste.

Vials (Contact time)	Basal spacing of Ca-montmorillonite* (Å)	Basal spacing of Na-montmorillonite (Å)	
		From 1st peak	From 2nd peak
TCE (56 days)	17.9	18.8	NP
PCE waste (18 days)	17.7	20.9	14.0
PCE waste (180 days)	18.5	19.4	13.0

Beakers (Contact time)	Basal spacing of Na-bentonite (Å)	
	From 1st peak	From 2nd peak
PCE (319 days)	19.5	NP
TCE waste (105 days) (sample from the surface)	18.3	14.5
TCE waste (105 days) (sample from below the surface)	19.4	15.7

*For Ca-montmorillonite samples, only a single peak was found. NP indicates that a second peak was not present.

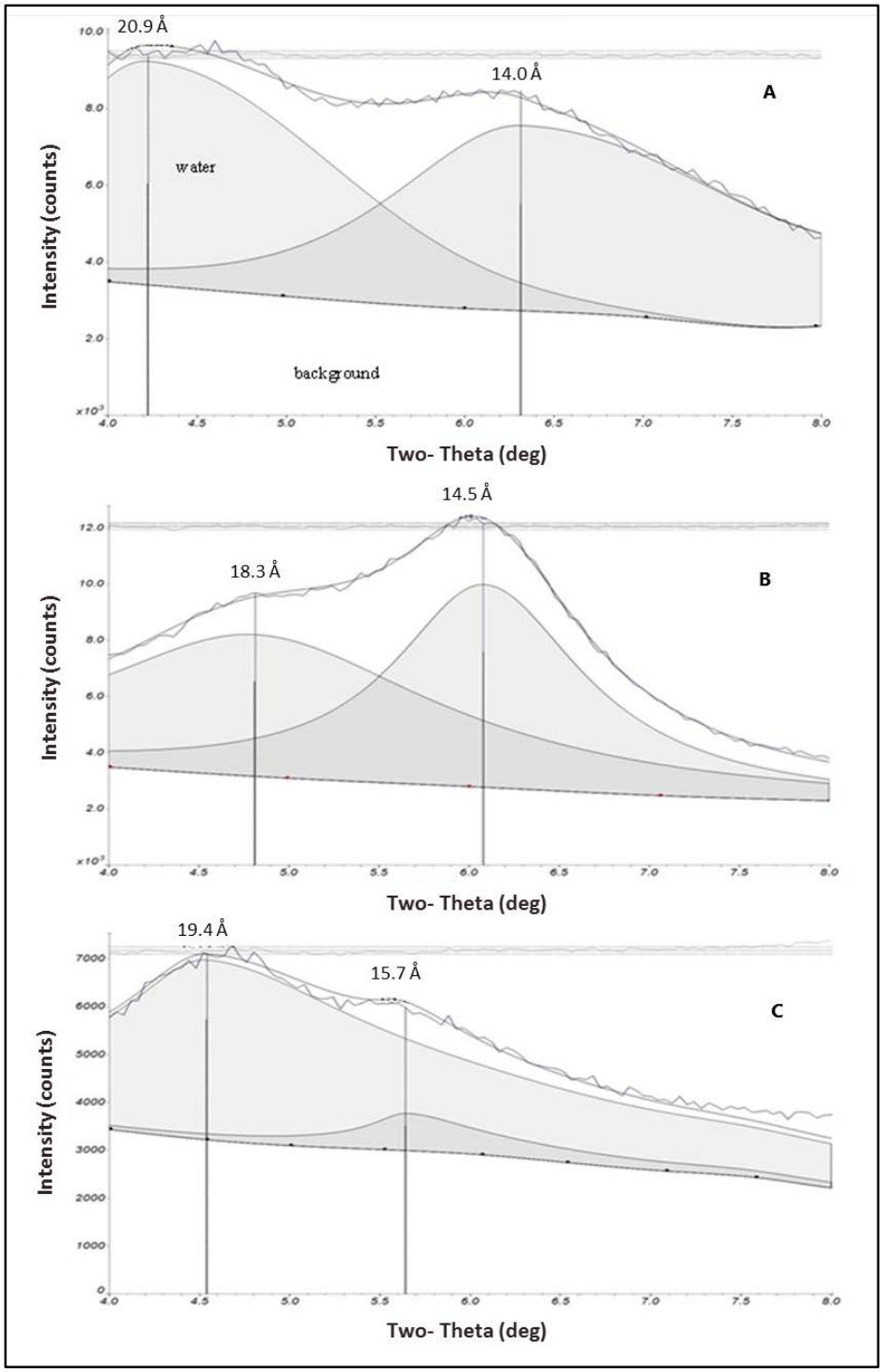

Figure 4.4 XRD profiles for A) water-saturated Na-montmorillonite in contact with PCE-based DNAPL waste for 18 days, B) Na-bentonite taken from the clay layer surface from a beaker containing TCE-based DNAPL waste ponded on top of the water-saturated clay for 105 days; and C) Na-bentonite taken from beneath the clay layer surface from a beaker containing TCE-based DNAPL waste ponded on top of the water-saturated clay layer for 105 days.

Decreases in the basal spacing of the sodium smectites caused by the contact with DNAPL wastes were accompanied by cracking. Cracking of the waste microcosms started after about ten days of contact (Figure 4.5.a). At 40 days of contact, the length and number of cracks had grown considerably, forming polygonal patterns on the surface of the clay. Fourteen days later, new cracks were still forming and the existing cracks were growing both in length and aperture (Figure 4.5.b). After 175 days of contact, the pattern of the cracks had essentially stabilized; only one additional crack seemed to have formed (Figure 4.5.c). Although no changes had occurred in the pattern of the clay between days 175 and 251 (Figure 4.5.d), the aperture of the cracks continued to grow. Therefore, it seems that approximately within the first fifty days, the general pattern of cracking is established and, as time proceeds, the pattern does not change, but the aperture of the cracks continues to grow, albeit at a reduced rate.

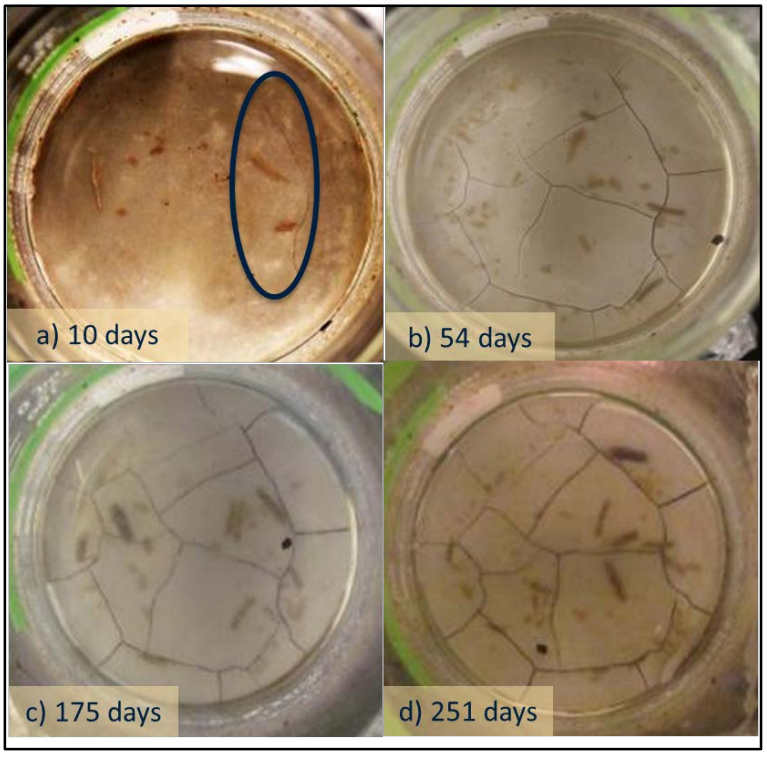

Figure 4.5 Photographs showing the cracking of Na-bentonite in contact with PCE-based DNAPL waste over time a) 10 days, b) 54 days, c) 175 days, and d) 251 days.

On the surface of the bentonite shown in Figure 4.5.d, 15 segments were formed with 18 intersections resulting in a segment per intersection value of 0.83. Four out of five segments in the middle of the surface are polygons with more than five sides. Compared to cracks resulting from desiccation, the number of segments per intersection is lower than the reported range (1.5-2), and the more common square or quadrangle shape segments were not observed. The lengths and apertures of the cracks were determined from the photographs shown in Figure 4.5.c and Figure 4.5.d using ImageJ (Table 4.5). The average crack length at 251 days was 6.3 mm and the average aperture size was 0.68 mm. The area of the cracks was also calculated using the aperture size and length. Based on this, the fraction of crack area per unit surface area was found to be almost 5% after 251 days of contact. Although the total crack length and the aperture percentage between 400 and 1000 μm are almost the same at 175 and 251 days, the aperture percentage over 800 μm has increased three-fold.

Table 4.5 Crack apertures in water-saturated Na-montmorillonite in contact with PCE-based DNAPL waste at 175 and 251 days of contact.

Aperture (μm)	Percent of total length at 175 days*	Percent of total length at 251 days*
200-400	14.6	9.8
400-600	36.6	24.7
600-800	39.9	41.4
800-1,000	5.4	14.2
>1000	3.3	9.9

*Total crack length is 56.7 cm and 57.3 cm at 175 and 251 days, respectively, on a surface of 78.5 cm^2.

Figure 4.6.a shows cracks in Na-montmorillonite in a vial containing PCE waste at 18 days, and Figure 4.6.b shows cracks in Na-montmorillonite in the beaker containing TCE waste at 105 days. The side of the beaker at 146 days of contact with PCE waste showed that some of the cracks have extended through the clay layer to the sand beneath.

At this point, the crack in Figure 4.6.c was sufficiently large that it was beginning to serve as a conduit for the DNAPL to migrate into the sand layer below. On the other hand, water-saturated bentonite in contact with pure PCE did not show cracking even after 319 days (Figure 4.6.d), consistent with the lack of change in the basal spacing measurements (Figure 4.2). This observation is in contrast with that by McCaulou and Huling (1999) who reported cracking of bentonite in contact with chromatography-grade TCE. It should be noted that in the experimental observations reported here, the applied hydraulic head was minimal (only 2.5 cm of organic solvent was ponded on top of the saturated clay), whereas in the case of the experiments of McCaulou and Huling (1999), a hydraulic head of up to 7 m was applied, which may have precipitated the cracking.

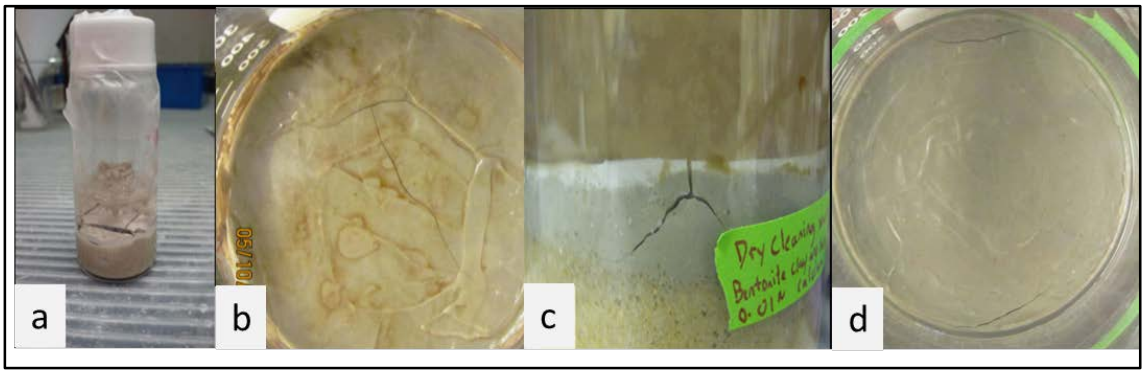

Figure 4.6 Photographs of cracks (from left to right) a) water-saturated Na-montmorillonite in contact with PCE-based DNAPL waste for 18 days in a vial; b) water-saturated Na-bentonite in contact with TCE-based DNAPL waste for 105 days: top view of microcosm in beaker; and c) water-saturated Na-bentonite in contact with PCE-based DNAPL waste for 146 days: side view of microcosm in beaker; d) water-saturated Na-bentonite in contact with pure PCE for 319 days.

4.4 Conclusions

The basal spacing of air-dry Na-montmorillonite clay contacted with chlorinated solvents is similar to the basal spacing in contact with air, and is consistent with the basal spacing of such materials in contact with low-miscibility nonchlorinated solvents. Contact

of water-saturated clays with pure chlorinated solvents did not lead to basal spacing changes, even after extended contact (up to 319 days). Similarly, contact of water-saturated Ca-montmorillonite with DNAPL wastes did not result in basal spacing changes. However, contact of water-saturated Na-smectites with DNAPL wastes led to basal spacing changes and significant cracking over the time frame of weeks to months. This finding suggests that passive contact with chlorinated DNAPLs over the time frame associated with hazardous waste sites may lead to basal spacing changes in the sodium smectite clay minerals in the clay layers at these sites. The shrinkage of the basal spacing may result in cracking allowing enhanced transport into the clay layers and may be the reason behind the greater than expected storage observed in the field and the extended remediation times associated with this phenomenon.

4.5 Implications of Crack Formation on Mass Storage

Chapter 3 showed that the measured effective diffusion coefficient of TCE was five times to two orders of magnitude lower than that deduced from field measurements. Calculations of mass accumulation reported in Section 3.5 suggest that the discrepancy in diffusion coefficients would result in a 2-17 fold overestimate of the mass storage in an aquitard over a 30-year time period attributed to diffusion. The research presented in this chapter shows that cracks can form in a clay layer in a relatively short time period. These cracks could enhance the solute transport into aquitards, or alternatively, permit the entrance of free phase DNAPL directly into the aquitard.

As illustrated in Section 3.5, the total mass of TCE in a model aquitard (Figure 3.17) was 4 - 29 g (Table 3.22) when the diffusion of TCE into the aquitard was modeled

as diffusion into a competent clay layer. To assess the impact of cracks, it was assumed that the crack length per unit surface area was the same as that reported in Table 4.5, or 0.73 m/m^2, giving a length of 7.3×10^3 cm on the 10^4 cm^2 surface of the model aquitard. The cracks were also assumed to form circles of a set diameter packed openly, rather than polygons of varying diameters. Based on these assumptions, the number of crack circles on the surface of the 1 m^2 model aquitard was calculated as 540, and the diameter of one circle was 4.3 cm (Figure 4.7). The information was not collected on the depth of the cracks; however, the photograph in Figure 4.6.c showed that the crack extended almost through the entire clay layer in the beaker. Based on this, the cracks were taken as 1 cm in depth. Two different scenarios were then considered: first, it was assumed that DNAPL did not enter into cracks directly; rather the cracking resulted in advective transport of TCE as a solute into the cracks. The mass accumulated in this scenario would have three different components: mass storage due to diffusion into a plane sheet, mass storage due to advection into the cracks, and mass storage due to diffusion from the cracks into the cylinders (Figure 4.7). The mass per unit area due to diffusion into a plane sheet was calculated in the same manner as in Section 3.5, neglecting the horizontal surface area of the cracks. The mass storage due to advection into the cracks was calculated by assuming that at t = 30 years, the distance travelled by the advective front was at least 1 cm. Thus, this was computed using the dissolved TCE concentration of 100 mg/L and the volume of the cracks. The volume was calculated as 50 cm^3 based on a length = 7.3×10^3 cm, a depth = 1 cm, and a median aperture of the cracks = 6.8×10^{-3} cm, based on the distribution shown in Figure 4.8.

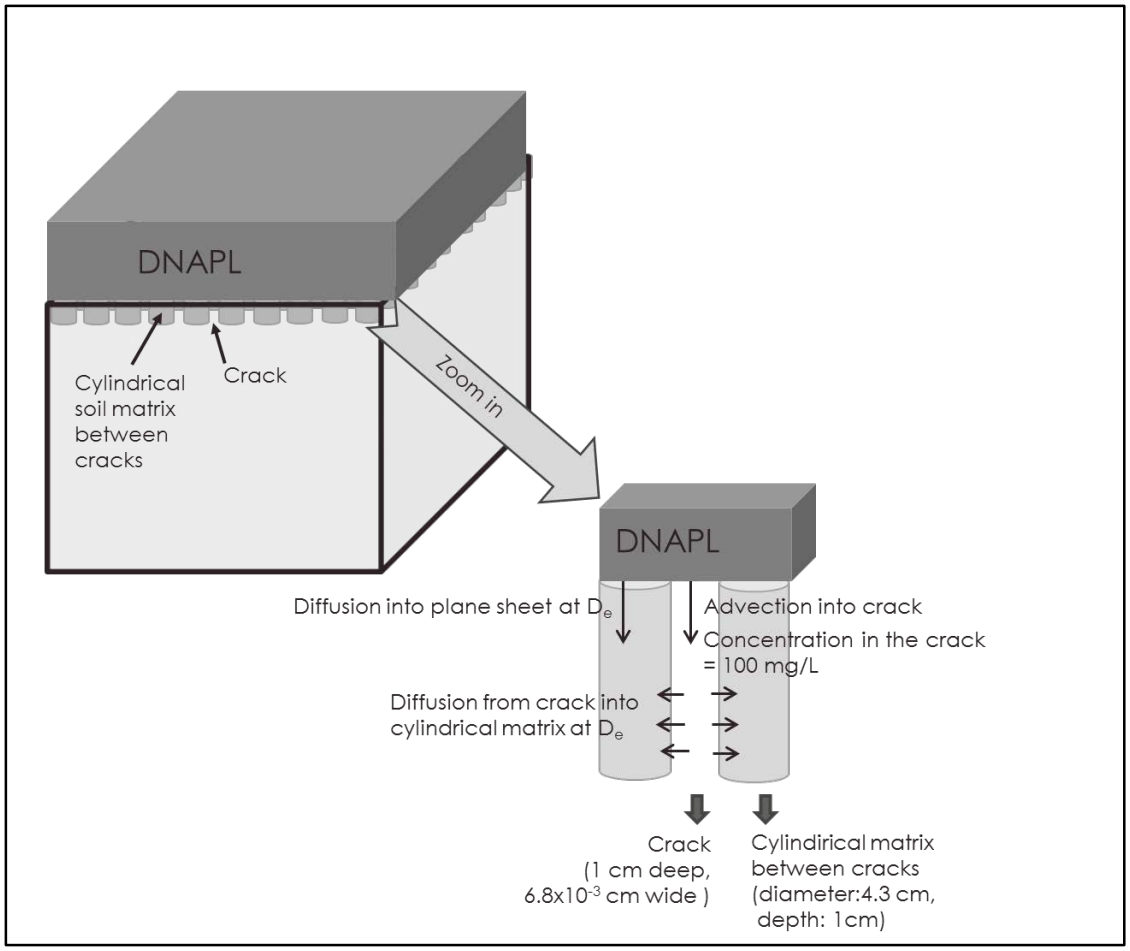

Figure 4.7 First scenario where DNAPL does not occupy the cracks but the moves into the cracks with advection.

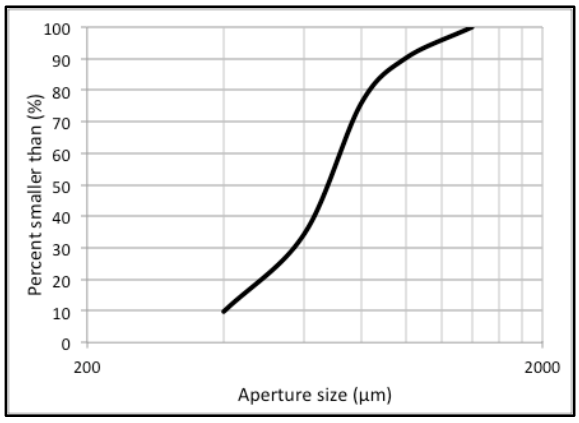

Figure 4.8 Distribution of crack aperture size on the bentonite surface as a result of 251 days of contact with PCE-based DNAPL waste (data from Table 4.5).

The mass entering the cylindrical soil matrix in between cracks can be calculated by Equation 4.1 at small times (Crank, 1975).

$$\frac{M_t}{M_\infty} = \frac{4}{\pi^{1/2}}\left(\frac{D_e t}{r^2}\right)^{1/2} - \frac{D_e t}{r^2} - \frac{1}{3\pi^{\frac{1}{2}}}\left(\frac{D_e t}{r^2}\right)^{\frac{3}{2}} + \cdots \qquad \text{(Equation 4.1)}$$

where M_t is the total amount of diffusing substance per unit area which enters the cylinder in time t; r is the radius of the cylinder; and M_∞ is defined by:

$$M_\infty = r\left\{\frac{1}{2}C_s\right\} \qquad \text{(Equation 4.2)}$$

where C_s is the initial, uniform concentration at the surface of the cylinder.

In the scenario modeled here with cylinders of a diameter = 4.3 cm, the maximum amount per surface area (M_∞) would be achieved in less than a year. As the mass storage calculations were based on 30-year time frame in this study, M_∞ was used as the mass per surface area in one cylinder due to diffusion into cylinders in between cracks. Thus, the total mass in the cylinders was calculated by multiplying M_∞ by the surface area of each cylinder and the total number of cylinders, 540.

In this case, the mass diffused into the aquitard from the top surface was found to be 29 g, the mass transported through advection into the cracks was 0.005 g, and mass diffused from the cracks into the cylindrical soil matrix was 0.8 g (Table 4.6). So, the overall mass (around 29.8 g) was only 3% higher than the mass attributed to diffusion into a plane sheet (29 g in Section 3.5) and failed to explain the mass storage in the aquitard of 62.6 g based on the diffusion coefficient reported by Johnson et al (1989).

In the second scenario, it needs to be assessed if DNAPL can overcome the entry pressure and enter into a crack which is water-wet and water-saturated. The height of the DNAPL pool required for a DNAPL to penetrate into the crack is given by Equation 2.2. The interfacial tension of the TCE-based field waste was 3 dyn/cm, the density was 1.30

g/cm^3, and the contact angle was 30^o (Table 3.7) (Hsu, 2005). Using the median aperture size of 680 µm, determined from the crack aperture sizes at day 251 (Figure 4.8), it was determined that the depth of pooling necessary for free phase DNAPL to enter a crack of this aperture is only 6 cm. As this pool height is well below the observed range (Oolman et al., 1995; Parker et al., 2003; Parker et al., 2004), the entrance of DNAPL into such a crack is a distinct possibility.

Using the assumed length and depth of the cracks in addition to the median aperture size, similar to the first scenario, the volume of the cracks was calculated 50 cm^3 in the 1 m x 1 m x 5 m domain shown in Figure 4.9. Based on the volume of the cracks and the density of the DNAPL waste, the additional mass accumulation due to the presence of free phase DNAPL in the cracks is 64.5 g. Thus, the total mass stored in the aquitard increases to 94.3 g, which is substantial enough to explain the mass calculated from the diffusion coefficient observed in the field (Table 3.22).

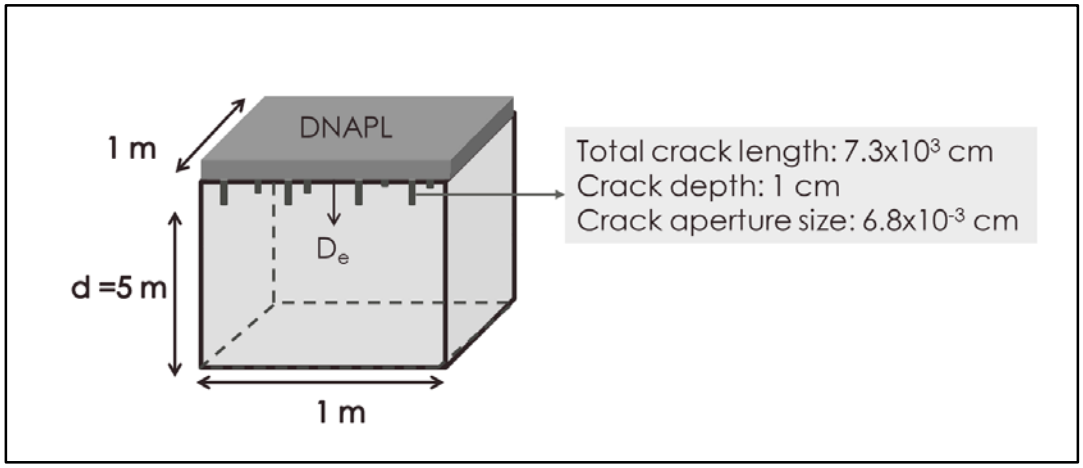

Figure 4.9 Second scenario where DNAPL is in the cracks.

Table 4.6 Mass storage in the model aquitard after 30 years.

	Mass due to diffusion into domain from top surface (g)	Mass due to advection into domain (g)	Mass due to diffusion from the cracks (g)	Mass due to DNAPL presence in the cracks (g)	Total mass (g)
Diffusion into cracks	29.0	0.005	0.8	-	29.8
DNAPL present in the cracks	29.0	-	0.8	64.5	94.3

These results imply that the high observed "diffusion rates" observed in the field may be attributable to small-scale cracking in the clay lenses or aquitards. Because of the possible significant ramifications, the mechanism of cracking needs to be elucidated. Thus, the following chapter summarizes the investigation into the mechanism by which the basal spacing is reduced when such clays are saturated with water.

Chapter 5
Investigation of Possible Mechanism Leading to Modification of Basal Spacing and Cracking of Smectitic Clays

Work reported in Chapter 4 demonstrated that pure chlorinated solvents cannot modify the basal spacing of water-saturated smectitic clays, whereas the passive contact with DNAPL waste caused the cracking of water-saturated Na-montmorillonite in a time frame on the order of weeks, accompanied by a decrease in the basal spacing of the clay. This finding indicated a key role played by other components in DNAPL waste. The question now becomes what are the chemical components necessary for the contraction of the basal spacing of water-saturated montmorillonite in the presence of DNAPL waste, and how is the reduction accomplished.

To determine a mechanism, it is essential to know what components of the DNAPL waste are important. Screening experiments were designed utilizing different combinations of compounds, based on an understanding of what might be present in the DNAPL wastes utilized in this study. The mixture that caused cracking and basal spacing reductions in a time frame similar to the actual DNAPL wastes was utilized in XRD, sorption and Fourier Transform Infrared Spectroscopy (FTIR) experiments to elucidate a possible mechanism for basal spacing reduction.

5.1. Background

The characteristics of the DNAPL wastes obtained from the field are presented in Table 3.7. One of the wastes comes from a dry cleaner, the other from an Air Force base and is a degreasing waste. Tetrachloroethylene used at dry cleaners is rarely used in its pure form. For example, Linn and Stupak (2009) provides a list of dry cleaning cosolvents, including propanol and 2-butoxyethanol, among other glycol ethers. Moreover, the report lists pre-cleaning agents such as potassium hydroxide and oxalic acid for water-based spotting agents, and amyl acetate and acetone for solvent-based spotting agents that may be applied prior to using PCE. In another report, prepared by Earnest et al. (1997), some additional spotting agents were reported: Pyratex is among the most commonly used. Based on the Material Safety Data Sheet (MSDS) for Pyratex (http://www.autolaundrysystems.com/msds/Pyratex.pdf), this agent contains an aliphatic carboxylic ester (e.g., n-butyl acetate), a glycol ether (e.g., 2-butoyethanol), and an aliphatic ketone (e.g., methyl isobutyl ketone). Therefore, six groups of water-soluble compounds that may be present in the PCE waste were identified: inorganic compounds (e.g., potassium hydroxide), alcohols (e.g., propanol), aliphatic carboxylic esters (e.g., n-butyl acetate and amyl acetate), glycol ethers (e.g., 2-butoxyethanol), aliphatic ketones (e.g., methyl isobutyl ketone and acetone), and acids (e.g., oxalic acid).

In addition to these solutes, surfactants are another common ingredient of DNAPL waste (Hsu, 2005). Surfactants can change the interfacial properties of the solvent even at low concentrations (Rosen, 2004), thereby enhancing the solvent's cleaning performance (Myers, 2006). The significance of surfactants lies in their amphipathic chemical structure: a hydrophilic head and hydrophobic tail which allow the surfactants to interact with both

polar and nonpolar compounds. Depending on the charge of the head group, they are classified as cationic, anionic, or nonionic; anionic (e.g., dioctyl sodium sulfosuccinate [AOT]) or nonionic (e.g., polyethylene glycoltert-octylphenyl ether [TritonX-100] and hexaethylene glycol monododecyl ether [$C_{12}E_6$]) surfactants are preferred in dry cleaning or degreasing mixtures (Hsu, 2005).

Smectite surfaces are negatively charged and hydrophilic (Moore and Reynolds, 1997). As a consequence of the electrostatic attraction, cationic surfactants can readily sorb onto clay (Shen, 2001; Sanchez-Martin et al., 2008). Once the cationic surfactants have sorbed, they can enhance the sorption of nonpolar solvents, as increased sorption of organic compounds like aniline and benzene on smectite treated with cetyltrimethylammonium bromide (CTAB) has been reported (Zhu et al., 1998). Similarly, the sorption of chlorophenols on montmorillonite modified by nonionic surfactants was found to increase (Deng et al., 2003). However, the sorption of nonionics usually occurs through hydrogen bonding (Somasundaran and Krishnakumar, 1997; Zhang and Somasundaran, 2006), a weaker type of interaction than electrostatic interaction, resulting in less sorption (Somasundaran and Krishnakumar, 1997; Shen, 2001; Levitz, 2002; Deng et al., 2003; Sanchez-Martin et al., 2008). Due to the negatively-charged head group, anionic surfactants sorb considerably less due to the repulsion between the clay surface and the surfactant molecule, with sorption almost an order of magnitude lower than that of a nonionic surfactant (Del Hoyo et al., 2008; Sanchez-Martin et al., 2008).

The basal spacing of smectite minerals has been measured to complement the measurements of surfactant sorption. In the case of cationic surfactants such as octadecyltrimethylammonium (ODTMA) or hexadecyltrimethylammonium (HDTMA)

bromide, the basal spacing increased up to 19.5-21 Å (Lee et al., 2004, Lee et al., 2005, Sanchez-Martin et al., 2008). Even larger basal spacings were observed with the cationic surfactant cetyltrimethylammonium bromide (CTAB), ranging from 14.4 to 37.7 Å as the surfactant loading increased from 23% to 257% of Na-montmorillonite's cation exchange capacity (98 meq/100 g) (Hu et al., 2013). This expansion was interpreted as intercalation of the cationic surfactant into the interlayer space of the smectite (Shen, 2001; Lee et al., 2004; Hu et al., 2013), with the conformation of the sorbed cationic surfactant molecules changing from a lateral monolayer to a lateral bilayer, a paraffin monolayer and a paraffin bilayer, leading to basal spacings even higher than that with water. Williams-Daryn and Thomas (2002) contacted vermiculite clays treated with alkyltrimethylammonium bromides with several organic compounds (toluene, hexane, cyclohexane, and ethanol) and measured the basal spacing. With exposure to these solvents, further increases in the basal spacing, up to 48 Å, were observed.

Nonionic surfactants (polyethylene glycol ether, polyoxyethylene-(20)-stearyl-ether, polyoxyethylene (10) cetyl ether, polyoxyethylene (12) nonylphenyl ether, polyoxyethylene-(23)-lauryl-ether, polyethylene glycol tert-octylphenyl ether) caused an expansion of the lattice of smectite clay with the sample, with a dry basal spacing of up to around 17 Å. But, unlike the situation with cationic surfactants, a continuous expansion of the clay structure greater than that with water was not observed (Shen, 2001; Deng et al., 2003; Sonon and Thompson, 2005; Sanchez-Martin et al., 2008). Additionally, the basal spacing of bentonite modified by nonionic surfactants was studied, but it was found that the intercalation of nonionic surfactants did not enhance the sorption of cyclohexane, toluene, octanol, or glycerol, as in the case with smectites treated with cationic surfactants

(Deng et al., 2003). Based on this finding, it was proposed that the surfactants were not entering the interlayer space and the hydrophilicity of the interlayer space was not affected. Thus, the sorption of surfactants that was observed was occurring on the exterior of the clay particles. With respect to anionic surfactants, the lack of any change in basal spacing has led researchers to surmise that anionic surfactants are excluded from the interlayer space montmorillonite (Sanchez-Martin et al., 2008), and any sorption that is occurring is probably on the exterior of the clay particles.

The studies cited above considered the interaction of a single surfactant with clay. However, a DNAPL waste contains a surfactant mixture. The degree of sorption of an individual surfactant can be modified due to synergistic interaction among the different surfactant molecules, depending on the surface properties of the sorbent and sorbate as well as the concentration of the surfactants. For example, the sorption of an anionic surfactant onto kaolinite from a mixture of anionic-nonionic surfactants was greater than that in the presence of the anionic surfactant by itself, when the concentration was lower than the critical micelle concentration (CMC). However, the sorption of the anionic surfactant was less when the concentration was above CMC (Xu et al., 1991). The same study observed an enhanced sorption of the nonionic surfactant from the anionic-nonionic surfactant mixture both below and above the CMC. In another study, the sorption of a nonionic surfactant on silica decreased in the presence of an anionic surfactant in the mixture when the concentration was above CMC and no impact was observed below the CMC (Gao et al., 1984). The hydrophobic chain-chain interaction of the surfactants and the reduction of the repulsive forces between the negatively-charged heads of anionic surfactants by the nonionic surfactant were offered as possible explanations for such synergism (Xu et al.,

1991; Zhang and Somasundaran, 2006). However, contradictory results suggest that there are other properties of the system playing a role: for instance, Somasundaran and Huang (2000) determined that the chain lengths of the nonionic and anionic surfactants influence the shielding of charge and, in turn, the degree of sorption. It should be noted that all the studies cited above examined surfactant sorption from aqueous solutions, and there are not comparable studies looking at sorption from nonpolar solvents.

To obtain greater detail of the interlayer space of clays during dehydration and surfactant sorption, FTIR spectroscopy has been used. The band at a wavenumber around 1635 cm^{-1} is assigned to the bending vibration of water (H-O-H) that is structurally bonded in the interlayer space (Madejová and Komadel, 2001). The location of this band is correlated with the water content of the clay, with a decrease in the wavenumber occurring as a result of dehydration (Russell and Farmer, 1964; Johnston et al., 1992). On the other hand, the sorption of surfactants into the interlayer space of clay minerals may cause an increase, as, for instance, Ma et al. (2010) reported an increase from 1634 to 1649 cm^{-1} in the H-O-H bending band with increasing cationic surfactant loading. Similarly, it was observed that after being treated with nonionic surfactants, the location of H-O-H bending band of water in smectites shifted from a wavenumber of 1633 to 1645 cm^{-1} (Deng et al. 2003), and from 1636 to 1643 cm^{-1} (Del Hoyo et al., 2008). All of these studies attribute this increase in wavenumber to the partial displacement of water molecules from the interlayer space. Yet, again, these studies examined the changes in the H-O-H bending band as a result of changes in the aqueous chemistry, and complementary work in nonpolar organic solvent systems is not available.

In summary, evidence reported in the literature suggests that water miscible organic solutes and aqueous solutions of nonionic surfactants increased the basal spacing of dry smectites up 16-17 Å. Aqueous solution of anionic surfactants caused less swelling of dry smectite, up to a basal spacing of 14-15 Å. Since the clay minerals found in the aquitards are water-saturated, the impact of these components on the basal spacing of water-saturated smectites needs to be assessed. However, there appears to be little work examining the basal spacing of water-saturated smectites exposed to organic solvents or surfactants; the presumption is if they are sufficiently small molecules, are water-miscible, and are not negatively-charged, they can enter the interlayer space of water saturated smectitic clay minerals. As a result of this entrance, a decrease in the basal spacing of water-saturated smectites from 18-19 Å to 16-17 Å may be postulated. On the other hand, the results presented in Chapter 4 suggest that non-polar low solubility chlorinated organic solvents do not appear have the ability to adjust the basal spacing if the interlayer space is already occupied by water. However, the basal spacing for samples of bentonite that cracked was found to be around 15 Å (Table 4.4), implying that the presence of water-soluble organic compounds, surfactants, or chlorinated organic solvents fail to explain this observation if they are considered individually. Therefore, it is hypothesized that the reduction in basal spacing is a synergistic phenomenon, with components of the DNAPL waste modifying the basal spacing of water-saturated smectites only when they are present together.

The first hypothesis as to how the basal spacing reduction might occur is that water-soluble organic compounds present in the waste dissolve into the water present in the interlayer spacing of clay, creating a solution with a reduced polarity. Acting as a co-

solvent, they then facilitate the dissolution of high concentrations of a chlorinated compound into the interlayer spacing, with the net result of a reduction in the basal spacing.

A similar hypothesis can be developed based on the surfactant content. Studies have shown that surfactants can sorb in the interlayer spacing and the sorption can lead to increased sorption of nonpolar organic compounds. Thus, if the surfactants present in the DNAPL waste sorb in the interlayer space, they provide an organic-rich site for the nonpolar chlorinated compounds in the interlayer space, leading to a reduction in the basal spacing.

With these hypotheses in mind, screening experiments were performed to ascertain which components of DNAPL needed to be present to cause cracking and a decrease in basal spacing. Sorption experiments were also performed to determine the degree of sorption of the various necessary components. Lastly, FTIR measurements were made to determine whether water molecules were displaced from the interlayer space. Based on these experimental results, a mechanism was proposed to explain how a decrease in basal spacing in water-saturated Na-montmorillonite may occur due to contact with DNAPL waste.

5.2. Materials and Methods

5.2.1. Screening Experiments

To ascertain which components of DNAPL waste may be responsible for the reduction in the basal spacing of Na-smectites, a series of experiments were performed. To determine whether water soluble organic components in the DNAPL wastes were enhancing the solubility of the chlorinated organics, the dry cleaning PCE waste and the

degreasing TCE waste were contacted with water at a volume ratio of 4:1 (waste:water) for 56 days. After this period of equilibration, the aqueous phase was extracted with toluene at a 5:1 volume ratio (toluene:water). The toluene phase was then analyzed for concentrations of PCE and TCE by the method described in Section 3.2.2.b.

In addition, a suite of 20 vials was set up. About one gram of bentonite put into each 20 mL glass vial and contacted with 10 mL of a 0.005M $CaSO_4$ solution to saturate it. After two weeks, any excess water was removed. The solutions summarized in Table 5.1 were prepared using the water-soluble compounds at concentrations given in Table 5.2 and surfactants, whose structures are shown in Figure 5.1, at concentrations given in Table 5.3. Then, 15 mL of one of these solutions was added on top of the clay, using a pipette. The vials were capped, stored at room temperature and observed over 90 days. Pictures were taken periodically to record visual changes such as the relative degrees of horizontal and vertical cracking as well as changes in clay color over time.

5.2.2. Basal Spacing Measurements

Bentonite was contacted with water in glass vials as in the screening experiments. After two weeks, the excess water at the surface was removed and the clay paste was mixed for homogeneity. Two grams of the clay paste were then transferred into a 30-mL centrifuge tube (Nalgene, Rochester, NY). 20 mL of a solution containing combinations of TritonX-100, AOT and $C_{12}E_6$ as solutes, dissolved in either water or PCE, were added into the tubes. The first set of tubes were rotated for at least four days followed by passive contact of at least one week; the second set of tubes were rotated for three weeks. The clay-solution mixture was centrifuged at 600xg relative centrifugal force (RCF) for 20 minutes and the solid phase was analyzed by XRD.

Table 5.1 Mixtures prepared to observe structural changes in water-saturated bentonite clay.

Vial	Surfactant			Alcohol	Aliphatic ketone	Glycol ether	Aliphatic carboxylic ester	Solvent
	Triton X-100	$C_{12}E_6$	AOT					
1				✓	✓	✓	✓	Water
2	✓							Water
3	✓	✓	✓	✓	✓	✓	✓	Water
4	✓							PCE
5	✓						✓	PCE
6	✓			✓	✓		✓	PCE
7		✓	✓					PCE
8		✓	✓	✓	✓	✓	✓	PCE
9	✓	✓	✓					PCE
10	✓	✓	✓	✓	✓			PCE
11	✓	✓	✓	✓	✓	✓		PCE
12	✓	✓	✓	✓	✓	✓	✓	PCE
13	✓	✓	✓				✓	PCE
14	✓	✓	✓	✓	✓		✓	PCE
15				✓				PCE
16					✓			PCE
17						✓		PCE
18				✓	✓	✓	✓	PCE

Table 5.2 Concentration of compounds used in screening experiments.

Chemical group	Compound	Concentration (mg/L)
Alcohol	Propanol	50
Aliphatic ketone	Acetone	10
	Methyl isobutyl ketone	2550
Aliphatic carboxylic esters	Amyl acetate	525
	n-Butyl acetate	528
Glycol ethers	2-Butoxyethanol	8992

Table 5.3 Properties of surfactants used in screening experiments.

	AOT	TritonX-100	$C_{12}E_6$
Chemical formula	$C_{20}H_{37}NaO_7S$	$C_{14}H_{22}O(C_2H_4O)_n$ (n = 9-10)	$C_{24}H_{50}O_7$
Concentration used in screening experiment (mM)	3.3	3.3	6.7
Molecular weight (g/mol)	456	625	451
Critical micelle concentration (mM)	1.56[a]	0.22[b]	0.071[a]
Source	Fisher Scientific (anhydrous)	ICN Biomedicals	Sigma Aldrich

[a]Hsu (2005); [b]Cuypers et al. (2002)

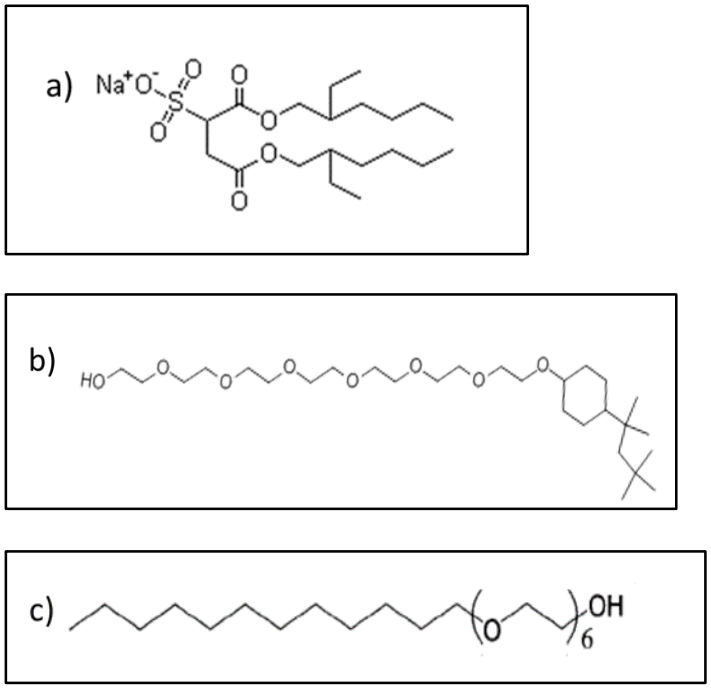

Figure 5.1 Molecular structure of a) AOT, b) TritonX-100, c) $C_{12}E_6$

5.2.3. Fourier Transform Infrared Spectroscopy (FTIR)

After XRD analysis, the samples were placed back into the centrifuge tubes. The same samples were then analyzed by using FTIR (Spectrum BX, Perkin Elmer, Boston, MA) with a MIRacle attenuated total reflectance (ATR) accessory. First, the background was scanned in a range of 650 cm^{-1} to 4000 cm^{-1} at a resolution of 4 cm^{-1}. Then, the sample

was placed on the ATR crystal, and the data was collected in the transmission mode. The spectra were corrected using the background scan and the peaks on each spectrum greater than the threshold (5% of transmission) were labeled. Similar to basal spacing measurements, two sets of experiments with different rotation and contact times were used. In the first set, bentonite clay in contact with either aqueous surfactant solutions or PCE-based surfactant solutions were rotated for at least four days and contacted with the liquid for almost 6 months. In the second set of experiments, the samples were rotated for three weeks with no additional passive contact. For comparison, scans were also made for solvents and solutions in the absence of clay; the total matrix of FTIR measurements is shown in Table 5.4.

Table 5.4 Experimental matrix for FTIR measurements.

FTIR of solvents and solutions	
Solute	**Solvent**
-	Water
TritonX-100	Water
AOT	Water
TritonX-100 and AOT	Water
-	PCE
TritonX-100	PCE
AOT	PCE
TritonX-100 and AOT	PCE
FTIR of air-dry bentonite	
Solute	**Solvent**
-	-
-	Water
-	PCE
FTIR of water-saturated bentonite contacted with solutions*	
Solute	**Solvent**
TritonX-100	Water
AOT	Water
TritonX-100 and AOT	Water
TritonX-100	PCE
AOT	PCE
TritonX-100 and AOT	PCE

*Concentrations are the same as in Table 5.3.

5.2.4. Sorption Experiments

One gram of Na-montmorillonite clay was saturated with 10 mL of Milli-Q water for two weeks. Similar to the protocol in the basal spacing measurements, excess water was removed from the surface and the clay paste was mixed. Then, two or four grams of the clay were transferred to a 30-mL centrifuge tube. The same surfactant solutions used for FTIR experiments (Table 5.4) were prepared in 50 mL volumetric flasks, and in the case of the surfactant solutions prepared in PCE, 0.06 mL ^{13}C-labeled TCE (Cambridge Isotope Laboratory, MA, >98%) was also injected into the volumetric flasks to examine the sorption of chlorinated solvent onto water-saturated Na-montmorillonite. 20 mL of the surfactant solutions were added into the centrifuge tube on the water-saturated Na-montmorillonite. Following one week of rotation, the tubes were centrifuged at 600xg RCF for 20 minutes. The supernatant phase was sampled to determine the concentration of surfactant left in the solution from which the sorption of surfactant on the Na-montmorillonite was calculated by mass balance.

Determination of AOT concentration

The AOT concentration in the aqueous phase was determined by the same method described in Chapter 3.2.2.c. Calibration standards were prepared in the range of 20-67.5 mg/L and samples were diluted in the range of 28 to 40 times using Milli-Q water. AOT concentrations in PCE were measured using the same analytic column and the same methodology as in Section 3.2.2.c and Table 3.9. A calibration curve was determined over the range of 20-65 mg/L and the samples were diluted 20-40 times using PCE.

Determination of TritonX-100 concentration

TritonX-100 concentrations in the aqueous phase were analyzed using a HPLC (Hewlett-Packard HP 1090, Palo Alto, CA) instrument with a Sedere Sedex 75 ELSD (Richard Scientific, Novato, CA) detector. A Hypersil ODS C18 security guard (ID: 2 mm, L: 4 mm) was used to separate the compound. The liquid program and other parameters used in the method are summarized in Table 5.5 and Table 5.6. The range for the calibration standards was 20-65 mg/L. Samples taken from the supernatant in the centrifuge tubes were diluted 25 to 40 times using Milli-Q water.

The TritonX-100 concentration in PCE was measured using a Hypersil Gold column (1.9 μm , ID: 2.1 mm, L: 50 mm). Method details are given in Table 5.5 and Table 5.7. A calibration curve was obtained over the range of 20-60 mg/L and samples were diluted 5-40 times using PCE.

Table 5.5 HPLC-ELSD method parameters for detection of TritonX-100 in water and PCE.

Injection volume (μL)	20	20
Oven temperature (°C)	60	60
Detector temperature (°C)	69	69
Pressure (bar)	2.2	2.2
Gain	8	8

Table 5.6 Solvent program for TritonX-100 analysis in water.

Time	Acetonitrile (%)	Water (%)	Flowrate (mL/min)
1.00	10	90	0.5
8.50	80	20	0.5
8.60	80	20	3.0
8.80	10	90	3.0
Stop time	10 min		

Table 5.7 Solvent program for TritonX-100 analysis in PCE.

Time	Acetonitrile (%)	Water (%)	Flowrate (mL/min)
1.50	35	65	0.2
4.50	95	5	0.2
8.50	95	5	0.2
8.51	35	65	0.2
Stop time	12 min		
Post-run	3 min		

Determination of ^{13}C-labeled TCE concentration

The concentration of ^{13}C-labeled TCE was analyzed using the same method described in Section 3.2.2.d and Table 3.10.

5.3. Results and Discussions

5.3.1. Screening Experiments

The PCE concentration in the aqueous phase contacted with dry cleaning PCE waste was measured to be 9500 mg/L, with no measurable concentrations of TCE. The concentrations in the aqueous phase contacted with the degreasing TCE waste were 125 mg/L and 500 mg/L for PCE and TCE respectively. The aqueous solubilities of PCE and TCE at 25°C are 150 mg/L and 1370 mg/L, respectively (Riddick et al., 1986). Thus, the components in the dry cleaning PCE-based waste increased the aqueous solubility of PCE significantly, but the components in the TCE-based waste reduced somewhat the aqueous phase solubility of TCE and PCE. Since both the PCE and TCE wastes cracked the clay, but the aqueous solubility increased only in the case of the PCE waste, it does not appear that enhanced solubility of the chlorinated compounds in the interlayer water is the mechanism by which basal spacing reduction occurs.

The main goal of screening experiments was to determine the components of DNAPL waste that cause cracking. The results are summarized in Table 5.8. When only one of the water-soluble organic solutes listed in Table 5.2 was dissolved in the chlorinated solvent (PCE), no crack was observed even in a time frame of longer than 75 days. Moreover, combinations of these compounds dissolved in PCE did not induce cracking, either (Figure 5.2). In addition, vials containing only TritonX-100 or AOT or $C_{12}E_6$ dissolved in PCE did not cause cracking. (Figure 5.3.a and b, respectively). On the other hand, cracking of the water-saturated bentonite occurred in less than two weeks in the vial containing nonionic and anionic surfactants dissolved in PCE (Figure 5.4.a). Therefore, it was concluded that a surfactant combination was vital to observe cracking. As the same surfactants dissolved in water did not cause the formation of cracks (Figure 5.4.b), the implication is that the chlorinated solvent is also an indispensable constituent.

Table 5.8 Summary of screening experiments comparing the relative severity of cracks.

Vial	0-7 days Horizontal crack	7-14 days Horizontal crack	14-25 days Horizontal crack	25-50 days Horizontal crack	50-75 days Horizontal crack	>75 days Horizontal crack	Cracked within 2 weeks
1							✗
2	*	*		***			✗
3							✗
4							✗
5							✗
6							✗
7							✗
8				*****	*****		✗
9		*****			****	****	✓
10		**					✓
11							✗
12		***			***	****	✓
13		***		****			✓
14		***		***			✓
15							✗
16							✗
17							✗
18				*****	*****		✗

Number of stars indicates the relative severity of the cracking.

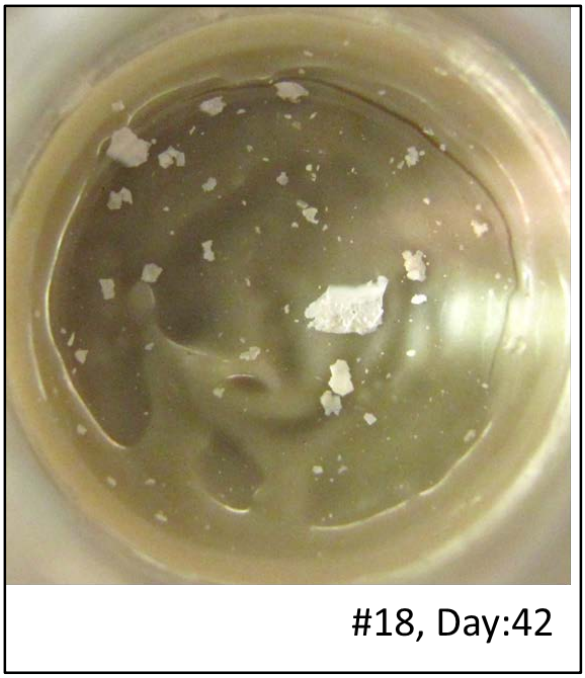

Figure 5.2 A mixture of propanol, acetone, methyl isobutyl ketone, 2-butoxyethanol, amyl acetate, and n-butyl acetate dissolved in PCE ponded on water-saturated bentonite for 42 days. No cracking was observed.

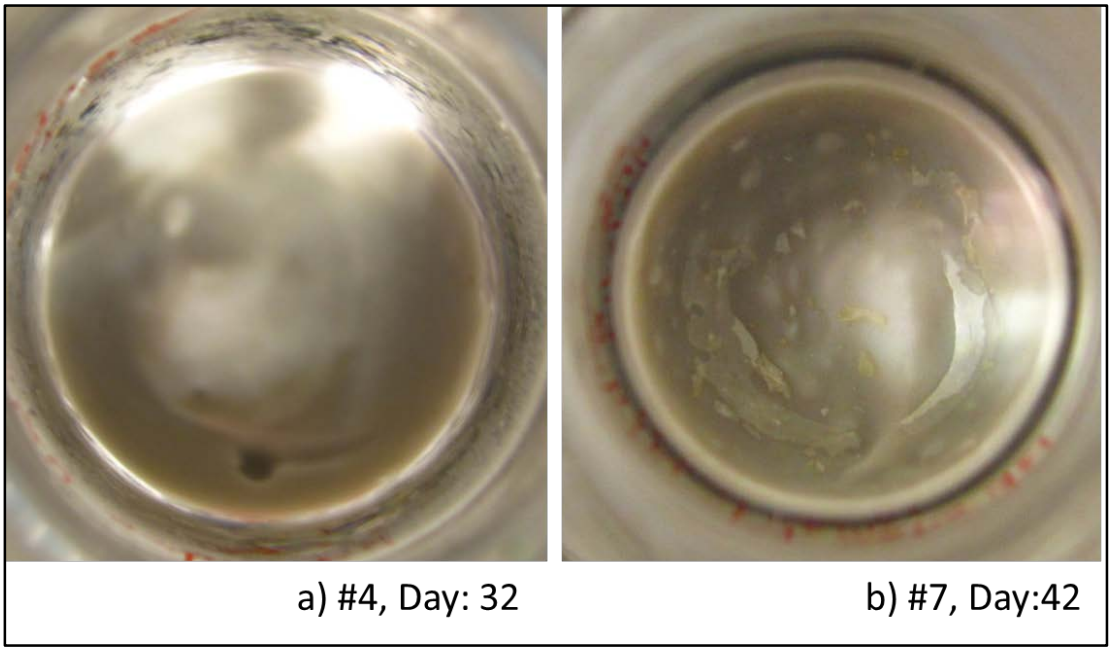

Figure 5.3 a) TritonX-100 dissolved in PCE, b) AOT and $C_{12}E_6$ dissolved in PCE, ponded on water-saturated bentonite for 32 and 42 days, respectively. No cracking was observed.

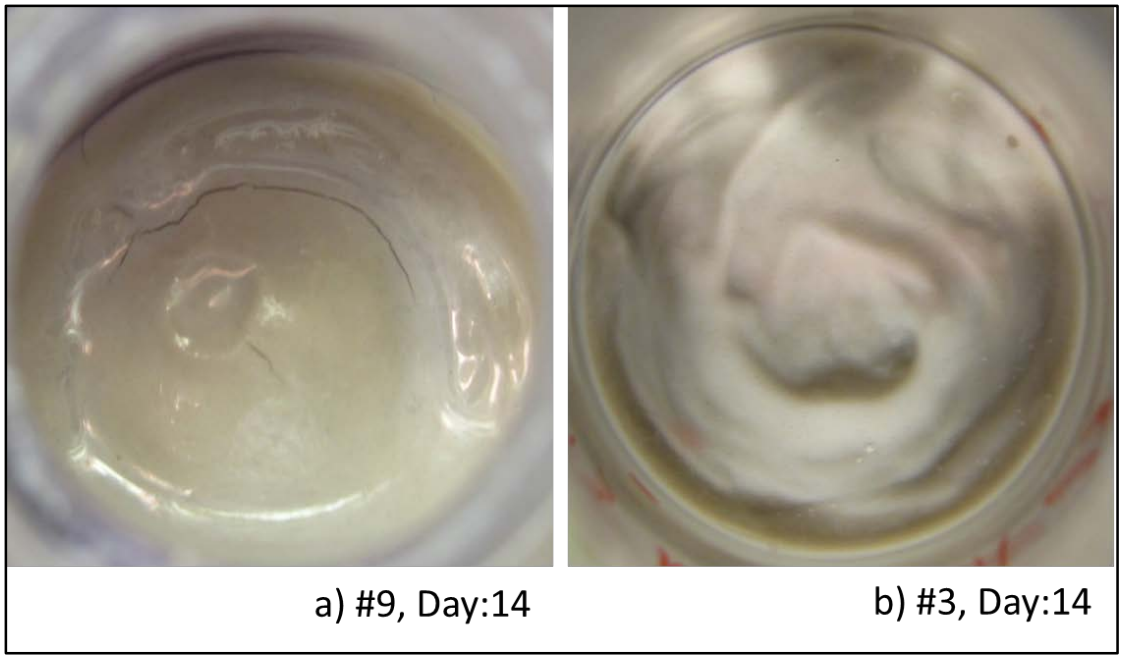

Figure 5.4 a) TritonX-100, AOT, $C_{12}E_6$ dissolved in PCE. Cracking was observed. b) TritonX-100, AOT, $C_{12}E_6$, propanol, acetone, methyl isobutyl ketone, 2-butoxyethanol, amyl acetate, and n-butyl acetate dissolved in water, ponded on water-saturated bentonite for 14 days. No cracking was observed.

5.3.2. Basal Spacing Measurements

The vial experiments showed that a mixture of anionic and nonionic surfactants dissolved in a chlorinated solvent was necessary in order to observe a magnitude and rate of cracking comparable to the real DNAPL waste. The beaker experiments described in Chapter 4 showed that a basal spacing decrease was always observed in the case of cracking. To corroborate this result with respect to the screening experiments reported in this chapter, the basal spacing of bentonite samples in contact with surfactant mixtures was measured.

The XRD results showed that an aqueous solution of TritonX-100 reduced the basal spacing of water-saturated bentonite from 19 Å to 17.5 Å; the combination of TritonX-100 and AOT had the same impact on basal spacing, as well (Table 5.9). On the other hand,

when the three surfactants (TritonX-100, AOT, and $C_{12}E_6$) were present together in water, the basal spacing increased to 20 Å. In contrast, bentonite in contact with the same surfactant mixture (TritonX-100, AOT, and $C_{12}E_6$) in PCE showed a reduction in the basal spacing to 15.8 Å, similar to that observed when water-saturated bentonite was contacted with DNAPL waste. Similarly, the basal spacing of water-saturated bentonite in contact with a PCE solution of TritonX-100 and AOT decreased to 15.4 Å, suggesting that the second nonionic surfactant $C_{12}E_6$ was not necessary. The basal spacing of water-saturated bentonite in contact with PCE containing these surfactants decreased even further to 12.7 Å after three weeks of rotation, most likely due to the more rigorous interaction between the clay and solution for an extended time frame. These results suggested that the minimum mixture needed for clay behavior similar to that observed with DNAPL waste is a combination of TritonX-100, AOT, and PCE.

Table 5.9 Basal spacing of water-saturated bentonite in contact with various surfactant solutions.

	Basal spacing (Å) (4 days of rotation and one week passive contact)		**Basal spacing (Å) (3 weeks of rotation)**	
Surfactant	**Dissolved in water**	**Dissolved in PCE**	**Dissolved in water**	**Dissolved in PCE**
No surfactant	19	19	NM	NM
TritonX-100 (3.3 mM)	17.5	17.5	17.4	15.6
TritonX-100 (3.3 mM) and AOT (3.3 mM)	17.9	15.4	17.1	12.7
TritonX-100 (3.3 mM) and $C_{12}E_6$ (6.7 mM)	NM	18.8	NM	NM
TritonX-100 (3.3 mM), AOT (3.3 mM) and $C_{12}E_6$ (6.7 mM)	20.2	15.8	NM	NM

NM: not measured.

Figure 5.5 shows the XRD pattern of water-saturated bentonite contacted with the mixture of AOT and TritonX-100 dissolved in PCE for one week following four days of

rotation. The broad peak suggests that not all of the interlayer space contracts to the same degree. The XRD pattern appears to be comprised of three overlapping peaks: one corresponding to a basal spacing of 18.9 Å (25% of total area as calculated by the profile fitting software), another one corresponding to 15.5 Å (50% of total area), and the third one corresponding to 11.5 Å (25% of total area). The magnitude of the basal spacings suggests that about 25% of the interlayer space was still fully hydrated, 50% of the interlayer space was partially hydrated and 25% of the interlayer space of bentonite was dehydrated up to air-dry conditions, as 11.5 Å is the basal spacing of air-dry bentonite. Sheng and Boyd (1998) and Lee et al. (2004) observed a similarly broadened peak in the case of naphthalene sorption onto smectite treated with a cationic surfactant. They attributed this to collapse of some of the interlayer space due to the removal of water molecules as a result of naphthalene sorption.

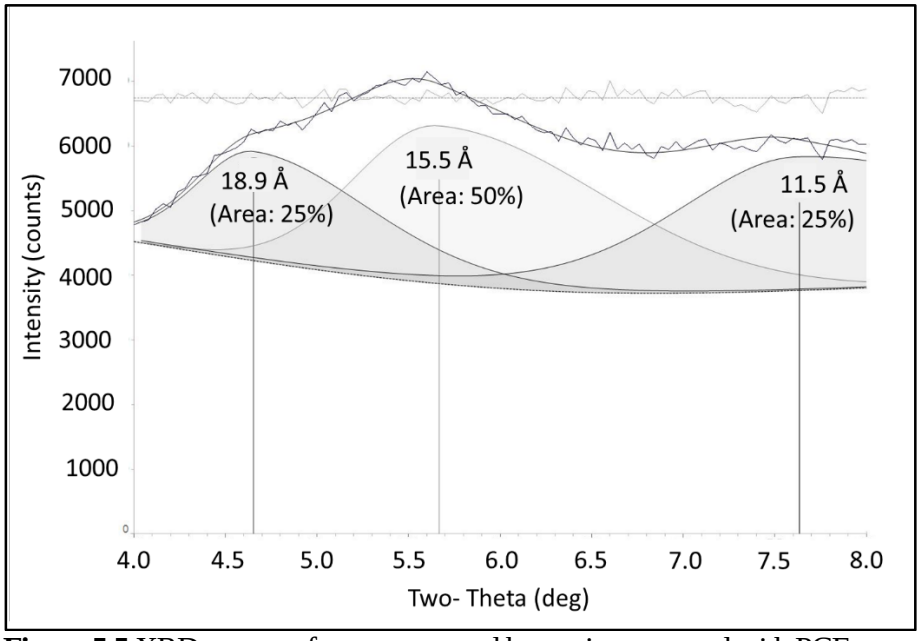

Figure 5.5 XRD pattern of water-saturated bentonite contacted with PCE containing 3.3 mM AOT and 3.3 mM TritonX-100.

5.3.3. FTIR Experiments

The question being addressed with the FTIR measurements was whether the decrease in basal spacing occurred through the displacement of water molecules from the interlayer space. In order to evaluate this, the location of the H-O-H bending band of water in the interlayer space was observed. Also, any sign of an interaction between the clay surface, PCE and the surfactants was sought. Figure 5.6 showed that air-dry bentonite had a very small band at wavenumber 1652 cm^{-1} attributed to H-O-H bending band of water whereas this band was located at 1636 cm^{-1} for water-saturated bentonite. Figure 5.6 also shows that six months of contact with a TritonX-100 solution in PCE did not change the location of the H-O-H bending band relative to that for water-saturated clay, suggesting that the interlayer water was not impacted by the presence of the nonionic surfactant and chlorinated solvent. This observation agrees with the results of the screening experiments and basal spacing measurements since neither cracking nor a reduction in the basal spacing was observed for that system. However, after six months of contact with a mixture of TritonX-100, AOT and PCE, bending band of interlayer water increased to 1652 cm^{-1}, similar to the location in air-dry clay. This shift in wave number towards the wave number of air-dry clay suggests a displacement of water molecules from the interlayer space, similar to the process of dehydration. The shift in the water-bending band was only from 1636 to 1639 cm^{-1} for the samples that were only aged for three weeks (Figure 5.7). This less pronounced change in the location of water bending band at shorter contact times implies that displacement of water molecules from the interlayer space of clay minerals is a time-dependent process, with perhaps progressively more water being displaced over time.

Although some evidence was found suggesting an interruption of the hydration layers in clay, surfactant specific bands were not detected. In previous studies using FTIR to examine surfactants in clays, the clays were exposed to high concentration surfactant solutions and then dried. Here, the clays were exposed to relatively dilute concentrations of surfactants and were analyzed wet. Because of these differences in measurement conditions, changes in surfactant specific bands as reported by Del Hoyo et al. (2008) could not be observed.

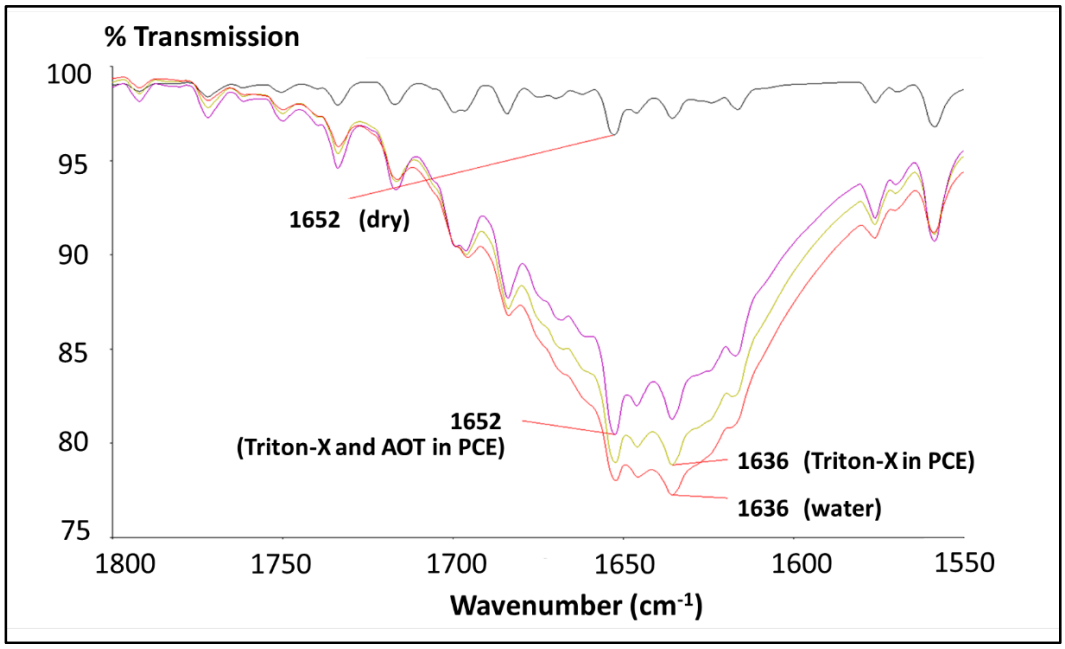

Figure 5.6 FTIR spectra of water-saturated bentonite in contact with different fluids for six months in comparison with air-dry bentonite.

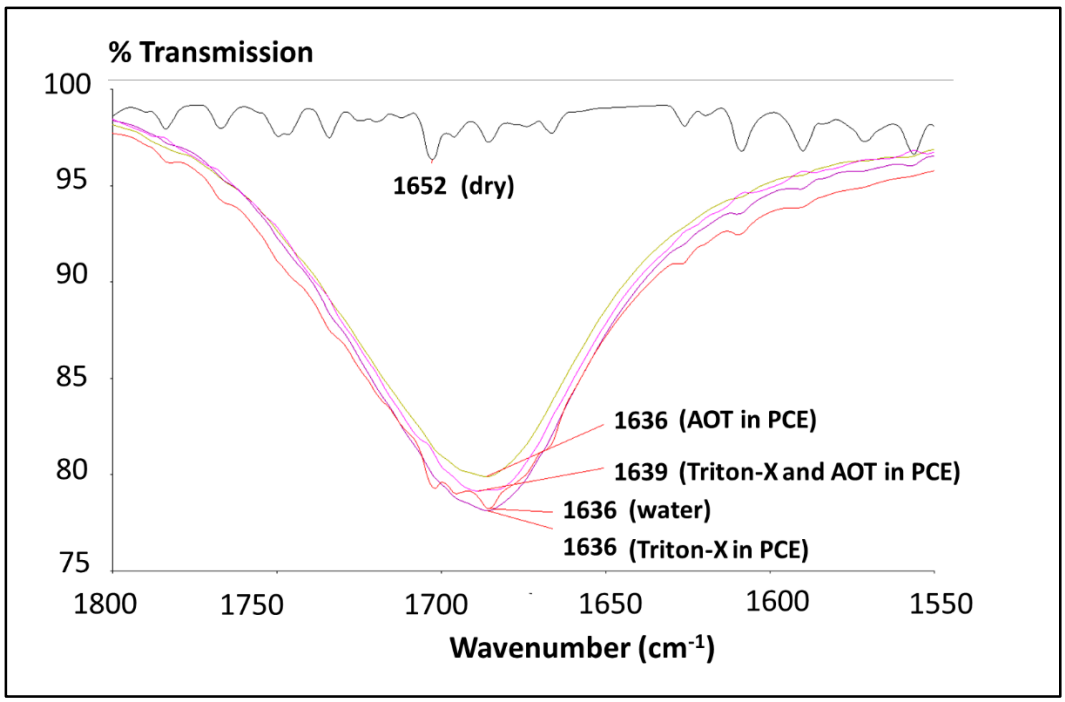

Figure 5.7 FTIR spectra of water-saturated bentonite in contact with different fluids for three weeks in comparison with air-dry bentonite.

5.3.4. Sorption Experiments

Surfactant sorption

The screening experiments and XRD measurements suggested that both an anionic and a nonionic surfactant needed to be present to decrease the basal spacing of water-saturated smectitic clay. The FTIR measurements suggest water displacement only in the case of contact with two surfactants and PCE. As synergistic activity of surfactants has been reported in the literature, it was thought that enhanced sorption may occur in the mixture. To investigate this hypothesis, batch experiments were conducted, and the sorption of TritonX-100 and AOT on water-saturated Na-montmorillonite was determined. The results showed that 65% of TritonX-100 was sorbed from an aqueous solution of TritonX-100, whereas the degree of sorption of TritonX-100 decreased slightly to 57% if

the aqueous solution consisted of TritonX-100 and AOT (Figure 5.8). On the other hand, the degree of AOT sorption increased from 7% to 14% if AOT and TritonX-100 were present in the solution together (Table 5.10, Figure 5.9). Thus, the presence of TritonX-100 increased the sorption of AOT two fold, giving a sorbed molar ratio of TritonX-100: AOT of around 5:1 from the aqueous solution. Similar experiments were conducted with the surfactants dissolved in PCE. The results showed that the degree of TritonX-100 sorption increased slightly, from 72% to 85%, in the presence of AOT. On the other hand, the degree of AOT sorption increased almost eight fold by the presence of TritonX-100 (Table 5.10, Figure 5.9). In the case of sorption from PCE, the sorbed molar ratio of TritonX-100: AOT was 3:2. Although AOT is an ionic surfactant, its sorption increased considerably through its association with a chlorinated solvent and a nonionic surfactant.

Table 5.10 Sorbed concentration of surfactant from solutions either in water or in PCE.

Solvent	Solute (Initial concentration)	Mass of wet soil (g)	Sorption of	C_{sorbed} (mmol/ g wet soil)	Percent sorption (%)
Water	TritonX-100 (3.3 mM)	2	TritonX-100	0.0242	64.9
	TritonX-100 (3.3 mM) **&** AOT (3.3 mM)	2		0.0238	57.1
	AOT (3.3 mM)	2	AOT	0.0022	6.5
	TritonX-100 (3.3 mM) **&** AOT (3.3 mM)	2		0.0050	14.3
PCE	TritonX-100 (3.3 mM)	4	TritonX-100	0.0120	72.4
	TritonX-100 (3.3 mM) **&** AOT (3.3 mM)	4		0.0126	84.9
	AOT (3.3 mM)	4	AOT	0.0011	7.3
	TritonX-100 (3.3 mM) **&** AOT (3.3mM)	4		0.0082	57.8

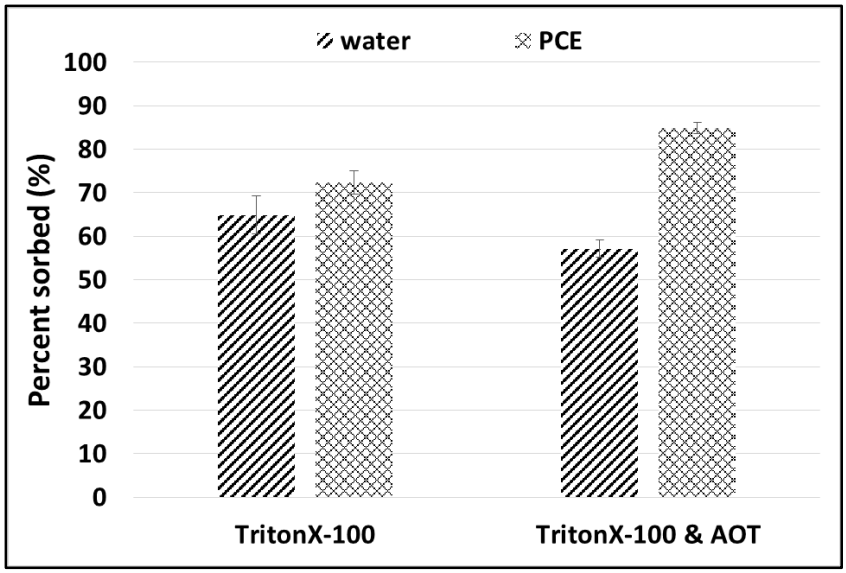

Figure 5.8 Percent sorption of TritonX-100 from solutions in water or PCE.

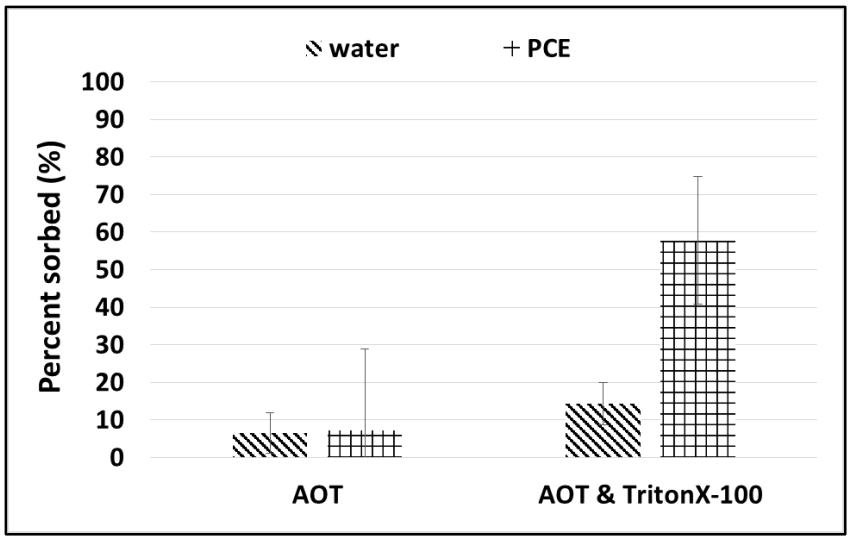

Figure 5.9 Percent sorption of AOT from solutions in water or PCE.

^{13}C-labeled TCE sorption

The XRD results presented in Chapter 4 showed that the basal spacing of water-saturated Na-montmorillonite contacted with DNAPL waste decreased to that of air-dry clay, so it was speculated that the surfactants penetrated into the interlayer space of water-saturated smectite, allowing the chlorinated solvent to then enter. To investigate the

possibility of an increased uptake of the chlorinated compound by the clay in the presence of surfactants, measurements of the sorption of ^{13}C-labeled TCE were performed in the presence and absence of surfactants. Table 5.11 shows the results of those measurements. These data show that the quantity of TCE sorbed is higher (33%) in case where AOT and TritonX-100 were dissolved in PCE. Therefore, it appears that presence of the surfactant mixture enhanced the sorption of the chlorinated solvent somewhat but considerably less than the increase as observed for sorption of AOT (around 800%). This result suggests that an explanation based solely on increased quantities of TCE in the interlayer space of water-saturated smectitic clays is not reasonable as this quantity of sorption could occur on the outer edge of the clay minerals. The fundamental difference noted in the presence of the chlorinated solvent is an increased sorption of the surfactants, in particular, the anionic surfactant AOT.

Table 5.11 Sorption of ^{13}C-labeled TCE from synthetic DNAPL waste.

Solution	C_{sorbed} (mmol/g wet soil)	% sorbed
AOT in PCE	0.006 (0.007)	7 (7)
AOT &TritonX-100 in PCE	0.008 (0.008)	33 (23)
TritonX-100 in PCE	0.003 (0.003)	5 (4)
No surfactant in PCE	-0.003* (0.02)	-1* (27)

*negative sorption was determined within the instrumental error, numbers in parentheses are standard deviations.

5.4. Proposed Mechanism for Basal Spacing Decrease

Screening experiments helped to determine that a mixture of anionic and nonionic surfactants and chlorinated solvent as the mixture responsible for the decrease in basal spacing and cracking. The sorption results suggested that there was increased sorption in the presence of PCE, with about 85% of the nonionic surfactant, TritonX-100, and nearly

60% the anionic surfactant, AOT, sorbed onto water-saturated Na-montmorillonite, giving a sorption ratio of 3:2. The location and orientation of the molecules relative to the clay surface of the interlayer space will depend, in part, on the size of the molecules. The basal spacing is the sum of the TOT layer and the interlayer space (Figure 5.10). The TOT structure of smectite clay minerals has a thickness of around 9.6 Å (Moore and Reynolds, 1997); thus, the interlayer space will have a thickness of around 5.5 Å, if the basal spacing is 15 Å. TritonX-100 can conceivably penetrate and sorb into the water-filled interlayer space since it is miscible in water and nonionic. However, due to its length (around 51 Å, Table 5.12), it cannot be aligned vertically in the interlayer space. So, TritonX-100 is thought to lie generally parallel to the interlayer surfaces. However, AOT is unlikely to enter into the interlayer space because it has a negatively-charged head, whose diameter is 5 Å. But, AOT can interact with TritonX-100 through the hydrophobic moieties of these two surfactants; this interaction is suggested by its enhanced sorption in the presence of TritonX-100. Furthermore, if there is water retained on the exterior surfaces, it is anticipated that AOT can sorb there as AOT shows preferential partitioning into water over PCE ($K_{PCE,water}$ = 0.001) (Hsu, 2005). Assuming interactions between the hydrophobic portions of TritonX-100 and AOT, a 3:2 ratio of sorption, that TritonX-100 can penetrate into the interlayer space, but AOT cannot, the configuration of sorbed surfactant may be represented as shown in Figure 5.11.

With the sorption of TritonX-100, some of the water molecules in the interlayer space at the edges of the clay particle are displaced which is consistent with the shifts in the water-bending band observed in FTIR experiments that suggest dehydration. This partial dehydration is also consistent the XRD pattern shown in Figure 5.5. In addition to

the displacement of some of the water molecules residing in the interlayer space of clay minerals, it is speculated that Na^+ cation in the anhydrous AOT molecules attract interlayer water molecules and stimulate further displacement of these water molecules leading to a collapse of the basal spacing.

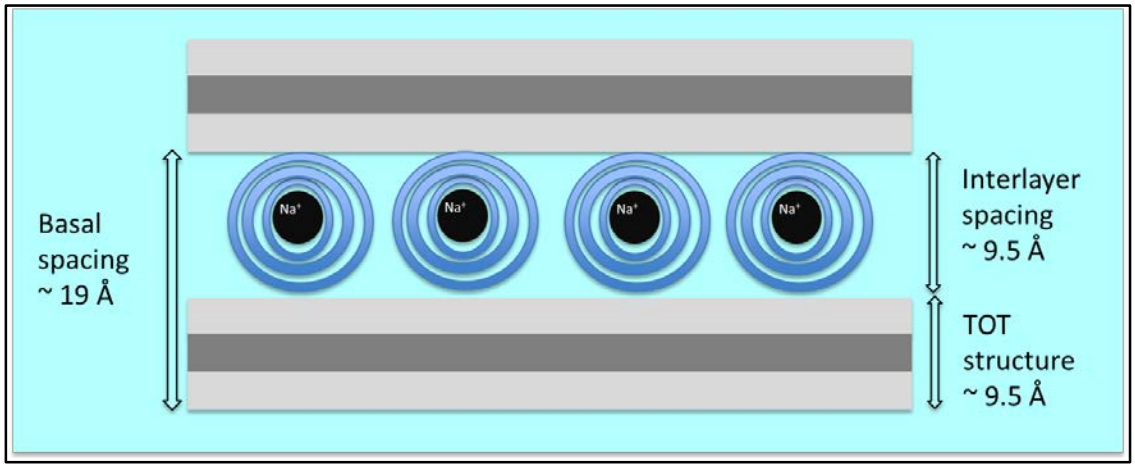

Figure 5.10 Diagram illustrating interlayer space of water-saturated Na-montmorillonite (blue color corresponds to bulk water).

Table 5.12 Size of molecules that play role in basal spacing decrease.

Head diameter of AOT (Å) (Moulik and Mukherjee, 1996)	5.0
Tail length of AOT (Å) (Moulik and Mukherjee, 1996)	12.6
Total length of TritonX-100 (Å) (Paradies, 1980)	51
Width of PCE molecule (Å) (Zhou, 1994)	3.6
Width of water molecule (Å) (Cheng et al., 2001)	2.8

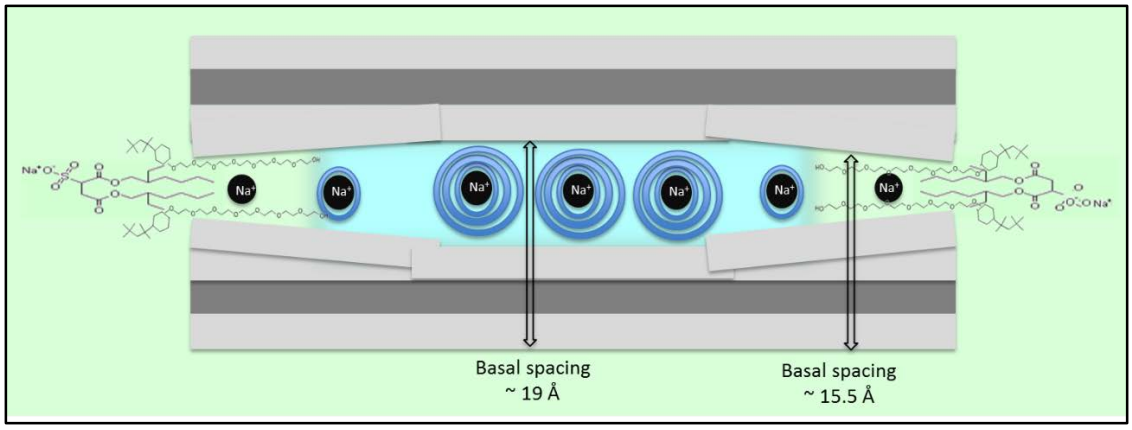

Figure 5.11 Diagram illustrating the partially collapsed interlayer space of water-saturated Na-montmorillonite in contact with PCE containing AOT and TritonX-100 (green color represents PCE and blue represents water).

5.5. Conclusions

DNAPL waste is a mixture of many different compounds. Traditionally, the focus of research has been on the solvent matrix of the waste, with the contribution of the other components receiving less attention. However, the work presented in Chapter 4 showed that PCE or TCE by itself does not cause a collapse of the clay structure as do PCE-based or TCE-based field wastes. Screening experiments were performed to determine the critical components of the field wastes. The modified structure of Na-montmorillonite clays was observed at two different scales: basal spacing was measured at the microscale and the formation of cracks was monitored at the macroscale. These experiments showed that the minimum mixture required to match the observations of a real DNAPL waste mixture was comprised of an anionic and nonionic surfactant, specifically AOT and TritonX-100, dissolved in a chlorinated solvent, PCE. With passive contact with this mixture, the basal spacing decreased from around 19 Å to 15 Å, and the water-saturated clay cracked within about a two-week time period.

Since all three components must be present for cracking to occur and none caused cracking individually, possible synergistic interactions were investigated. It was found that, in the presence of PCE, the nonionic surfactant, TritonX-100, sorbed onto water saturated Na-montmorillonite in greater quantities than from water and, in addition, it significantly increased the sorption of the anionic surfactant, AOT. Thus, the presence of PCE and TritonX-100 allowed the sorption of AOT, which, generally, is not thought to sorb on clays due to the repulsion between negatively-charged clay surfaces and the negative charge of the surfactant. Furthermore, the presence of the surfactants increased the sorption of TCE, although to a considerably lesser extent. Thus, it appears that the role of the chlorinated solvent is to increase the sorption of the surfactants, particularly AOT. FTIR data suggested a partial displacement of water molecules as a result of contact with the synthetic DNAPL waste. When this information is considered in concert with the sorption data, it was concluded that the surfactants sorbed on the water-saturated Na-smectite, displacing some water molecules. Because of its length, TritonX-100 is hypothesized to lie horizontally relative to the interlayer surface. Since the sorption of AOT increased in the presence of TritonX-100, it is speculated that it interacts with TritonX-100 through an interaction between hydrophobic moieties. However, the AOT lies external to the clay particle, due to the size of its head and the repulsion between the negatively-charged clay surface and the negatively-charged head group. Interlayer water molecules move toward the AOT molecule to hydrate Na^+ cation in the anhydrous structure of AOT, resulting in additional water displacement over time.

As the displacement of water molecules is not uniform, there is a range of basal spacings; this is reflected in the XRD pattern as a very broad peak which actually represents

overlapping peaks, with each peak indicating an interlayer space with a different thickness. This partial decrease in basal spacing and shrinkage of the lattice structure, accompanied by cracking, analogous to the situation with desiccation.

Chapter 6
Conclusions and Recommendations for Future Work

Chlorinated solvents such TCE and PCE were released to the subsurface due to improper waste disposal practices before the passage of the Resource Conservation and Recovery Act (RCRA) in 1976, and are some of the most prevalent contaminants at hazardous waste sites in the U.S. Due to its low water solubility and high density, the solvent waste tends to migrate vertically as a separate organic liquid phase in the subsurface and pool on top of low permeability layers and lenses. Despite years of remedial action at many of these waste sites, the concentrations of these contaminants in the groundwater continue to be above the MCL. Recent studies aimed at understanding why attribute the failure of the concentrations to fall below the MCL to a phenomenon referred to as back diffusion, in which contaminants that have accumulated in low permeability layers over time are slowly released back to the groundwater through diffusion. Furthermore, it is speculated that the mechanism by which the contaminants accumulate in the low permeability layers is through diffusion. However, there is field evidence that the mass storage of the contaminants in these layers is greater than that which can be accounted for by diffusion. Because of the dependence of the remedial actions on estimates of the amount of contamination in the subsurface, this research conducted for this dissertation investigated the reasons for high accumulations of chlorinated contaminants in clay layers and lenses.

Studies about diffusion of organic solutes in clayey soils were reviewed in depth:

The literature discussing the diffusion of organic solutes in water-saturated low permeability soils was reviewed as diffusion is hypothesized to be the dominant transport process into low permeability layers. Despite the prevalence of chlorinated organic solutes at hazardous waste sites, the literature contains surprisingly few measurements of the effective diffusion coefficient for these compounds. Consequently, most studies examining the diffusive movement of such compounds employ estimates. However, commonly used correlations for the estimation of the diffusion coefficient of inorganic species in unsaturated sandy soils overestimate the diffusion coefficient for soils with a clay content of more than 25%, as they give relative diffusivity as an exponential function of porosity, and clays have an increased porosity, but decreased diffusivities. Relative diffusivities reported for field studies were also examined but it was concluded that they overpredict the diffusion coefficient, as well. Based on data reported in the literature for tritiated water, two additional methods were evaluated which decreased the error significantly but these methods have not been widely adopted. Thus, there seems to be a general trend of overpredicting the rate of diffusion; however, due to the limited amount of data for chlorinated compounds, this finding could be attributed to the data themselves or to the correlations.

Effective diffusion coefficients in water-saturated silt-clay mixtures were measured.

In an effort to ascertain mass transport rates into low permeability media due to diffusion, the effective diffusion coefficients of iodide, trichloroethylene and the anionic surfactant AOT in silt and in a silt-clay mixture were measured. The measurements were

consistent with measurements reported in the literature for comparable systems. The measured values of effective diffusion coefficients were compared with the estimates and the overestimation by correlations developed for sandy soils was confirmed. The methods proposed for the diffusion of tritiated water in clay soils proved to be more appropriate for the prediction of the effective diffusion coefficient of TCE also, suggesting that the use of these correlations could be expanded to the diffusion of nonpolar organic species as well.

Johnson et al. (1989) reported the effective diffusion coefficient of TCE in the field to be 1.7 times higher than the estimated diffusion coefficient of TCE. As the estimations were found to overestimate the diffusion coefficient measured here, the overall discrepancy between the diffusion coefficient observed in the field and measured diffusion coefficient is five fold. Furthermore, the diffusion coefficient of TCE in the water-saturated silt-clay mixture that had been contacted with DNAPL waste for 18 months was measured, and it was found that it was two orders of magnitude smaller than diffusion coefficient of TCE through a silt-clay mixture that had not been contacted with waste. Consequently, the rate of diffusion in the field could be dramatically lower than reported based on the experimental diffusion coefficients in silt-clay mixtures.

Field implications of the discrepancy between measured and observed diffusion coefficients were evaluated.

The measured diffusion coefficient of TCE was found to be lower than the diffusion coefficient estimates used in field studies (Parker, 1996; Ball et al., 1997; Parker et al., 2004) and the diffusion coefficient observed in the field (Johnson et al., 1989). The impact of the different diffusion coefficients on mass storage was estimated through hypothetical calculations of the mass storage of TCE in an aquitard. It was concluded that mass storage

estimates determined using diffusion coefficients measured in the lab were half of that mass calculated using diffusion coefficients observed in the field. Therefore, it suggests that there are additional mechanisms other than diffusion contributing to mass accumulation in clay layers at sites contaminated with DNAPL waste.

Structural changes in clay minerals as a result of contact with organic solvents were investigated as a hypothesis to explain elevated mass storage in low permeable layers.

As it appeared that the amount of mass accumulated in the aquitards cannot be explained solely by diffusion, it was hypothesized that the structure of clay minerals in aquitards was altered as a result of contact with DNAPL waste and this structural change caused increased storage of the chlorinated compound in the aquitard. Measurements of basal spacing showed that pure TCE and PCE were not able to contract the lattice structure of water-saturated Na-montmorillonite clays, whereas DNAPL waste could. Additionally, this structural change was accompanied by the formation of cracks of up to 1 mm within weeks, a phenomenon which could play a significant role in the transport of chlorinated solvents into low permeability layers.

Field implications of the cracks on the amount of mass storage were evaluated.

The impact of cracks on mass storage was evaluated by considering two scenarios. Calculations of the increase in diffusion due to cracks, assuming that the contaminants enter the cracks as a solute in the aqueous phase, did not increase the mass storage significantly. However, additional calculations suggested that, given the size of crack apertures that formed and the pool depths observed at hazardous waste sites, it is possible

that the cracks could fill with DNAPL. In this scenario, the mass storage increased substantially, giving estimates that could match field observations.

A mechanism that enables the structural modification of clay minerals was proposed.

Given that DNAPL waste was able to contract the structure of water-saturated Na-smectites unlike pure chlorinated solvents, the next step was the determination of the mechanism of this contraction. As components of DNAPL waste did not have this impact individually, the combination of necessary compounds was determined by screening experiments. These experiments indicated that a mixture of anionic and nonionic surfactants dissolved in a chlorinated solvent decreased the basal spacing and caused cracking similarly to the field DNAPL wastes.

Since the collapse of the basal spacing suggested dehydration, the question of whether this surfactant-chlorinated organic solvent mixture displaced water molecules from the interlayer space was addressed. Fourier transform infrared (FTIR) spectroscopy suggested a partial displacement of water from the interlayer space, but no signal resulting from PCE or the surfactants was detected. Sorption measurements showed an enhanced synergistic sorption of the surfactants in the presence of the chlorinated solvent; in fact, the sorption of the anionic surfactant increased by a factor of eight in the presence of nonionic surfactant and chlorinated solvent. However, sorption of the solvent did not appear to increase to a similar degree, suggesting that the entrance of the chlorinated solvent into the interlayer space was not the primary mechanism by which the basal spacing was decreased, and the main role of the chlorinated solvent was to increase sorption. Based on all the accumulated evidence, it was hypothesized that the nonionic surfactant sorbs in the

interlayer space, displacing some of the interlayer water, but with a portion of the molecule extending beyond the interlayer space. It interacts with the anionic surfactant through a its hydrophobic moiety. Na^+ cations in the AOT molecule attract interlayer water molecules to stay hydrated and this leads to a greater collapse of the interlayer space at the edges. This hypothesis is consistent with the broad peak in the XRD pattern, which showed variable interlayer spacings, with only about 25% of the space showing dehydration.

Future Work

This study revealed that Na-smectite clays undergo structural changes like lattice structure contraction and cracking due to contact with DNAPL waste. This modification of the structure may influence the fate of the contaminants in the subsurface, leading to high accumulations of the contaminants in clay layers, which conventionally have been viewed as barriers to contaminant movement. However, this research focused on basal spacing and cracking of Na-smectites in a laboratory setting.

1. Extension of work to field sites: This study observed the structure of pure smectites contacted with DNAPL wastes in a laboratory setting. Although the wastes were taken from the field, the clays were commercially purchased. It would be invaluable to assess whether the structural modifications observed in the lab occur in the field. This verification might involve the isolation of clay from real waste sites and an analysis of the clay structure to determine whether such changes occur with impure clays or in the presence of an overburden pressure. Bentonite, which is mainly Na-montmorillonite, is frequently used in construction of impermeable

barriers at contaminated sites to prevent further migration of the contaminants. At sites where bentonite slurry walls have been constructed around DNAPL pools, it would be worthwhile to assess whether there is evidence of clay structure alteration due to contact with DNAPL waste.

2. Extension to clays other than Na-montmorillonite: This study focused on the changes in the structure of Na-montmorillonite clays since these clays are an important component of landfill liners and slurry walls. However, an aquitard contains other clay minerals other than just Na-smectites. There is some evidence that the structure of nonexpansive clay minerals, such as kaolinite, may also be affected by contact with DNAPL waste. The colloidal structure of nonexpansive clay minerals may be influenced by contact with waste, leading to greater flocculation. A more flocculated state can also lead to cracking and enhanced non-diffusive transport.
3. Extension to other hazardous wastes: This study demonstrated that the composition of waste plays a very important role in determining its fate in the subsurface. The field wastes examined here were a degreasing TCE-based waste from an Air Force Base and a PCE-based waste from a dry cleaner. Based on an analysis of these wastes a synthetic waste containing PCE, an anionic surfactant, AOT, and a nonionic surfactant, TritonX-100 could cause basal spacing reductions and cracking similar to real wastes. Further research is necessary to extend this research to other waste compositions and to understand the possible synergistic activity among chemicals in various types of waste and the resultant impact on their transport in the subsurface.

References

Abdul, A. S., Gibson, T. L., & Rai, D. N. (1990). Laboratory studies of the flow of some organic solvents and their aqueous solutions through bentonite and kaolin clays. *Groundwater*, *28*(4), 524–533.

Allen-King, R. M., Groenevelt, H., & Mackay, D. M. (1995). Analytical method for the sorption of hydrophobic organic pollutants in clay-rich materials, *29*(1), 148–153.

Allen-King, R. M., Grathwohl, P., & Ball, W. P. (2002). New modeling paradigms for the sorption of hydrophobic organic chemicals to heterogeneous carbonaceous matter in soils, sediments, and rocks. *Advances in Water Resources*, *25*(8-12), 985–1016. doi:10.1016/S0309-1708(02)00045-3

Amarasinghe, P. M., Katti, K. S., & Katti, D. R. (2009). Nature of organic fluid-montmorillonite interactions: an FTIR spectroscopic study. *Journal of Colloid and Interface Science*, *337*(1), 97–105. doi:10.1016/j.jcis.2009.05.011

Anderson, D. C., Brown, K. W., & Thomas, J. C. (1985). Conductivity of compacted clay soils to water and organic liquids. *Waste Management & Research*, *3*(1), 339–349. doi:10.1177/0734242X8500300142

Appelo, C. A. J., & Wersin, P. (2007). Multicomponent diffusion modeling in clay systems with application to the diffusion of tritium, iodide, and sodium in opalinus clay. *Environmental Science & Technology*, *41*(14), 5002–5007.

Archie, G. E. (1942). The electrical resistivity log as an aid in determining some reservoir characteristics. *I. Petroleum Technology*, *5*, 54–62.

ASTM International, ASTM D422-63(2007)e2, Standard Test Method for Particle-Size Analysis of Soils, West Conshohocken, PA, 2007.

ASTM International, ASTM D5856-95(2007), Standard Test Method for Measurement of Hydraulic Conductivity of Porous Material Using a Rigid-Wall, Compaction-Mold Permeameter, West Conshohocken, PA, 2007.

Ball, W. P., Liu, C., Xia, G., & Young, D. F. (1997). A diffusion-based interpretation of tetrachloroethene and trichloroethene concentration profiles in a groundwater aquitard. *Water Resources Research*, *33*(12), 2741–2757. doi:10.1029/97WR02135

Barone, F. S., Rowe, R. K., & Quigley, R. M. (1992). A laboratory estimation of diffusion and adsorption coefficients for several volatile organics in a natural clayey soil. *Journal of Contaminant Hydrology*, *10*(3), 225–250. doi:10.1016/0169-7722(92)90062-J

Barrer, R. M., & Rideal, E. K. (1939). Permeation, diffusion and solution of gases in organic polymers. *Transactions of the Faraday Society, 35*, 628–643. doi:10.1039/tf9393500628

Barshad, I. (1952). Factors affecting the interlayer expansion of vermiculite and montmorillonite with organic substances. *Soil Science Society of America Journal, 16*(2), 176–182.

Bear, J. (1972). *Dynamics of Fluids in Porous Media*, Eisevier, New York.

Berkheiser, V., and Mortland M. M. (1975). Variability in exchange ion position in smectite: dependence on interlayer solvent. *Clays and Clay Minerals, 23*(5), 404–410.

Bourg, I. C., Bourg, A. C. M., & Sposito, G. (2003). Modeling diffusion and adsorption in compacted bentonite: a critical review. *Journal of Contaminant Hydrology*, *61*(1-4), 293–302. doi:10.1016/S0169-7722(02)00128-6

Bourg, I. C., Sposito, G., & Bourg, A. C. M. (2006). Tracer diffusion in compacted, water-saturated bentonite. *Clays and Clay Minerals*, *54*(3), 363–374. doi:10.1346/CCMN.2006.0540307

Boving, T. B., & Grathwohl, P. (2001). Tracer diffusion coefficients in sedimentary rocks: correlation to porosity and hydraulic conductivity. *Journal of Contaminant Hydrology*, *53*(1-2), 85–100. doi:10.1016/S0169-7722(01)00138-3

Brady, N., & Weil, R. (1996). *The Nature and Properties of Soils*, 11th ed, Prentice-Hall, New Jersey.

Brindley, G. W., Wiewiora, K., & Wiewiora, A. (1969). Intracrystalline swelling of montmorillonite in some water-organic mixtures, Clay-organic studies-17. *American Mineralogist*, *54*(11), 1635–1644.

Brindley, G., & Brown, G. (1980). *Crystal structures of clay minerals and their X-ray identification,* Mineralogical Society, London (pp. 361–410).

Bronswijk, J. (1988). Modeling of water balance, cracking and subsidence of clay soils. *Journal of Hydrology*, *97*(3), 199–212.

Brown, K. W., & Thomas, J. C. (1984). Conductivity of three commercially available clays to petroleum products and organic solvents. *Hazardous Waste, 1*(4), 545–553.

Brown, K. W., & Thomas, J. C (1987). A mechanism by which organic liquids increase the hydraulic conductivity of compacted clay materials. *Soil Science Society of America Journal, 51*(6), 1451–1459.

Campbell, G. S. (1974). A simple method for determining unsaturated conductivity from moisture retention data. *Soil Science, 117*(6), 311–314.

Chapman, S. W., & Parker, B. L. (2005). Plume persistence due to aquitard back diffusion following dense nonaqueous phase liquid source removal or isolation. *Water Resources Research, 41*(12). doi:10.1029/2005WR004224

Cheng, L., Fenter, P., Nagy, K. L., Schlegel, M. L. (2001). Molecular-scale density oscillations in water adjacent to a mica surface. *Physical Review Letters*, *87*(15), 156103.

Chipera, S., & Bish, D. (2001). Baseline studies of the clay minerals society source clays: powder X-ray diffraction analyses. *Clays and Clay Minerals*, *49*(5), 398–409.

Cho, W. J., Oscarson, D. W., & Hahn, P. S. (1993). The measurement of apparent diffusion coefficients in compacted clays: an assessment of methods. *Applied Clay Science*, *8*(4), 283–294.

Crank, J. (1975). *The Mathematics of Diffusion*, 2nd ed, Oxford University Press, London.

Cuypers, C., Pancras, T., Grotenhuis, T., & Rulkens, W. (2002). The estimation of PAH bioavailability in contaminated sediments using hydroxypropyl-b-cyclodextrin and TritonX-100 extraction techniques. *Chemosphere*, *46*, 1235–1245.

D'Astous, A. Y., Ruland, W. W., Bruce, J. R. G., Cherry, J. A., & Gillham, R. W. (1989). Fracture effects in the shallow groundwater zone in weathered Sarnia-area clay. *Canadian Geotechnical Journal*, *26*(1), 43–56.

Dabestani, A. (2001). "Dry Cleaning Surfactants" in *Detergency of Specialty Surfactants*, Surfactant Science Series Volume: 98, Friedli, F. E. (Ed.), Marcel Dekker, New York, 239-254.

Day, M. J. (1977). *Analysis of Movement and Hydrochemistry of Groundwater in the Fractured Clay and Till Deposits of the Winnipeg Area, Manitoba*, M.Sc. thesis, Univ. of Waterloo,Waterloo, Ontario, Canada.

Del Hoyo, C., Dorado, C., Rodríguez-Cruz, M. S., & Sánchez-Martín, M. J. (2008). Physico-chemical study of selected surfactant-clay mineral systems. *Journal of Thermal Analysis and Calorimetry*, *94*(1), 227–234. doi:10.1007/s10973-007-8934-6

Demond, A., & Lindner, A. (1993). Estimation of interfacial tension between organic liquids and water. *Environmental Science & Technology*, *27*(12), 2318–2331.

Deng, Y., Dixon, J. B., & White, G. N. (2003). Intercalation and surface modification of smectite by two non-ionic surfactants. *Clays and Clay Minerals*, *51*(2), 150–161. doi:10.1346/CCMN.2003.0510204

Donahue, R. B., Barbour, S. L., & Headley, J. V. (1999). Diffusion and adsorption of benzene in Regina clay. *Canadian Geotechnical Journal*, *36*(3), 430–442. doi:10.1139/t99-017

Dou, W., Omran, K., Grimberg, S. J., Denham, M., & Powers, S. E. (2008). Characterization of DNAPL from the U.S. DOE Savannah River Site. *Journal of Contaminant Hydrology*, *97*(1-2), 75–86. doi:10.1016/j.jconhyd.2008.01.002

Dullien, F. (1991). *Porous Media: Fluid Transport and Pore Structure*, Academic Press, New York, NY.

Dwarakanath, V., Jackson, R. E., & Pope, G. A. (2002). Influence of wettability on the recovery of NAPLs from alluvium. *Environmental Science & Technology, 36*(2), 227–231.

Epstein, N. (1989). On tortuosity and the tortuosity factor in flow and diffusion through porous media. *Chemical Engineering Science*, *44*(3), 777–779.

Freeze, R., & Cherry, J. (1979). *Groundwater,* Prentice-Hall, New Jersey.

Gao, Y., Yue, C., Lu, S., Gu, W., & Gu, T. (1984). Adsorption from mixed solutions of TritonX-100 and sodium n-alkyl sulfates on silica gel. *Journal of Colloid and Interface Science, 100*(2), 581–583.

García-Gutiérrez, M., Cormenzana, J. L., Missana, T., & Mingarro, M. (2004). Diffusion coefficients and accessible porosity for HTO and ^{36}Cl in compacted FEBEX bentonite. *Applied Clay Science*, *26*(1-4), 65–73. doi:10.1016/j.clay.2003.09.012

García-Gutiérrez, M., Cormenzana, J. L., Missana, T., Mingarro, M., & Molinero, J. (2006). Overview of laboratory methods employed for obtaining diffusion coefficients in FEBEX compacted bentonite. *Journal of Iberian Geology, 32*(1), 37–53.

Goodall, D., & Quigley, R. (1977). Pollutant migration from two sanitary landfill sites near Sarnia, Ontario. *Canadian Geotechnical Journal, 14*(2), 223–236.

Grathwohl, P. (1998). *Diffusion in Natural Porous Media: Contaminant Transport, Sorption/Desorption and Dissolution Kinetics,* Kluwer Academic Publishing, Boston.

Greene-Kelly, R. (1954). Sorption of aromatic organic compounds by montmorillonite. Part 1. Orientation studies. *Transactions of the Faraday Society, 51*, 412–424.

Griffin, R. A., Hughes, R. E., Follmer, L. R., Stohr, C. J., Morse, W. J., Johnson, T. M., Bartz, J.K., Steele, J. D., Cartwright, K., Killey, M. M. & DuMontelle, P. B. (1984). "Migration of Industrial Chemicals and Soil-Waste Interactions at Wilsonville, Illinois" in *Land Disposal of Hazardous Waste, Tenth Annual Research Symposium*, Fort Mitchell, KY, 61-77.

Hayduk, W., & Laudie, H. (1974). Prediction of diffusion coefficients for nonelectrolytes in dilute aqueous solutions. *AIChE Journal*, *20*(3), 611–615.

Hayduk, W., & Minhas, B. (1982). Correlations for prediction of molecular diffusivities in liquids. *The Canadian Journal of Chemical Engineering*, *60*(2), 295–299.

Headley, J. V., Boldt-Leppin, B. E., Haug, M. D., & Peng, J. (2001). Determination of diffusion and adsorption coefficients for volatile organics in an organophilic clay-sand-bentonite liner. *Canadian Geotechnical Journal*, *38*(4), 809–817.

Hendry, M. (1982). Hydraulic conductivity of a glacial till in Alberta. *Groundwater*, *20*(2), 162–169.

Hinsby, K., McKay, L. D., Jørgensen, P., Lenczewski, M., & Gerba, C. P. (1996). Fracture aperture measurements and migration of solutes, viruses, and immiscible creosote in a column of clay-rich till. *Groundwater*, *34*(6), 1065–1075.

Hsu, H.-L. (2005). *Determination of Interfacial Tension and Contact Angle of Dense Non-Aqueous Phase Liquid Waste Mixtures*, PhD dissertation, University of Michigan, Ann Arbor, MI, USA.

Hu, Z., He, G., Liu, Y., Dong, C., Wu, X., & Zhao, W. (2013). Effects of surfactant concentration on alkyl chain arrangements in dry and swollen organic montmorillonite. *Applied Clay Science*, *75-76*, 134–140. doi:10.1016/j.clay.2013.03.004

Itakura, T., Airey, D. W., & Leo, C. J. (2003). The diffusion and sorption of volatile organic compounds through kaolinitic clayey soils. *Journal of Contaminant Hydrology*, *65*(3-4), 219–43. doi:10.1016/S0169-7722(03)00002-0

Jin, Y., & Jury, W. (1996). Characterizing the dependence of gas diffusion coefficient on soil properties. *Soil Science Society of America Journal*, *60*(1), 66–71.

Johnson, R. L., Cherry, J. A., & Pankow, J. F. (1989). Diffusive contaminant transport in natural clay: A field example and implications for clay-lined waste disposal sites. *Environmental Science & Technology*, *23*(3), 340–349.

Johnston, C. T., Sposito, G., & Erickson, C. (1992). Vibrational probe studies of water interactions with montmorillonite. *Clays and Clay Minerals*, *40*(6), 722–730.

Keller, C. K., Kamp, G. V. D., & Cherry, J. A. (1986). Fracture permeability and groundwater flow in clayey till near Saskatoon, Saskatchewan. *Canadian Geotechnical Journal*, *23*(2), 229–240.

Khandelwal, A., Rabideau, A. J., & Shen, P. (1998). Analysis of diffusion and sorption of organic solutes in soil-bentonite barrier materials. *Environmental Science & Technology*, *32*(9), 1333–1339.

Kueper, B. H., Stroo, H. F., Vogel, C. M., & Ward, C. H. (2014). *Chlorinated Solvent Source Zone Remediation*, Springer, New York, NY. doi:10.1007/978-1-4614-6922-3

Lee, S., & Kim, S. (2002). Expansion of smectite by hexadecyltrimethylammonium. *Clays and Clay Minerals*, *50*(4), 435–445.

Lee, S. Y., Kim, S. J., Chung, S. Y., & Jeong, C. H. (2004). Sorption of hydrophobic organic compounds onto organoclays. *Chemosphere*, *55*(5), 781–785. doi:10.1016/j.chemosphere.2003.11.007

Lee, S., Cho, W., Hahn, P., Lee, M., Lee, Y., & Kim, K. (2005). Microstructural changes of reference montmorillonites by cationic surfactants. *Applied Clay Science*, *30*(3-4), 174–180. doi:10.1016/j.clay.2005.03.009

Lerz, V. H., & Kraemer, V. (1966). Ein verfahren zur herstellung texturfreier rontgen-pulverpraeparate von tonmineralen fur zaehlrohrgoniometer mit senkrechter drehachse. *Neues Jahrb. Minerol, Monatsh*, 50-59.

Lever, D., Bradbury, M., & Hemingway, S. (1985). The effect of dead-end porosity on rock-matrix diffusion. *Journal of Hydrology*, *80*(1), 45–76.

Levitz, P. E. (2002). Adsorption of non ionic surfactants at the solid/water interface. *Colloids and Surfaces A: Physicochemical and Engineering Aspects*, *205*(1-2), 31–38. doi:10.1016/S0927-7757(01)01139-6

Lexa, D. (1998). Hermetic holder for x-ray powder diffraction of air-sensitive differential scanning calorimetry samples. *Review of Scientific Instruments*, *69*(12), 4249–4250.

Li, J. H., & Zhang, L. M. (2010). Geometric parameters and REV of a crack network in soil. *Computers and Geotechnics*, *37*(4), 466–475. doi:10.1016/j.compgeo.2010.01.006

Li, J., Smith, J. A., & Winquist, A. S. (1996). Permeability of earthen liners containing organobentonite to water and two organic liquids. *Environmental Science & Technology*, *30*(10), 3089–3093.

Linn, B., & Stupak, S. (2009). Chemicals Used in Dry Cleaning Operations. Retrieved from http://www.drycleancoalition.org/chemicals/ChemicalsUsedInDrycleaningOperations.pdf

Liu, C., & Ball, W. P. (2002). Back diffusion of chlorinated solvent contaminants from a natural aquitard to a remediated aquifer under well-controlled field conditions: Predictions and measurements. *Groundwater*, *40*(2), 175–184.

Ma, Y., Zhu, J., He, H., Yuan, P., Shen, W., & Liu, D. (2010). Infrared investigation of organo-montmorillonites prepared from different surfactants. *Spectrochimica Acta. Part A, Molecular and Biomolecular Spectroscopy*, *76*(2), 122–9. doi:10.1016/j.saa.2010.02.038

MacEwan, D. (1948). Complexes of clays with organic compounds. I. Complex formation between montmorillonite and halloysite and certain organic liquids. *Transactions of the Faraday Society*, *44*, 349–367.

Mackay, D., & Cherry, J. (1989). Groundwater contamination: Pump-and-treat remediation. *Environmental Science & Technology*, *23*(6), 630–636.

Mackay, D. M., Wilson, R. D., Brown, M. J., Ball, W. P., Xia, G., & Durfee, D. P. (2000). A controlled field evaluation of continuous vs. pulsed pump-and-treat remediation of a VOC-contaminated aquifer: site characterization, experimental setup, and overview of results. *Journal of Contaminant Hydrology*, 41(1), 81-131.

Madejová, J., & Komadel, P. (2001). Baseline studies of the Clay Minerals Society Source Clays: infrared methods. *Clays and Clay Minerals*, *49*(5), 410–432.

Marshall, T. (1959). The diffusion of gases through porous media. *Journal of Soil Science*, *10*(1), 79–82.

Matthieu III, D. E., Brusseau, M. L., Johnson, G. R., Artiola, J. L., Bowden, M. L., & Curry, J. E. (2013). Intercalation of trichloroethene by sediment-associated clay minerals. *Chemosphere*, *90*(2), 459–463.

McCaulou, D. R., & Huling, S. G. (1999). Compatibility of bentonite and DNAPLs. *Groundwater Monitoring & Remediation*, *19*(2), 78–86.

McKay, L. D., Cherry, J. a., & Gillham, R. W. (1993). Field experiments in a fractured clay till: 1. Hydraulic conductivity and fracture aperture. *Water Resources Research*, *29*(4), 1149–1162. doi:10.1029/92WR02592

Mering, J. (1946). On the hydration of montmorillonite. *Trans. Faraday Soc.*, *42*, B205–B219.

Meunier, A., & Fradin, N. (2005). *Clays*, Springer, Berlin.

Michaels, A. S., & Bixler, H. J. (1961). Flow of gases through polyethylene. *Journal of Polymer Science*, *50*(154), 413–439. doi:10.1002/pol.1961.1205015412

Middleton, T.A., Cherry, J.A. (1996). "The Effects of Chlorinated Solvents on the Permeability of Clay" in *Dense Chlorinated Solvents and Other DNAPLS in Groundwater: History, Behavior, and Remediation*, Pankow, J.F., and Cherry, J.A., (Eds.), Waterloo Press, Portland, 313-335.

Miller, C. J., Mi, H., & Yesiller, N. (1998). Experimental analysis of desiccation crack propagation in clay liners. *Journal of the American Water Resources Association*, *34*(3), 677–686.

Millington, R., & Quirk, J. (1960). "Transport in Porous Media" in *Transactions of 7th International Congress of Soil Science*, Vol. 1, F. A. van Baren. (Ed.), 97–106.

Millington, R., & Quirk, J. (1961). Permeability of porous solids. *Transactions of the Faraday Society*, *57*, 1200–1207.

Miyahara, K., Ashida, T., Kohara, Y., Yusa, Y., & Sasaki, N. (1991). Effect of bulk density on diffusion for cesium in compacted sodium bentonite. *Radiochimca Acta*, *52*(2), 293–298.

Moldrup, P., Olesen, T., Gamst, J., Yamaguchi, T., & Rolston, D. E. (2000). Predicting the gas diffusion coefficient in repacked soil: Water-induced linear reduction model. *Soil Science Society of America Journal*, *64*(5), 1588–1594.

Montavon, G., Guo, Z., Tournassat, C., Grambow, B., & Le Botlan, D. (2009). Porosities accessible to HTO and iodide on water-saturated compacted clay materials and relation with the forms of water: A low field proton NMR study. *Geochimica et Cosmochimica Acta*, *73*(24), 7290–7302. doi:10.1016/j.gca.2009.09.014

Montgomery, J. H. (2007). *Groundwater chemicals desk reference*, 4th ed, CRC Press, Florida.

Moore, D. M., & Reynolds, R. C. (1989). *X-ray Diffraction and the Identification and Analysis of Clay Minerals*, Oxford university press, Oxford.

Moran, M. J., Zogorski, J. S., & Squillace, P. J. (2007). Chlorinated solvents in groundwater of the United States. *Environmental Science & Technology*, *41*(1), 74–81. doi:10.1021/es061553y

Morris, P. H., Graham, J., & Williams, D. J. (1992). Cracking in drying soils. *Canadian Geotechnical Journal*, 29(2), 263-277.

Mott, H. V., & Weber Jr, W. J. (1991). Factors influencing organic contaminant diffusivities in soil-bentonite cutoff barriers. *Environmental Science & Technology*, *25*(10), 1708–1715.

Moulik, S. P., & Mukherjee, K. (1996). "On the Versatile Surfactant Aerosol-OT (AOT): Its Physicochemical and Surface Chemical Behaviours and Uses" In *Proceedings-Indian National Science Academy*, Part A, 62, 215–236.

Murray, R. S., & Quirk, J. P. (1982). The physical swelling of clays in solvents. *Soil Science Society of America Journal*, *46*(4), 856–868.

Muurinen, A. (1990). Diffusion of uranium in compacted sodium bentonite. *Engineering Geology*, *28*(3), 359–367.

Myers, D. (2006). *Surfactant Science and Technology*, 3rd ed, John Wiley & Sons, New Jersey.

Myrand, D., Gillham, R. W., Sudicky, E. A., O'Hannesin, S. F., & Johnson, R. L. (1992). Diffusion of volatile organic compounds in natural clay deposits : Laboratory tests. *Journal of Contaminant Hydrology*, *10*(2), 159–177.

Nahlawi, H., & Kodikara, J. K. (2006). Laboratory experiments on desiccation cracking of thin soil layers. *Geotechnical and Geological Engineering*, *24*(6), 1641–1664. doi:10.1007/s10706-005-4894-4

Nowak, E. J. (1983). "Diffusion of Colloids and Other Waste Species in Brine–saturated Backfill Materials" in *Symposium D–Scientific Basis for Nuclear Waste Management VII, Materials Research Society Proceedings*, Vol. 26, Cambridge University Press, Cambridge, UK, 59-68.

O'Hara, S. K., Parker, B. L., Jørgensen, P. R., & Cherry, J. A. (2000). Trichloroethene DNAPL flow and mass distribution in naturally fractured clay: Evidence of aperture variability. *Water Resources Research*, *36*(1), 135–147. doi:10.1029/1999WR900 212

Olejnik, S., Posner, A. M., & Quirk, J. P. (1974). Swelling of montmorillonite in polar organic liquids. *Clays and Clay Minerals*, *22*, 361–365.

Olesen, T., Moldrup, P., & Gamst, J. (1999). Solute diffusion and adsorption in six soils along a soil texture gradient. *Soil Science Society of America Journal*, *63*(3), 519–524.

Oliviera, I. B., Demond, A. H., & Salehzadeh, A. (1996). Packing of sands for the production of homogeneous porous media. *Soil Science Society of America Journal*, *60*(1), 49–53.

Olphen, H. Van, & Fripiat, J. (1979). *Data Handbook for Clay Minerals and Other Non-Metallic Materials*, Pergamon, New York.

Omidi, G., Thomas, J., & Brown, K. (1996). Effect of desiccation cracking on the hydraulic conductivity of a compacted clay liner. *Water, Air, and Soil Pollution*, *89*(1-2), 91–103.

Oolman, T., Godard, S. T., Pope, G. A., Jin, M., & Kirchner, K. (1995). DNAPL flow behavior in a contaminated aquifer: Evaluation of field data. *Groundwater Monitoring & Remediation*, *15*(4), 125–137.

Oscarson, D. W., Hume, H. B., Sawatsky, N. G., & Cheung, S. C. H. (1992). Diffusion of iodide in compacted bentonite. *Soil Science Society of America Journal*, *56*(5), 1400–1406.

Oscarson, D. W. (1994). Diffusion coefficients for iodide in compacted clays. *Clay Minerals*, *29*, 145–151.

Oscarson, D., & Hume, H. (1994). Diffusion of ^{14}C in dense saturated bentonite under steady-state conditions. *Transport in Porous Media*, *14*(1), 73–84.

Paradies, H. H. (1980). Shape and size of a nonionic surfactant micelle: TritonX-100 in aqueous solution. *The Journal of Physical Chemistry*, *84*(6), 599–607.

Parker, Beth L., Robert W. Gillham, and J. A. C. (1994). Diffusive disappearance of immiscible-phase organic liquids in fractured geologic media. *Groundwater*, *62*(5), 805–820.

Parker, B. L. (1996). *Effects of Molecular Diffusion on the Persistence of Dense, Immiscible Phase Organic Liquids in Fractured Porous Media*, PhD dissertation, University of Waterloo, Waterloo, Ontario, Canada.

Parker, B. L., Cherry, J. a., Chapman, S. W., & Guilbeault, M. A. (2003). Review and analysis of chlorinated solvent dense nonaqueous phase liquid distributions in five sandy aquifers. *Vadose Zone Journal*, *2*(2), 116. doi:10.2136/vzj2003.0116

Parker, B. L., Cherry, J. a, & Chapman, S. W. (2004). Field study of TCE diffusion profiles below DNAPL to assess aquitard integrity. *Journal of Contaminant Hydrology*, *74*(1-4), 197–230. doi:10.1016/j.jconhyd.2004.02.011

Parker, B. L., Chapman, S. W., & Guilbeault, M. A. (2008). Plume persistence caused by back diffusion from thin clay layers in a sand aquifer following TCE source-zone hydraulic isolation. *Journal of Contaminant Hydrology*, *102*(1-2), 86–104. doi:10.1016/j.jconhyd.2008.07.003

Penman, H. (1940). Gas and vapour movements in the soil: I. The diffusion of vapours through porous solids. *The Journal of Agricultural Science*, *30*(3), 437–462.

Petersen, L. W., Rolston, D. E., Moldrup, P., & Yamaguchi, T. (1994). Volatile organic vapor diffusion and adsorption in soils. *Journal of Environmental Quality*, *23*(4), 799–805.

Poling, B., Prausnitz, J., Paul, O. J., & Reid, R. (2001). *The Properties of Gases and Liquids,* McGraw-Hill, New York.

Porter, L. K., Kemper, W. D., Jackson, R. D., & Stewart, B. A. (1960). Chloride diffusion in soils as influenced by moisture content. *Soil Science Society of America Journal, 24*(6), 460–463.

Rayhani, M. H., Yanful, E. K., & Fakher, A. (2007). Desiccation-induced cracking and its effect on the hydraulic conductivity of clayey soils from Iran. *Canadian Geotechnical Journal, 44*(3), 276–283. doi:10.1139/t06-125

Riddick, J., Bunger, W., & Sakano, T. (1986). *Organic Solvents: Physical Properties and Methods of Purification*, John Wiley & Sons, New Jersey.

R. R. Street & Co. (2014, October 24). Pyratex. [Material Safety Data Sheet]. Retrieved from http://www.autolaundrysystems.com/msds/Pyratex.pdf

Robinson, R. A., and Stokes, R.H. (1959). *The Measurement and Interpretation of Conductance, Chemical Potential and Diffusion in Solutions of Simple Electrolytes,* 2nd ed, Butterworths, London.

Roehl, K., & Czurda, K. (1998). Diffusion and solid speciation of Cd and Pb in clay liners. *Applied Clay Science, 12*(5), 387–402.

Rosen, M. J. (2004). *Surfactants and Interfacial Phenomena*, 3rd ed, John Wiley & Sons, New Jersey.

Rudolph, D. L., Cherry, J. A. and Farvolden, R. N. (1991). Groundwater flow and solute transport in fractured lacustrine clay near Mexico City. *Water Resources Research, 27*(9), 2187–2201.

Russell, J. D., & Farmer, V. C. (1964). Infrared spectroscopic study of the dehydration of montmorillonite and saponite. *Clay Minerals Bulletin, 5*(32), 443–464.

Sale, T., Illangasekare, T., Zimbron, J., Rodriguez, D., Wilking, B., Marinelli, F. (2007). AFCEE Source Zone Initiative. Final Report. Submitted to Air Force Center for Engineering and the Environment, Brooks City-Base, TX, USA.

Sale, T., Newell, C., Stroo, H., Hinchee, R., & Johnson, P. (2008). *Frequently Asked Questions Regarding Management of Chlorinated Solvents in Soils and Groundwater*. Environmental Security Technology Certification Program, Arlington, VA, USA.

Sallam, A., Jury, W., & Letey, J. (1984). Measurement of gas diffusion coefficient under relatively low air-filled porosity. *Soil Science Society of America Journal, 48*(1), 3–6.

Sánchez-Martín, M. J., Dorado, M. C., del Hoyo, C., & Rodríguez-Cruz, M. S. (2008). Influence of clay mineral structure and surfactant nature on the adsorption capacity of surfactants by clays. *Journal of Hazardous Materials, 150*(1), 115–23. doi:10.1016/j.jhazmat.2007.04.093

Saripalli, K., Serne, R., Meyer, P., & McGrail, B. (2002). Prediction of diffusion coefficients in porous media using tortuosity factors based on interfacial areas. *Groundwater*, *40*(4), 346–352.

Sato, H., Ashida, T., Kohara, Y., Yui, M., & Sasaki, N. (1992). Effect of dry density on diffusion of some radionuclides in compacted sodium bentonite. *Journal of Nuclear Science and Technology*, *29*(9), 873–882. doi:10.1080/18811248.1992.9731607

Sawatsky, N., Feng, Y., & Dudas, M. J. (1997). Diffusion of 1 -naphthol and naphthalene through clay materials: Measurement of apparent exclusion of solute from the pore space. *Journal of Contaminant Hydrology*, *27*(1), 25–41.

Schaefer, C. E., Arands, R. R., Van der Sloot, H. A., & Kosson, D. S. (1995). Prediction and experimental validation of liquid-phase diffusion resistance in unsaturated soils. *Journal of Contaminant Hydrology*, *20*(1), 145–166.

SERDP and ESTCP. (2006). *Expert Panel Workshop on Reducing the Uncertainty of DNAPL Source Zone Remediation, Final Report*. Retrieved from https://www.serdp-estcp.org/News-and-Events/Conferences-Workshops/Past-ER-Workshops

Shackelford, C. D., Daniel, D. E., & Liljestrand, H. M. (1989). Diffusion of inorganic chemical species in compacted clay soil. *Journal of Contaminant Hydrology*, *4*(3), 241–273.

Shackelford, C. D. (1991). Laboratory diffusion testing for waste disposal: A review. *Journal of Contaminant Hydrology*, *7*(3), 177–217.

Shackelford, C. D., & Moore, S. M. (2013). Fickian diffusion of radionuclides for engineered containment barriers: Diffusion coefficients, porosities, and complicating issues. *Engineering Geology*, *152*(1), 133–147. doi:10.1016/j.enggeo.2012.10.014

Shen, Y.-H. (2001). Preparations of organobentonite using nonionic surfactants. *Chemosphere*, *44*(5), 989–995. doi:10.1016/S0045-6535(00)00564-6

Sheng, G., & Boyd, S. A. (1998). Relation of water and neutral organic compounds in the interlayers of mixed Ca/trimethylphenylammonium-smectites. *Clays and Clay Minerals*, *46*(1), 10–17.

Shimamura, K. (1992). Gas diffusion through compacted sands. *Soil Science*, *153*(4), 274–279.

Sims, J. E., Elsworth, D., & Cherry, J. A. (1996). Stress-dependent flow through fractured clay till: A laboratory study. *Canadian Geotechnical Journal*, *33*(3), 449–457.

Somasundaran, P., & Krishnakumar, S. (1997). Adsorption of surfactants and polymers at the solid-liquid interface. *Colloids and Surfaces A: Physicochemical and Engineering Aspects*, *123-124*(96), 491–513. doi:10.1016/S0927-7757(96)03829-0

Somasundaran, P., & Huang, L. (2000). Adsorption/ aggregation of surfactants and their mixtures at solid-liquid interfaces. *Advances in Colloid and Interface Science*, *88*(1), 179–208.

Sonon, L. S., & Thompson, M. L. (2005). Sorption of a nonionic polyoxyethylene lauryl ether surfactant by 2:1 layer silicates. *Clays and Clay Minerals*, *53*(1), 45–54. doi:10.1346/CCMN.2005.0530106

Stroo, H. F., & Ward, C. H. (2010). *In situ remediation of chlorinated solvent plumes*, Springer, New York.

Stroo, H. F., Leeson, A., Marqusee, A., Johnson, P. C., Ward, C. H., Kavanaugh, M. C., Sale, T. C., Newell, C. J., Pennell, K. D., Lebrón, C. A., and Unger, M. (2012). Chlorinated ethene source remediation: Lessons learned. *Environmental Science & Technology*, *46*(12), 6348–6447.

Tang, C., Shi, B., Liu, C., Zhao, L., & Wang, B. (2008). Influencing factors of geometrical structure of surface shrinkage cracks in clayey soils. *Engineering Geology*, *101*(3-4), 204–217. doi:10.1016/j.enggeo.2008.05.005

Tang, C.-S., Shi, B., Liu, C., Suo, W.-B., & Gao, L. (2011). Experimental characterization of shrinkage and desiccation cracking in thin clay layer. *Applied Clay Science*, *52*(1-2), 69–77. doi:10.1016/j.clay.2011.01.032

Tang, C.-S., Shi, B., Cui, Y.-J., Liu, C., & Gu, K. (2012). Desiccation cracking behavior of polypropylene fiber–reinforced clayey soil. *Canadian Geotechnical Journal*, *49*(9), 1088–1101. doi:10.1139/t2012-067

Thompson, D. (1990). *Hydraulic Evidence of Wisconsinan-aged Open Fractures in a Deep Clayey Till*, M. Sc. thesis, Univ. of Waterloo, Waterloo, Ontario, Canada.

Timms, W. A., & Hendry, M. J. (2007). Quantifying the impact of cation exchange on long-term solute transport in a clay-rich aquitard. *Journal of Hydrology*, *332*(1-2), 110–122. doi:10.1016/j.jhydrol.2006.06.025

Troeh, F., Jabro, J., & Kirkham, D. (1982). Gaseous diffusion equations for porous materials. *Geoderma*, *27*(3), 239–253.

Tyn, M., & Calus, W. (1975). Diffusion coefficients in dilute binary liquid mixtures. *Journal of Chemical and Engineering Data*, *20*(1), 106–109.

Van Loon, L. R., Glaus, M. A., & Müller, W. (2007). Anion exclusion effects in compacted bentonites: towards a better understanding of anion diffusion. *Applied Geochemistry*, 22(11), 2536-2552.

Velde, B. (1992). *Introduction to Clay Minerals: Chemistry, Origins, Uses and Environmental Significances, Geolog.* J. Chapman-Hall, London.

Velde, B. (1999). Structure of surface cracks in soil and muds. *Geoderma*, *93*(1-2), 101–124. doi:10.1016/S0016-7061(99)00047-6

Waterloo Centre for Ground Water Research (1989). *Dense Immiscible Phase Liquid Contaminants in Porous and Fractured Media.* Kitchener, Ontario: University of Waterloo.

Weber Jr, W. J., & DiGiano, F. A. (1996). *Process Dynamics in Environmental Systems*, John Wiley & Sons, New York.

Wilke, C., & Chang, P. (1955). Correlation of diffusion coefficients in dilute solutions. *AIChE Journal*, *1*(2), 264–270.

Williams-Daryn, S., & Thomas, R. K. (2002). The intercalation of a vermiculite by cationic surfactants and its subsequent swelling with organic solvents. *Journal of Colloid and Interface Science*, *255*(2), 303–311. doi:10.1006/jcis.2002.8673

Williams-Johnson, M., Eisenmann, C. J., & Donkin, S. G. (1997). *Toxicological profile for trichloroethylene*, Agency for Toxic Substances and Disease Registry, Atlanta, GA.

Wilson, J. (1997). "Removal of Aqueous Phase Dissolved Contamination: Non-chemically Enhanced Pump-and-treat" in *Subsurface Restoration*, Ward, M. R., Cherry, C.H., and Scalf, J.S. (Eds.), Ann Arbor Press, Ann Arbor, 271-285.

Xu, Q., Vasudevan, T. V., & Somasundaran, P. (1991). Adsorption of anionic—nonionic and cationic—nonionic surfactant mixtures on kaolinite. *Journal of Colloid and Interface Science*, *142*(2), 528–534. doi:10.1016/0021-9797(91)90083-K

Yang, Y., & Aplin, A. C. (2010). A permeability–porosity relationship for mudstones. *Marine and Petroleum Geology*, *27*(8), 1692–1697. doi:10.1016/j.marpetgeo.2009.07.001

Yesiller, N., Miller, C., Inci, G., & Yaldo, K. (2000). Desiccation and cracking behavior of three compacted landfill liner soils. *Engineering Geology*, *57*(1), 105–121.

Young, D. F., & Ball, W. P. (1998). Estimating diffusion coefficients in low-permeability porous media using a macropore column. *Environmental Science & Technology*, *32*(17), 2578–2584. doi:10.1021/es9711324

Zhang, R., & Somasundaran, P. (2006). Advances in adsorption of surfactants and their mixtures at solid/solution interfaces. *Advances in Colloid and Interface Science*, *123-126*, 213–29. doi:10.1016/j.cis.2006.07.004

Zheng, J., & Powers, S. E. (2003). Identifying the effect of polar constituents in coal-derived NAPLs on interfacial tension. *Environmental Science & Technology*, *37*(14), 3090–3094.

Zhou, X. (1994). *The Study of Restacked Single Molecular Layer Molybdenum Disulfide with Organic Tetrachloroethylene Included*, B. Sc. thesis, Simon Fraser University, Burnaby, British Columbia, Canada.

Zhu, L., Ren, X., & Yu, S. (1998). Use of cetyltrimethylammonium bromide-bentonite to remove organic contaminants of varying polar character from water. *Environmental Science & Technology*, *32*(21), 3374–3378. doi:10.1021/es980353m

Zogorski, B. J. S., Carter, J. M., Ivahnenko, T., Lapham, W. W., Moran, M. J., Rowe, B. L., Squillace, P.J., and Toccalino, P. L. (2006). *Volatile Organic Compounds in the*

Nation's Ground Water and Drinking Water Supply Wells. US Geological Survey Circular 1292 (Vol. 1292), Reston, Virginia.